

For Reference

NOT TO BE TAKEN FROM THIS ROOM

For Reference

NOT TO BE TAKEN FROM THIS ROOM

Ex libris
UNIVERSITATIS
ALBERTAENSIS





Digitized by the Internet Archive
in 2020 with funding from
University of Alberta Libraries

<https://archive.org/details/Murthy1969>

THE UNIVERSITY OF ALBERTA

PALEOMAGNETIC STUDIES IN THE CANADIAN SHIELD

by



GUMMULURU S. MURTHY

A THESIS

SUBMITTED TO THE FACULTY OF GRADUATE STUDIES
IN PARTIAL FULFILMENT OF THE REQUIREMENTS FOR THE DEGREE
OF DOCTOR OF PHILOSOPHY

DEPARTMENT OF PHYSICS

EDMONTON, ALBERTA

FALL, 1969

UNIVERSITY OF ALBERTA
FACULTY OF GRADUATE STUDIES

The undersigned certify that they have read,
and recommend to the Faculty of Graduate Studies for
acceptance, a thesis entitled PALEOMAGNETIC STUDIES
IN THE CANADIAN SHIELD submitted by Gummuluru S.
Murthy in partial fulfilment of the requirements for
the degree of Doctor of Philosophy.

ABSTRACT

Paleomagnetic studies have been made of two rock units in the Canadian shield. The first is an anorthosite intrusion near Michikamau Lake in northern Labrador, which has been reliably dated at 1400 m.y. by the potassium-argon method. The stability of magnetization of this body has been established through alternating-field demagnetization, and it is concluded that the observed magnetization is thermoremanent and represents the direction of the earth's field at the place and time of formation of the intrusion. A fold test has been applied to the paleomagnetic results after alternating field demagnetization. This test suggests that the magnetization was acquired with the rocks in their present attitudes. The paleomagnetic pole position for the intrusion lies at 0.5°S , 144.7°W with $A_{95}=5.6^{\circ}$. A comparison of this result with recently published results for well-dated rocks suggests that the geomagnetic field was essentially dipolar 1400 m.y. ago and that there have been no large relative movements between sampling sites widespread in North America during the last 1400 million years.

The Michikamau anorthosite has been shown to possess extremely high coercivities of the order of 1800

oersteds. Petrographic studies were made to investigate the nature of the magnetic mineral. It was shown that the contained magnetic mineral was magnetite occurring in the plagioclase feldspar in the form of rods of axial ratio of at least 20:1 and of typical length 12 microns. Theoretical estimates showed that grains in the shape of rods and of axial ratio 20:1 or more can be as long as 10 microns and still behave as single domains. It was shown that some of the magnetite grains of Michikamau anorthosites were in the single domain range. The observed high coercivity can then be explained in terms of the shape anisotropy of magnetite. A test of the field required to saturate the rock showed that magnetite and not hematite was the magnetic mineral.

The diabase dikes intruding in the Grenville province formed the second rock unit studied paleomagnetically. K-Ar age determinations by the Geological Survey of Canada gave scattered results between 437 and 970 m.y. for these dikes. The stability of magnetization of these dikes was tested both by alternating field and thermal demagnetization. While the responses of the specimens to both demagnetizations were similar, most of the sites had varying degrees of stability represented by a large range in coercive forces. Petrographic studies

indicated that all samples contained titanomaghemite and titanomagnetite in varying abundances. It was shown that while samples with higher stability of magnetization do have smaller grain sizes for titanomagnetites, a specially good correlation was obtained between the relative abundance of titanomaghemite and the magnetic stability factor. It was shown that titanomaghemite, probably formed by the low temperature oxidation of titanomagnetite, is responsible for the observed drop in magnetic stability of certain dikes. Petrological observations of the titanomaghemite/titanomagnetite ratio were used to assist in the exclusion of certain dikes whose magnetization was affected by secondary alteration. The mean paleomagnetic pole for the Grenville dike swarm was computed to lie at 3.0°N , 29.0°W with $A_{95}=11.0^{\circ}$. Comparison of this result with other Precambrian pole positions of North America suggests that the dikes were intruded after the Grenville orogeny.

The above results, along with other published results, were used in tracing a very tentative polar wander path relative to North America during Precambrian time.

ACKNOWLEDGEMENTS

I wish to express my sincere thanks and gratitude to Dr. D. I. Gough for supervising the research project. I am also grateful for his continuous encouragement and invaluable advice at various stages of this project.

I am also thankful to Dr. D. L. Jones, now at the University College of Rhodesia, for supervising the research project during the initial stages and for making the work possible by organizing the paleomagnetic laboratory instrumentation.

I am grateful to Dr. W. F. Fahrig of the Geological Survey of Canada for kindly providing me with the samples of the Michikamau anorthosites and for helping me with the field work on the Grenville dikes. I benefited greatly from his discussions on the diabase dike swarms of the Canadian shield.

I am particularly thankful to Dr. R. Morton of the Department of Geology for allowing me to use the ore-microscope in his laboratory and for his helpful discussions of the various aspects of microscopic studies under reflected light.

I wish to thank Drs. A. L. Hales and C. E. Helsley for allowing me to use their laboratory facilities at the Southwest Center for Advanced Studies, Dallas, Texas.

I am grateful to Dr. M. E. Evans, Dr. E. W. McMurry and Mr. A. B. Reid of this department for helpful comments and suggestions and particularly to Mr. Reid for assisting me with the collection of diabase dike samples from Sudbury.

The Geological Survey of Canada kindly prepared the polished sections used in this study and their service is greatly appreciated. During the course of this study, financial support was received from the National Research Council of Canada and the University of Alberta.

TABLE OF CONTENTS

	Page
ABSTRACT	iii
ACKNOWLEDGEMENTS	vi
TABLE OF CONTENTS	viii
LIST OF TABLES	xii
LIST OF ILLUSTRATIONS	xiii
LIST OF PLATES	xv
 CHAPTER 1 INTRODUCTION	
1.1 Principles of rock magnetism	1
1.2 Laboratory and field techniques	12
1.3 Analysis of data	17
1.4 Importance of Precambrian paleomagnetic results	21
1.5 Importance of petrographic studies in rock magnetism	24
1.6 Summary of the Thesis	24
 CHAPTER 2 LABORATORY INSTRUMENTATION	
2.1 Preliminary remarks	26
2.2 PAR spinner magnetometer	26
2.3 Alternating field demagnetizer	29
 CHAPTER 3 PALEOMAGNETISM OF THE MICHIKAMAU ANORTHOSITES	
3.1 Objectives of the study	38

3.2	Geologic setting and paleomagnetic sampling	39
3.3	Natural remanent magnetization of the anorthosite specimens	42
3.4	Alternating field demagnetization	47
3.5	Analysis of data	54
3.6	Comparison with paleomagnetic results from rocks of similar age in North America	57
3.7	Summary	63

CHAPTER 4 STABILITY OF MAGNETIZATION OF MICHIKAMAU ANORTHOSITES

4.1	High magnetic stability exhibited in Michikamau anorthosites	65
4.2	Magnetic stability of igneous rocks	67
4.3	Polished section studies of Michikamau anorthosites	69
4.4	Studies on isothermal remanent magnetization	77
4.5	Critical size of a single-domain grain	79
4.6	High coercive force of single-domain particles	85

	Page
4.7 Discussion	85
CHAPTER 5 THE PALEOMAGNETISM OF DIABASE DIKES FROM THE GRENVILLE PROVINCE: EXPERIMENTAL RESULTS	
5.1 Objectives of the study	89
5.2 Geologic setting and paleomagnetic sampling	91
5.3 Measurement of magnetization	93
5.4 Alternating field and thermal demagnetization	97
CHAPTER 6 STUDIES ON STABILITY OF MAGNETIZATION OF GRENVILLE DIABASE	
6.1 Objectives of the study	114
6.2 Opaque petrological properties of the Grenville diabase	116
6.3 Correlation between petrological properties and magnetic stability factor	124
6.4 Possible causes for the occurrence of titanomaghemite	132
CHAPTER 7 PALEOMAGNETISM OF THE DIABASE DIKES FROM THE GRENVILLE PROVINCE: INTERPRETATION AND CONCLUSIONS	
7.1 Analysis of data	134

Page

7.2 Discussion	137
----------------	-----

CHAPTER 8 REVIEW OF PRECAMBRIAN PALEOMAGNETISM OF
NORTH AMERICA

8.1 Preliminary remarks	140
-------------------------	-----

8.2 Discussion	147
----------------	-----

CHAPTER 9 SUMMARY AND CONCLUSIONS	152
-----------------------------------	-----

REFERENCES	158
------------	-----

APPENDIX A

APPENDIX B

APPENDIX C

APPENDIX D

LIST OF TABLES

Table		Page
2.1	Results of ten consecutive measurements of a specimen with the PAR Spinner.	28
2.2	Characteristics of demagnetizing solenoid.	34
3.1	Site mean directions of Michikamau anorthosites: natural remanent magnetization.	46
3.2	Site mean directions and pole positions of Michikamau anorthosites after optimum demagnetization.	53
3.3	Application of fold test to the data of anorthosites	56
3.4	Pole positions for 1400 m.y. age from North American rock units.	58
4.1	Summary of observations on polished sections of Michikamau anorthosites.	72
5.1	Site mean directions of Grenville dikes (NRM).	95
5.2	Site mean directions of Grenville dikes after optimum demagnetization.	109
5.3	Paleomagnetic pole positions for Grenville dikes.	111
6.1	Summary of observations on polished sections of Grenville diabase dikes.	117
6.2	Magnetic and petrologic parameters of Grenville diabase.	123
7.1	Magnetization directions and parameter B/A for Grenville dikes.	136
8.1	Paleomagnetic results for the Precambrian of North America.	143

LIST OF ILLUSTRATIONS

Figure		Page
2.1	Infinitely variable transformer for raising and lowering current in the demagnetizing solenoid.	32
2.2	Circuit for alternating field demagnetizer.	32
2.3	Calibration curve for demagnetizing solenoid.	36
3.1	Geologic map of Michikamau Intrusion showing the paleomagnetic sampling sites.	40
3.2	Sample magnetization directions of Michikamau anorthosites: natural remanent magnetization.	43
3.3	Mean site directions of Michikamau anorthosites: natural remanent magnetization.	45
3.4	Directional change of anorthosite specimens during a.f. demagnetization.	48
3.5	Sample magnetization directions of Michikamau anorthosites: after optimum demagnetization.	50
3.6	Mean site directions of anorthosites: after optimum demagnetization.	52
3.7	Intensity change of anorthosite specimens during a.f. demagnetization.	48
3.8	Paleomagnetic poles derived from North American rocks for 1400 million years.	60
4.1	Directional change of anorthosite specimens during a.f. demagnetization.	66
4.2	Intensity change of anorthosite specimens during a.f. demagnetization.	66
4.3	Saturation IRM of specimen AN041A.	78
4.4	Histogram of lengths of rod-shaped magnetite grains observed in Michikamau anorthosite.	78

Figure		Page
4.5	The critical single-domain size of magnetite as a function of axial ratio.	83
5.1	Location of diabase dikes intruding the Grenville province of Ontario and Quebec.	92
5.2	Mean site directions of Grenville dikes: natural remanent magnetization.	96
5.3	Response of specimens of Grenville diabase to a.f. demagnetization.	100
5.4	Intensity change of specimens of Grenville diabase during a.f. demagnetization.	102
5.5	Mean site directions of Grenville dikes: after optimum demagnetization.	110
5.6	Response of specimens of Grenville diabase to thermal demagnetization.	104
5.7	Intensity change of specimens of Grenville diabase during thermal demagnetization.	106
5.8	Paleomagnetic pole positions for Grenville dikes.	112
6.1	Histogram of grain-sizes of titanomagnetites observed in Grenville diabase.	127
6.2	Correlation of grain-size versus magnetic stability.	129
6.3	Correlation of relative abundance of titanomaghemite versus magnetic stability.	129
6.4	Correlation of titanomagnetite oxidation number versus magnetic stability.	129
8.1	A tentative Precambrian polar wander curve for North America.	148

LIST OF PLATES

Plate		Page
1	Photomicrographs of polished sections of anorthosites showing elongated magnetite grains in plagioclase.	75
2	Photomicrograph of Grenville diabase showing lamellae development in GR221.	121
3	Photomicrograph of Grenville diabase showing alteration of titanomagnetite to titanomaghemite in GR181.	121
4	Photomicrograph of Grenville diabase showing a titanomagnetite grain in GR364.	121
5	Photomicrograph of Grenville diabase showing a titanomaghemite grain in GR231.	121

CHAPTER 1

INTRODUCTION

1.1 Principles of Rock Magnetism

Paleomagnetism is fast developing into one of the most widely studied branches of geophysics. The interest in this subject originates mainly from the fact that knowledge of paleomagnetic directions can be effectively used to solve many physical, geological and mineralogical problems.

The magnetization in a rock can be expressed in terms of two components, the induced magnetization and the remanent magnetization. The former requires the presence of an external field and has the direction of the inducing field, while the latter can be present in the absence of such a field. It is this remanent or permanent magnetization which is of importance in paleomagnetism. For the remanent magnetization found in a rock when it is sampled, the customary term natural remanent magnetization (NRM) will be used.

The rocks owe their magnetism to the presence of one or more oxides of iron, while in some cases iron sulphides are also of importance. Usually these minerals constitute only a small part of the rock volume, being

distributed in a groundmass of paramagnetic or diamagnetic minerals. Magnetite (Fe_3O_4), titanomagnetite (solid solution between Fe_3O_4 and TiFe_2O_4), maghemite ($\gamma\text{-Fe}_2\text{O}_3$), hematite ($\alpha\text{-Fe}_2\text{O}_3$), ilmenite (TiFeO_3) and oxides in the solid solution hematite-ilmenite series are the oxides of iron most important in rock magnetism. In all cases the significance of these minerals lies in their property of ferromagnetism which enables them to have remanent magnetism in the absence of an external field. Thus before going over to the magnetic properties of these minerals, it would be advantageous to give a brief account of the theory of ferromagnetism. More complete discussions of the principles of ferromagnetism are given in the classic monographs on the subject by Bozorth (1951), Chikazumi (1964) and Morrish (1965).

An important property of ferromagnetic materials is that they occur in the form of crystals. The ferromagnetic character of the material is then derived from strong interaction of electron spins among neighbouring ions in the crystal lattice, which tends to align all the spin magnetic moment vectors against the randomizing effect of thermal agitation. The exchange energy is a minimum when the spins of the neighbouring ions or atoms become parallel or antiparallel. Thus there will be a net magnetization (the spontaneous magnetization) in the

absence of an external field. When the temperature is raised, the spins are increasingly deflected from their close alignment; hence the spontaneous magnetization decreases, falling to zero at the Curie temperature T_c ; this is a characteristic parameter of ferromagnetic materials, which become paramagnetic at temperatures above T_c .

Despite the property of spontaneous magnetization, ferromagnetic materials nearly always need an external field to acquire a remanent magnetization. This phenomenon can be explained by the domain theory (Weiss 1907, Bitter 1931), according to which even a single ferromagnetic crystal usually consists of numerous magnetic domains separated by discontinuous boundaries. The total energy of the crystal is a minimum when the domain magnetizations form a closed magnetic circuit, with minimal external field. Thus, while individual domains have parallel spin alignment, the vector sum of the moments of a large number of domains tends to zero. An external field gives the material a net magnetization by deflecting the average spin moment towards the field direction. This occurs in weak fields by migration of domain walls, a reversible process; and in stronger fields by switching of whole domains to a new direction of magnetization along a crystalline axis making a smaller

angle with the field. The latter process is irreversible and causes the crystal to retain remanent magnetization after removal of the field, as well as the other phenomena of magnetic hysteresis (Brailsford 1960).

With or without an external field, however, the arrangement of magnetic moments in the crystal depends upon the condition that the total energy per unit volume must be a minimum. If the entire volume of the crystal or grain were a single domain, the magnetostatic energy would become significant because of the presence of an external field of the crystal. Magnetostatic energy is always less in a multi-domain crystal than in a single-domain one. Magnetocrystalline energy is minimized when the parallel spin moments in each domain lie along a crystal axis of easiest magnetization. Application of an external field produces a new equilibrium of minimum energy, tending to enlarge domains whose magnetization lies near the direction of the external field, and to reduce the size of the others. Finally, a considerable amount of magnetoelastic energy, arising from internal stress, may be stored in the crystal, so that altogether four energy terms, exchange, magnetostatic, magneto-crystalline and magnetoelastic energy, contribute to determine the optimum number, size and shape of domains in a ferromagnetic substance.

Strictly, the magnetic properties of some of the minerals important in rock magnetism are derived from ferrimagnetism, a phenomenon closely related to ferromagnetism. Here the magnetic ions occupy two interleaved sublattices, A and B, in the unit cell of the crystal, where the spins in A are directed in opposition to those in B because of strong negative interaction between the two spin systems. The result is an antiparallel spin arrangement. The crystal is ferrimagnetic and has a net external magnetic moment if the number of ions, or their individual moments, or both, are different in sublattices A and B. Magnetite, titanomagnetite and pyrrhotite all exhibit ferrimagnetism. Oxides in the hematite-ilmenite solid solution series exhibit weak ferromagnetism caused probably by canting of spins from the direction normal to the triad basal plane (Néel 1949, 1953; Li 1956; Moriya 1960). Crystals are known in which the sublattices A and B contribute equal and opposite magnetizations. So far as is known, these antiferromagnetic substances play little part in rock magnetism.

A given crystal will require some definite energy from an applied field to switch a domain to a new direction. It thus has a characteristic energy or energy barrier for isothermal remanent magnetization by an external field. Fields below a corresponding limiting value will produce

only reversible induced magnetization, by reversible displacement of domain walls, in a multidomain crystal; and no magnetization in a single domain crystal.

Rocks acquire NRM in one or more of several ways depending on the formation of the rock and its subsequent history. Igneous rocks, which are formed by the cooling of liquid magma, tend to acquire most of their magnetization as they cool from above the Curie temperatures of their ferromagnetic constituents. Laboratory experiments by numerous workers (Irving 1964) indicate that the direction of magnetization acquired by this process, known as thermoremanent magnetization (TRM) in most cases lies accurately in the direction of the applied field. Néel (1955) has proposed a theory of the TRM for single-domain particles which explains many of the observed characteristics. In Néel's theory, the magnetic moment of each grain can lie along one of two mutually opposite directions consistent with minimum energy per unit volume of the grain. Opposing reversal of the magnetization is an energy barrier given by

$$E = \frac{vH_c J_s}{2} \quad (1.1)$$

where v is volume of the grain, H_c the coercive force and J_s is the spontaneous magnetization of the mineral. If E exceeds the thermal energy T (k = Boltzmann's constant,

T =absolute temperature), no change of the magnetic direction will result. When the temperature is sufficiently high, or the volume sufficiently small, however, the magnetic moments are easily reversed by thermal energy, and the crystal magnetization is unstable. The combined effect due to all the oriented domains results in a value J_0 of the initial magnetization.

After a time t , this value will decay to J_R given by

$$J_R = J_0 e^{-t/\tau_0} \quad (1.2)$$

and τ_0 is called the relaxation time. Néel derived τ_0 as

$$\frac{1}{\tau_0} = A \left(\frac{V}{T} \right)^{\frac{1}{2}} e^{-vH_c J_s / 2kT} \quad (1.3)$$

$$= A \left(\frac{V}{T} \right)^{\frac{1}{2}} e^{-\gamma v / T}$$

where constants A and γ depend on the elastic and magnetic properties of the mineral. From the known values of these constants for iron, Néel showed that the direction of magnetization in an iron grain of diameter less than 120\AA is quickly changed by the thermal fluctuations at room temperature, and the application of a weak field to a number of such grains causes a net magnetization in the direction of the field. On the other hand, an increase in v/T by a factor of 3 increases t_0 by a factor of 10^{17} . If τ_0 is of

the order of experimental times, then (1.3) can be solved for T which will be a maximum temperature at which the grain will show a stable magnetic moment with relaxation time τ_0 . Néel called this value of T the blocking temperature T_b of the grain. As a rock containing single domain crystals cools, each crystal becomes stabilized as it passes through its blocking temperature, which is always less than the Curie temperature T_c . If the rock cools in a field H , and contains many grains randomly oriented, a net magnetization parallel to H results. Nagata (1943) has shown that for fields of order of 1 oe. the TRM magnitude is proportional to H . Because of the exponential dependence of τ_0 on T , the resulting TRM may be stable in the geological time scale. Dunlop (1968) suggested a generalized Néel theory to include the effects of grain interaction.

Stacey (1963) has proposed a theory of TRM for multidomain grains. He showed that small grains have appreciable permanent moments called 'pseudo-single domain' moments because the equilibrium positions of domain walls do not in general coincide with the positions required to give zero total moments of the grains containing them. TRM of these grains, large enough to contain four domains, may be explained by Barkhausen discreteness, so that the domain walls have perfect locations in the samples leaving

a residual magnetic moment associated with the grain. The component of the TRM in the field direction is given by

$$I_{\text{TRM}} = \frac{m}{v} \cos\theta \tanh\left(\frac{m_B H}{kT_B} \cos\theta\right) \quad (1.4)$$

where v is volume of the grain, m and m_B the pseudo single domain moments at room temperature and at blocking temperature T_b , and θ is the angle the external field H makes with the p.s.d. moments. Alternative theories to explain the origin of TRM are given among others by Verhoogen (1959) and Ozima and Ozima (1965).

Sedimentary rocks, particularly red sandstones, acquire their natural magnetizations mainly in two ways. Preferential alignment of ferromagnetic mineral grains along the ambient field during their deposition, or in the unconsolidated sediment shortly after deposition, may give the rock a depositional remanent magnetization (DRM). A process which is probably more relevant to the magnetization of red sediments, from which a large fraction of all paleomagnetic results are derived, is chemical remanent magnetization (CRM). In equation (1.3) if T is held constant, but v increases through growth of a crystal by chemical reactions, a characteristic blocking volume v_b can be defined such that the relaxation time τ_0 is of the order of an experiment. Crystals with $v < v_b$ will not acquire

remanent magnetization. Creer (1961) used the term superparamagnetism to describe their behaviour. As crystals grow through v_b in an ambient field the rock acquires a stable CRM along the field direction. A problem which arises in paleomagnetic use of rocks having CRM is that their oxides may have been formed and therefore the CRM acquired, long after the sediments were deposited (Chamalaun and Creer 1964).

Other types of remanent magnetization which a rock can acquire include isothermal remanent magnetization (IRM) and viscous remanent magnetization (VRM). A rock placed in a magnetic field at room temperature and subsequently removed will acquire a remanent magnetization, known as isothermal remanent magnetization (IRM), provided the field is larger than the lowest coercive force of the magnetic minerals in the rock. The process involves alignment with the applied field of magnetic moments of the domains having magnetic energy barriers with corresponding coercive force less than the applied field. The large magnetic fields associated with lightning may impart a substantial IRM to rocks (Graham 1961). If a rock remains in a field too weak to cause IRM for sufficiently long period of time, it acquires a new component of remanent magnetization in the direction of the field. This component, known as viscous remanent magnetization (VRM),

is due to the Boltzmann distribution of thermal energy which, when converted to magnetic energy, allows the magnetic domains to cross energy barriers that they otherwise could not cross in the weak field of the earth. Cox and Doell (1960), Nagata (1961) and Irving (1964) have discussed in detail these various forms of magnetization and their origins.

The early classic work in paleomagnetism by Chevallier (1925) indicated that the remanent magnetism of lava flows on Mt. Etna was parallel to the earth's magnetic field as measured at nearby observatories at the times the flows erupted. Other workers such as Koenigsberger (1930) demonstrated in the laboratory that the remanent magnetization of rocks heated above the Curie points of their ferromagnetic constituents and cooled in an ambient field nearly always had the same direction and sense as that field. These early investigations served to establish confidence in the ultimate usefulness of the NRM of rocks as a fossil compass and dip needle. This confidence has been justified by more recent studies, which have also increasingly emphasized, however, that reliable conclusions from rock magnetism can be drawn only if a stable direction of magnetization can be isolated from isothermal and viscous components not related to the original field.

1.2 Laboratory and Field Techniques

The NRM of a rock often contains, in addition to the primary component of magnetization acquired at the time of formation of the rock, secondary components which it acquires during its later history. The secondary components may be in the form of IRM due to lightning, VRM acquired in the present earth's field and so on while the primary component may be a TRM for igneous or a CRM or DRM for sedimentary rocks. Tests must be devised to isolate the primary component of magnetization which is of importance in paleomagnetic research. Both field and laboratory tests can be performed to study the stability of magnetization of rocks. The field tests include Graham's classic fold test and conglomerate test (Graham 1949). Strangway (1967) has discussed some of these tests for the stability of magnetization of a rock unit. Laboratory tests use parameters which can distinguish between a very stable TRM or CRM and less stable isothermal components.

In the laboratory, the stability of NRM is tested by one or more demagnetization procedures, the most widely used being alternating field demagnetization (Thellier and Rimbert 1954; As and Zijderveld 1958; Creer 1959; McElhinny and Gough 1963) and thermal demagnetization (Thellier 1938; Wilson 1962). In the former method, the rocks are partly demagnetized in a smoothly decreasing alternating field,

with the aim of randomizing the directions of the magnetic moments in all domains having coercive force less than the highest value of the demagnetizing field; this would leave intact the magnetization due to the "hard" (high coercive force) domains, which may preserve the direction of the ambient field at the time the rock was formed. Thus if a rock is placed in an a.c. magnetic field with peak value \tilde{H} , all domains with coercive force less than \tilde{H} will follow the field and as the field is reduced to zero, these domains will have random orientations. If a constant magnetic field, such as the geomagnetic field, is superposed upon the a.c. field, an anhysteritic remanent magnetization (ARM) will develop which may mask the remaining remanent magnetization. Thus it is essential to perform the a.c. demagnetization of rocks in the absence of a constant field. The constant geomagnetic field at the location is usually cancelled by pairs of Helmholtz coils. Later improvements in the design of a.c. demagnetizers include tumbling of the specimen while the demagnetization is carried out. There are two purposes served by tumbling a) application of \tilde{H} along all directions in the specimen and b) avoidance of ARM by any small residual field. There is no danger of chemical modification of the specimen by the a.c. demagnetization.

In thermal demagnetization the rock is heated to a certain temperature T_1 and cooled in zero field to atmos-

spheric temperature, T_0 , the direction and intensity of remanent magnetization being measured before and after heat treatment. This process will destroy any magnetic component with blocking temperature $T_b < T_1$. Treatment is then repeated by heating to a temperature $T_2 > T_1$ and again cooling to T_0 in a zero field, and so on, where $T_1, T_2, T_3 \dots T_n < T_c$ and T_c corresponds to the component with the highest Curie temperature. The effectiveness of thermal demagnetization depends upon the fact that in many rocks the most stable magnetic component is due to a TRM acquired in grains with T_b just below the Curie temperature, which remains after less stable components (such as IRM or partial TRM acquired at relatively low temperature, and perhaps a significantly long time after the rock was formed) have been removed by the heat treatment. An alternative thermal demagnetization technique consists of taking measurements during continuous heating of the sample to a high temperature, and calculating the direction and magnitude of the components destroyed in each temperature interval (Wilson 1962).

Knowledge of the NRM of rocks has many useful applications. The evidence can be interpreted in terms of the geophysical hypotheses of continental drift and polar wandering. They have also found application in solving local tectonic problems, as well as in age correlation of

rocks. An important application arises from reversals in polarity, which are a frequent occurrence in rock formations of various ages: these have been cited by many workers as evidence for reversals of the geomagnetic field during geological times (Hospers 1955; Cox, Doell and Dalrymple 1963), but an alternative possibility is that in rare cases physico-chemical changes in the rock may cause it to acquire a magnetization directed in opposition to the applied field (Néel 1951; Uyeda 1958). The present state of the evidence indicates that actual reversals of the geomagnetic field have given rise to most occurrences of reversed NRM in rocks. The fact that frequent reversals of the geomagnetic field took place during the Quaternary may be utilized in estimating the rate of spreading of the ocean floors (Vine and Matthews 1963).

The collection of oriented rock samples and measurement of their remanent magnetization is difficult and is prone to error. Collections of oriented samples may be made either by the less cumbersome block method or by the more precise drill method, the latter being preferred by most workers in recent times. The drill method uses portable drilling equipment to obtain rock cores and a solar compass to orient them. The advantages of this method over the block method are the better marking accuracy and specially the fact that samples can be chosen from below

the surface weathered layer. The equipment used in this laboratory is a portable drilling equipment powered by a commercial single-cylinder two-stroke gasoline motor normally used to power a lumbering saw (McCullough model 35A). It develops approximately 2 h.p. at about 3000-4000 r.p.m.. The motor is fitted with a centrifugal clutch that engages a plate fitted to the transmission shaft. Water with some soluble oil is supplied to the coring crown through a shut-off valve and a plastic hose fitted to a commercial pressure type garden insecticide sprayer. The use of soluble oil enables more cores to be drilled with a single crown. Orientation of the drill core is done in situ with a solar compass and a slotted brass tube. The brass tube is lowered on the core and a mark is made on the bottom side of the core using a diamond scratcher. The azimuth of the shadow of the pointer on the brass plate of the solar compass is measured and this value and the local time are used in computing the orientation of the scratch relative to true north. Errors in orientation are restricted to about 1.5° . Descriptions of similar drilling equipment and solar compasses were given by Gough and Opdyke (1963), McElhinny and Neal (1967), Doell and Cox (1967), Helsley (1967) and Opdyke (1967).

Measurement of the remanent magnetization of rocks, in general, is carried out either electromagnetically or by

means of an astatic magnetometer. Johnson and Steiner (1937) and Nagata (1940) were the first to use the astatic magnetometer for the measurement of permanent magnetization of rocks. Blakett (1952) considerably improved the design of the astatic magnetometer and achieved a high sensitivity. Electromagnetic apparatus of the rock generator type was pioneered by Johnson and McNish (1938). Gough (1964) has described an improved spinner magnetometer. The instrument used in the present study is a spinner magnetometer commercially available through the Princeton Applied Research Corporation.

1.3 Analysis of Data

In paleomagnetic research, a principal aim is to establish the direction of magnetization of a particular rock unit. The directions observed in a rock never agree exactly, scatter being caused by various factors (Irving 1964). A satisfactory sampling scheme should take into account all the factors causing scatter. The sampling scheme employed in the present study is a hierarchical type comprising two levels. At least five oriented cores called "samples" were collected from each "site", a small separated exposure at least tens of meters wide. Two "specimens" in the form of cylinders were cut from each core and used in the measurements. Advantages of this site sampling method have been discussed by Gough (1967). Results

are presented as individual specimen observations, sample means, site means and rock unit mean. In the calculation of each mean, members of the next lower hierarchy are given unit weight. Thus the two specimen observations are combined to obtain the sample mean; the sample means are given unit weight to obtain the site mean; and the site means are given unit weight to obtain the rock-unit mean. A similar sampling plan is the two-tier method of Watson and Irving (1957).

Directions are usually combined by means of a statistical method developed by Fisher (1953) to give a mean direction and estimates of precision. Each directional vector is regarded as a point on a sphere of unit radius. In order to justify the use of Fisher's statistics, the population from which the sample is drawn must satisfy two conditions: 1. the vectors in the population must be distributed with axial symmetry about their mean direction; 2. the density of the vectors in the population must decrease with increasing angular displacement ψ from the mean direction according to the probability density function

$$P = \frac{\kappa}{4\pi \sinh \kappa} \exp(\kappa \cos \psi) \quad (1.5)$$

where κ is a constant called the precision parameter and describes the tightness of the group of vectors in the population about their mean direction. The best estimate

of the precision parameter κ is given by

$$k = (N-1)/(N-R) \quad (1.6)$$

where N is the number of vectors in the sample and R is the length of the resultant of the N unit vectors. At a probability level of $(1-P)$, the true mean direction of the population lies within a circular cone about the resultant vector R with a semi vertical angle $\alpha_{(1-P)}$ given by

$$\cos \alpha_{(1-P)} = 1 - \frac{N-R}{R} \left[\left(\frac{1}{P} \right)^{1/N-1} - 1 \right]. \quad (1.7)$$

In paleomagnetic analyses, P is usually taken as 0.05 and an approximate relationship for α_{95} , the semi angle of the cone of 95% confidence for the mean direction is given by

$$\alpha_{95} = 140/\sqrt{Nk}. \quad (1.8)$$

The parameter κ is a measure of the precision of the data; α_{95} gives a confidence limit for their mean. It will be observed that k is independent of the sample size, while α_{95} is proportional to $1/\sqrt{N}$.

For comparison of paleomagnetic results from different parts of the world, they must be represented by the same parameters. One convenient way is to represent data in terms of the geocentric dipole that would produce the measured field direction at the site. This position is referred to as the virtual paleomagnetic pole and is specified

by the present geographic coordinates of that position. In such calculations, the following assumption which is of fundamental importance in paleomagnetism is made: over a time interval which has been variously estimated at 10^4 , 10^5 or 10^6 years, the average geomagnetic field approximates that of a geocentric dipole along the axis of rotation. This is usually called the 'axial geocentric dipole' assumption. It has some support from theoretical considerations of the dominance of Coriolis force in the Earth's liquid core over motions in the core involved in any self-excited dynamo source of the field. The assumption also has empirical support from the good grouping, symmetrically about the present geographic pole, of virtual paleomagnetic poles found from rocks less than 50 m.y. old (Brynjólfson 1957; Cook and Belshé 1958; Roche 1960). In most earlier epochs the dipolar field can only be assumed. In principle it can be tested by work on two rock units of the same age widely separated on the same continent. Such a test, with a positive result, is reported in Chapter 3 of this thesis. On the axial geocentric dipole assumption, semi-axes δp and δm of the oval of confidence about the paleomagnetic pole are calculated as

$$\delta p = \frac{1}{2}(1+3\cos^2 p)$$

$$\delta m = \sin p / \cos I$$

where p is the distance from the sampling site to the paleomagnetic pole and I is the inclination of remanent magnetization from the horizontal. Alternatively, each site mean magnetization can be used to find a virtual pole and the site poles can then be combined by means of Fisher's statistics and expressed as a mean pole position with circle of confidence of radius A_{95} .

1.4 Importance of Precambrian Paleomagnetic Results

The Physics Department of the University of Alberta has initiated a comprehensive project in rock magnetism, centered on studies of the Precambrian paleomagnetism of the Canadian shield. Such a study is important in many respects. J. E. Gill and J. T. Wilson (quoted in Harrison 1963) have emphasized in recent times the probability that Precambrian time was marked by many orogenic cycles. This is the period during which biological evolution is supposed to have begun and developed. It encompasses roughly 85% of the earth's history.

Information on the magnetic field that existed on the earth's surface during the Precambrian could in many ways contribute to solving the problem of the state of its interior in the distant past and aid in selecting the most suitable model of the earth's development. In particular solution of the following problems would be of great value: 1) Has the earth's magnetic field been a

dipole field in the first approximation and what could its non-dipole components have been? 2) What were the nature and amplitude of the secular variation? 3) What was the strength of the earth's magnetic field, at least in order of magnitude? 4) Did polar wander or continental drift take place early in the earth's history? Although the dynamo theory of the geomagnetic field is embryonic, it seems clear that a large liquid core is required for the necessary fluid motions and magnetohydrodynamic interactions. The existence of a Precambrian field of comparable magnitude to the present field would thus support the view that the core was differentiated from the mantle early in the development of the earth. Answers to Questions 1, 2 and 3 would thus be relevant to the age of the core.

In addition to seeking answers for the above questions, it will be useful to compare the paleomagnetic results from different shield areas of the world. At present only the Southern African shield has been extensively studied and has yielded reliable paleomagnetic data. However some results are available from the Australian and Canadian shields. McElhinny et al. (1968) have attempted a comparison between the African polar wander curve and the very tentative pole positions from the Canadian Shield. The results of this comparison, although not conclusive, suggest no relative movement between the South African and Canadian shields by a

detectable amount between 2000 and 1300 m.y.. Extensive paleomagnetic data from the rocks of the Canadian shield are required before such comparisons can lead to reliable results. When such data are available for all shield areas, it is hoped the comparison of results may be decisive in choosing between the hypotheses of relative drift of the shields, polar wandering or a combination of the two.

As part of this endeavour, the author has obtained paleomagnetic results from two formations of the Canadian Shield. The first is the Michikamau anorthosite body from the Ungava Province of the Canadian Shield. The age of this formation has been well determined as 1400 m.y.. This formation was investigated 1) to obtain a reliable paleomagnetic pole for 1400 m.y. for the Canadian Shield, and 2) to study the usefulness of anorthosite bodies for paleomagnetic study. The latter objective is of importance particularly in view of recent observations by Herz (1969) on the importance of massive anorthosite bodies in studies of continental drift. Secondly, the diabase dikes intruded throughout the Grenville Province were studied to investigate the effect, if any, of Grenville orogeny on the magnetization of the dikes. The known ages of these dikes vary between 450 and 970 m.y.. It is hoped that the paleomagnetic results from these two formations yield two significant pole positions relative to the Canadian Shield which will be useful in intershield correlation.

1.5 Importance of Petrographic Studies in Rock Magnetism

It has long been a puzzling problem for researchers in paleomagnetism to explain the varying magnetic stability of igneous rocks. Of late many attempts have been made to correlate the magnetic stability of a rock with the degree of oxidation of the magnetic mineral (Ade-Hall et al. 1968; Wilson et al. 1968; Larson et al. 1969). Petrographic studies are often useful in identifying the magnetic mineral and finding its state of oxidation. Results of petrographic analysis of Michikamau anorthosite and Grenville diabase are reported in this thesis and attempts were made to explain their very different stabilities.

1.6 Summary of the Thesis

The subject matter of the thesis is divided as follows:

Chapter 2 gives a short account of the instruments used in the present study.

Chapter 3 deals with the paleomagnetic results from the Michikamau anorthosites and Chapter 4 with the explanation of magnetic stability of these anorthosites.

Paleomagnetic results from diabase dikes from the Grenville Province are reported in Chapter 5. Results of petrographic studies were used in explaining the magnetic behaviour of the diabase samples and these results are presented in Chapter 6. Chapter 7 deals with an attempted

interpretation of the results reported in Chapters 5 and 6.

Paleomagnetic results for the Precambrian of North America are reviewed in Chapter 8 and a tentative polar wander curve is suggested for this period. Summary and conclusions are presented in Chapter 9.

CHAPTER 2

LABORATORY INSTRUMENTATION2.1 Preliminary Remarks

Methods for the measurement of magnetic fields associated with igneous and sedimentary rocks have been known for a long time, but accurate measurements of the direction of natural remanent magnetization of weakly magnetized rocks were made possible only in recent times, after the design of very sensitive magnetometers. It was pointed out in Chapter 1 that in this regard, two basic instruments, the astatic magnetometer and the spinner magnetometer, are of importance.

2.2 PAR Spinner Magnetometer

The apparatus used in the present study, for the measurement of magnetization of rocks, is a spinner magnetometer commercially available through the Princeton Applied Research Corporation, Princeton, New Jersey (Model SM-1). This magnetometer has many advantages over earlier spinner magnetometers (Gough 1964), the chief of which is the speed of measurement and low drift rate. It provides direct and simultaneous measurement of two orthogonal components of the sample's magnetic moment in a plane perpendicular to the spin axis. This facilitates easy computation of the total magnetic vector as for an

astatic magnetometer.

In operation of the PAR spinner magnetometer, the specimen is inserted into a 'Permali' holder and oriented with respect to an index mark on the specimen holder. The specimen holder is inserted into the shielded spinner head where it is spun at 105 revolutions per second with the spin axis perpendicular to the common axis of two pick-up coils connected in series. The signal from the pick-up coils is amplified and synchronously detected with respect to two orthogonal signals generated by two photo-choppers mounted 90° apart with respect to known faces of the sample cup. The demodulated outputs of the synchronous detectors represent the magnitude and direction of the components of magnetic moment of the specimen in the plane normal to the spin axis. Reorienting the specimen by 90° in the holder and spinning enables the measurement of the third component of the magnetic moment of the specimen. Usually the specimen holder (with the specimen inside) is oriented in six different positions in the spinner head and is spun in the six positions. This procedure eliminates error caused by any asymmetric centering of the specimen in the holder. The manufacturers of the PAR spinner list the minimum detectable magnetization in the specimen as 7×10^{-9} emu/cc and claim an accuracy of 1% and $\pm 0.5^\circ$ in magnitude and phase calibration.

TABLE 2.1

RESULTS OF 10 CONSECUTIVE MEASUREMENTS OF A
SPECIMEN WITH THE PAR SPINNER

Azimuth(DEG)	Inclination(DEG)	Intensity(EMU/CC)
109.71	31.57	0.30788E-06
108.63	32.12	0.31056E-06
108.78	31.95	0.31159E-06
109.00	32.56	0.30943E-06
108.79	32.08	0.31052E-06
108.72	32.03	0.31206E-06
108.98	32.60	0.30762E-06
109.35	32.69	0.30916E-06
109.24	32.27	0.30817E-06
109.13	32.75	0.30805E-06

In actual practice, many factors contribute to the noise level of the magnetometer and the accuracy of measurements may not be of the same order as claimed by the manufacturers. While the various sources are partly random and partly systematic, so that it is difficult to estimate the contribution of each, one can estimate the total measurement error by repeating observations with the same specimen and noting the scatter in the results. Ten consecutive measurements were made of the intensity and direction of magnetization of one of the specimens of Grenville diabase. The specimen was reoriented in the specimen holder before each measurement. From the data listed in Table 2.1, the standard deviations from the mean in the measurements of the angle and intensity of magnetization were calculated as 0.1° and 1.5×10^{-9} emu/cc respectively, for this specimen of intensity 3.09×10^{-7} emu/cc.

Computer programs were designed so as to calculate the intensity and direction of magnetization from the spinner magnetometer readings.

2.3 Alternating Field Demagnetizer

It was pointed out in Chapter 1 that alternating field demagnetization has been recognized as an important means of selectively removing the soft secondary components of remanent magnetization. If a rock is placed in an a.c.

magnetic field with peak value H , all domains with coercive force less than H will follow the field as it alternates. As the a.c. field is then smoothly decreased to zero, domains with progressively lower coercive forces become randomly oriented. However if a constant field is superposed over the alternating field or if the variation of the magnetic field with time is not symmetrical, an anhysteretic magnetization will develop which may mask the remaining primary component. Thus it is essential in an a.c. demagnetization experiment to completely annul the geomagnetic field and to engineer a smooth reduction of the a.c. field to zero.

Remarkable improvements in design took place since the first a.c. demagnetizer was used by French workers. Creer (1959) introduced rotation of the specimen about two axes mainly to counteract the effects of imperfect cancellation of the geomagnetic field. It is now a standard practice to rotate the specimen in a decreasing a.c. field usually about two axes and sometimes about three axes (Doell and Cox 1967). Thellier (1966) states that excessive complication of rotation is not necessary except perhaps in high alternating fields.

The a.c. demagnetizer at the University of Alberta was installed, tested and calibrated by Dr. D. L. Jones and the writer. In this apparatus the demagnetizing

field is produced by means of a solenoid similar to that described by McElhinny (1966). The solenoid is wound with 16 SWG bicalex covered copper wire in twenty-seven layers of approximately 109 turns per layer. The solenoid has an inside diameter of 13.0 cm, an outside diameter of 23.0 cm, is 19.0 cm long and has a total of 2933 turns. It has an inductance of 0.8083 henries and a D.C. resistance of 13.83 ohms. While winding the solenoid, each layer of wire is covered with shellac and one layer of brown paper.

Smooth reduction of the current in the solenoid is achieved by means of an infinitely variable transformer similar to that described by McElhinny (1966). The device contains a laminated iron core which has two equal and oppositely wound coils AC and CB (Figure 2.1) of total length 60 cm. wound along the central portion. A shorter coil DE which is short-circuited is placed over either of the two coils previously described. The short-circuited coil rests on guides and can be moved smoothly over the two primary coils. Since the secondary coil is short circuited, the inductance of the primary coil which it encloses is reduced to near zero. When the mains supply at 60 c/s is connected across the two primary coils in series, the effect of the coil DE over the primary coil AC is to produce almost the full mains supply across CB, since the impedance of AC has been reduced to zero or very nearly so. As the coil DE moves over the other primary coil CB,



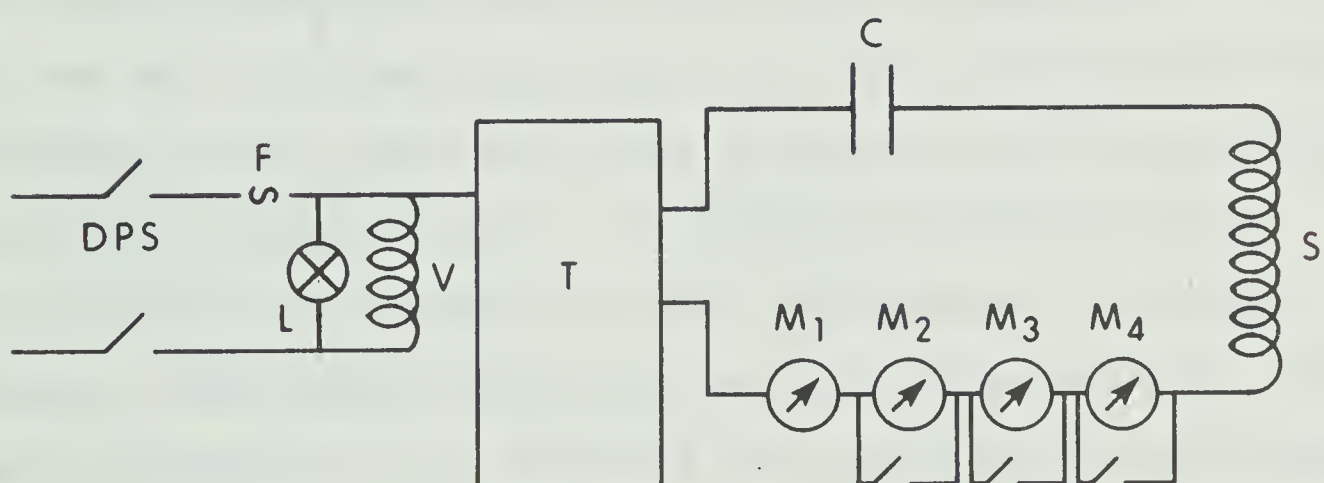
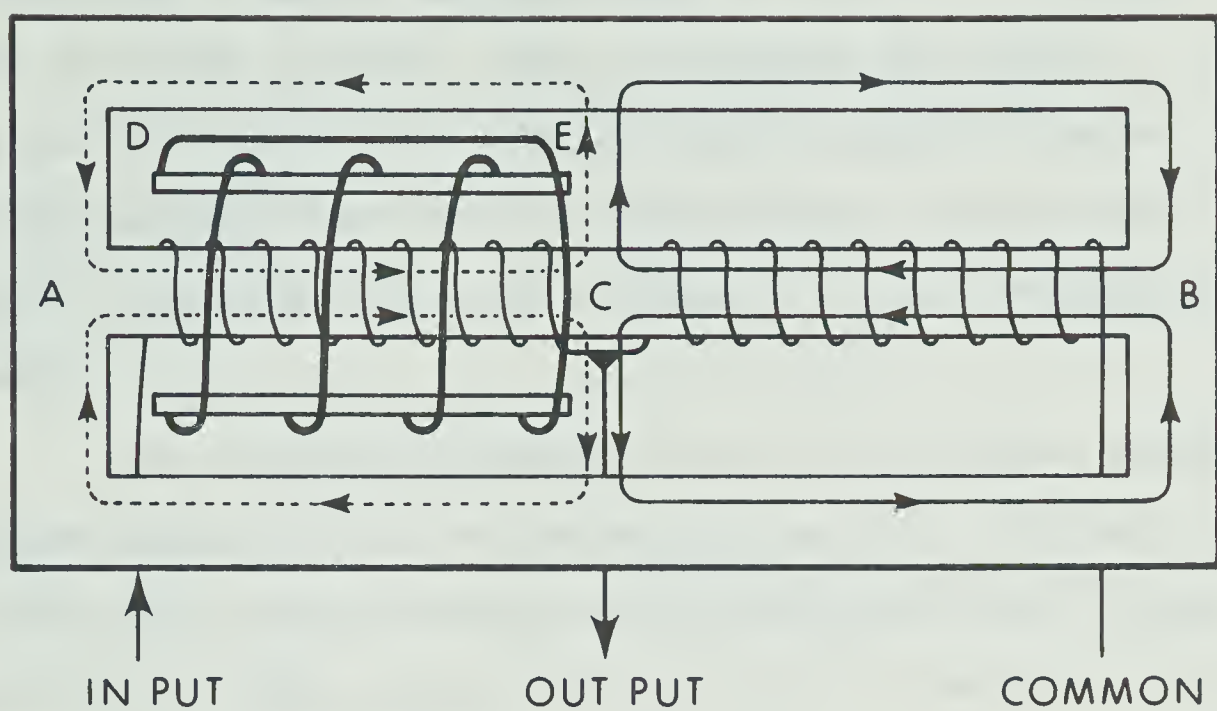
Figure 2.1 Infinitely variable transformer for raising and lowering the current in the demagnetizing solenoid.

Figure 2.2 Circuit for alternating field demagnetizer.

DPS: double pole switch; F: fuse; L: lamp;

T: variable transformer; C: bank of capacitors;

M: ammeters with shunt switches; S: demagnetizing solenoid.



the full mains supply appears across AC and the voltage across CB drops to zero. Thus by sliding the short-circuited coil from A to B the voltage across CB can be smoothly reduced from the full mains supply value nearly to zero. The output from CB is applied to the demagnetizing solenoid.

The solenoid is tuned to the 60 c/s mains supply by connecting a bank of condensers in series, the exact value of capacitance being determined by trial and error during tuning tests. The characteristics of the solenoid are listed in Table 2.2.

The solenoid rests in a cradle which runs on guides facilitating its easy withdrawal from the tumbling mechanism. The tumbling mechanism selected for this demagnetizer is of the two axis type and has a ratio of 11:16. McElhinny (1966), Hutchings (1967) and others have discussed the relative merits of various tumbling ratios. In particular McElhinny has shown that a 11:16 tumbler is more advantageous than some tumblers with simple ratios such as 1:2, 15:16 and 8:15. The short circuited coil is attached to a screw which runs along the side of the primary coils AB. The screw is driven by a motor the speed of which can be varied over a continuous range thereby allowing the a.c. field in the demagnetizing solenoid to be reduced in the desired time range. A time range from 122 seconds to 16 minutes for the reduction of the magnetic field from maximum to zero is possible with the present

TABLE 2.2

CHARACTERISTICS OF DEMAGNETIZING SOLENOID

Inner diameter	13.0 cm
Outer Diameter	23.0 cm
Number of turns	2933
Length of solenoid	19.0 cm
Inductance	0.8083 henry
D.C. resistance	13.83 ohms

CHARACTERISTICS OF PARRY COILS

Coil former	aluminum
Wire used	18 AWG heavy insulated copper wire
Vertical coils	
side	75.2 cm
separation of coils	41.0 cm
number of turns	40
resistance per coil	4.0 ohms
Horizontal coils	
side	79.8 cm
separation of coils	43.6 cm
number of turns	40
resistance per coil	4.3 ohms

CHARACTERISTICS OF TEST COIL

Internal diameter	1.396 cm
External diameter	2.152 cm
Number of turns	2000
Resistance	68.0 ohms
Area of cross section	2.47 sq cm

CALIBRATION CONSTANTS OF THE SOLENOID

Voltage induced in test coil (slope of the best fit by method of least squares)	2.67 volts/amp rms
Field at center of the solenoid	190.2 ± 2 gauss peak/amp rms

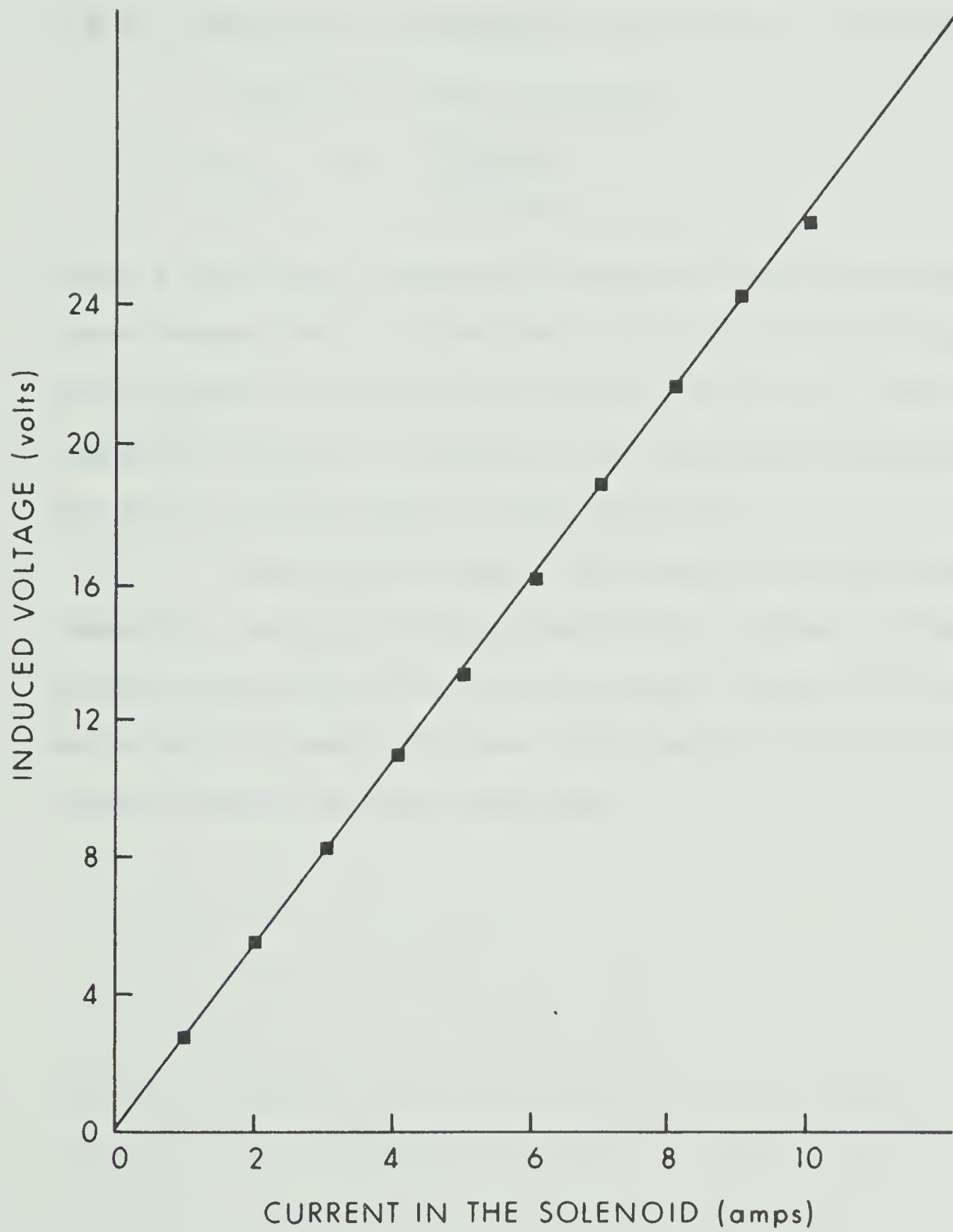
arrangement.

The cancellation of the geomagnetic field at the tumbling mechanism is accomplished by means of two pairs of Parry coils. The coils are arranged so that the horizontal axis of one pair of coils coincides exactly with the horizontal field in the laboratory, allowing the compensation of the total horizontal component by one pair of coils alone. The characteristics of Parry coils are listed in Table 2.2. A field cancellation to a minimum of 50γ was achieved by these coils.

Microswitches were arranged at either end of the variable transformer so that the process of increasing and decreasing the a.c. field is carried out automatically. The dial of the variac is calibrated and can be preset so that any given current up to 10 amp can be passed through the circuit. By operating a microswitch, the motor which drives the coil DE from B to A is turned on. When the coil DE reaches the end of its travel from B to A at A, it operates a microswitch which reverses the current to the motor. The coil DE moves in the opposite direction from A to B and as it reaches B, it operates a microswitch which switches off the motor. The demagnetizing circuit is shown in Figure 2.2.

The demagnetizing coil was calibrated by measuring the induced voltage in a small search coil placed at its center. The characteristics of the search coil are listed in Table 2.2. The values of the induced voltage were

Figure 2.3 Calibration curve for the demagnetizing solenoid.



measured for various currents in the demagnetizing solenoid. From the calibration curve shown in Figure 2.3, the voltage induced in the test coil may be estimated as 2.67 volts/amp r.m.s.. The e.m.f. induced in the test coil is given by

$$\begin{aligned} \text{e.m.f.} &= -AN \omega B_0 \cos \omega t \\ B_0 &= \frac{\sqrt{2} e_{\text{rms}}}{AN \cdot 2\pi f} \end{aligned}$$

where A and N are the area of cross section and number of turns respectively of the test coil and f is the frequency. Thus B_0 may be estimated as 203 oe./amp r.m.s.. This value compares with 194 oe. which is a theoretical estimate of the field at the center of the solenoid.

Thus the two basic instruments for paleomagnetic research, the spinner magnetometer and the a.c. demagnetizer were set up in the laboratory. Results of measurements made by means of these instruments form much of the subject matter of later chapters.

CHAPTER 3

PALEOMAGNETISM OF THE MICHIKAMAU ANORTHOSITES3.1 Objectives of the Study

Very few paleomagnetic studies have been made of anorthositic bodies. This is partly because massive anorthosite formations are relatively rare in parts of the world other than the Canadian shield. Even in this shield, most of the massive anorthosite bodies lie inside the Grenville structural province and were altered during the Grenville orogeny. As such they are not suitable for paleomagnetic work. Examples of anorthosites which have been subject to metamorphism are those at Allard Lake studied by Hargraves and Burt (1967), and the Adirondack anorthosites studied by Balsley and Buddington (1958). The Michikamau intrusion is one of a few anorthosite intrusions which lie north of the Grenville Front. It is essentially unaltered. Thus this body provides a good opportunity to study the use of anorthosites in paleomagnetic work.

The Michikamau intrusion has been dated at 1400 m.y. by the potassium-argon method. As rocks of this age suitable for paleomagnetic work are uncommon in the Canadian shield, the Michikamau intrusion provides an opportunity to obtain a reliable paleomagnetic pole position relative to this part of the shield for this period.

3.2 Geologic Setting and Paleomagnetic Sampling

The Michikamau intrusion has been described in detail by Emslie (1965) and the geologic data of Figure 3.1 and subsequent description are taken largely from his report. The intrusion is centered at latitude $54^{\circ}30'$ N, longitude $64^{\circ}00'$ W and underlies an area of approximately 2000 square kilometers. The intrusion consists of major units of leucotroctolite, anorthosite and leucogabbro, with a border group of fine grained olivine basalt, coarser olivine gabbros and pyroxene troctolites. Ferrous rich rocks of dioritic, granodioritic and syenitic compositions form part of the intrusion. All these units are remarkably fresh and unaltered. Rocks surrounding the intrusion are predominantly paragneisses, quartz feldspathic gneisses, migmatites, granite and syenite.

The Michikamau intrusion contains internal planar structures of two types. One is defined by planar orientation of plagioclase; the other consists of rhythmic mineralogic layering. The two types of structure are sensibly parallel where they occur together. Emslie concluded that the lamination and layering were formed by accumulation of crystals settling from a liquid magma and that some of the planes have had primary dips of about 30 degrees.

Along the west shore of Michikamau Lake the primary structures show consistent eastward dips of between 50 and

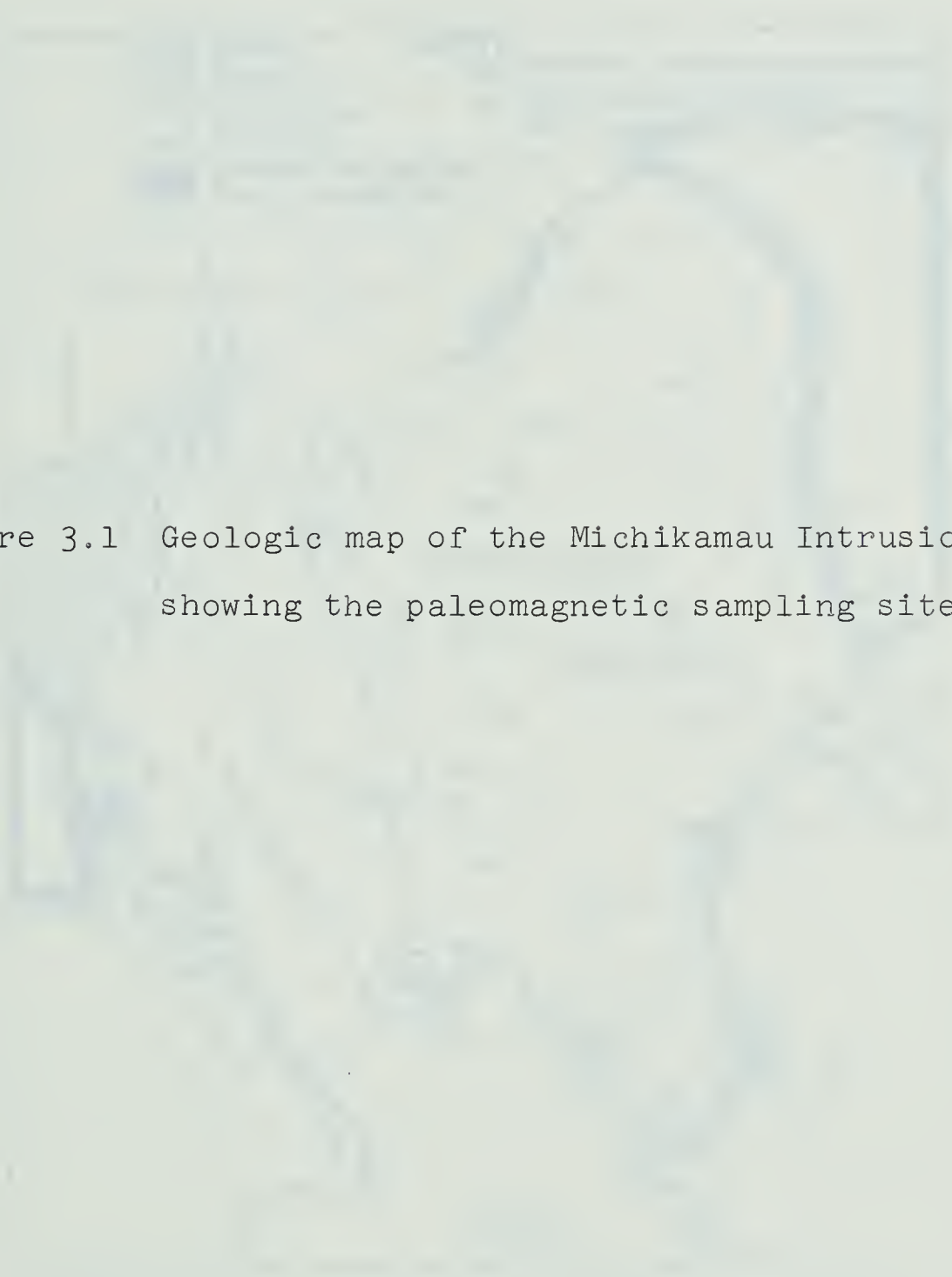
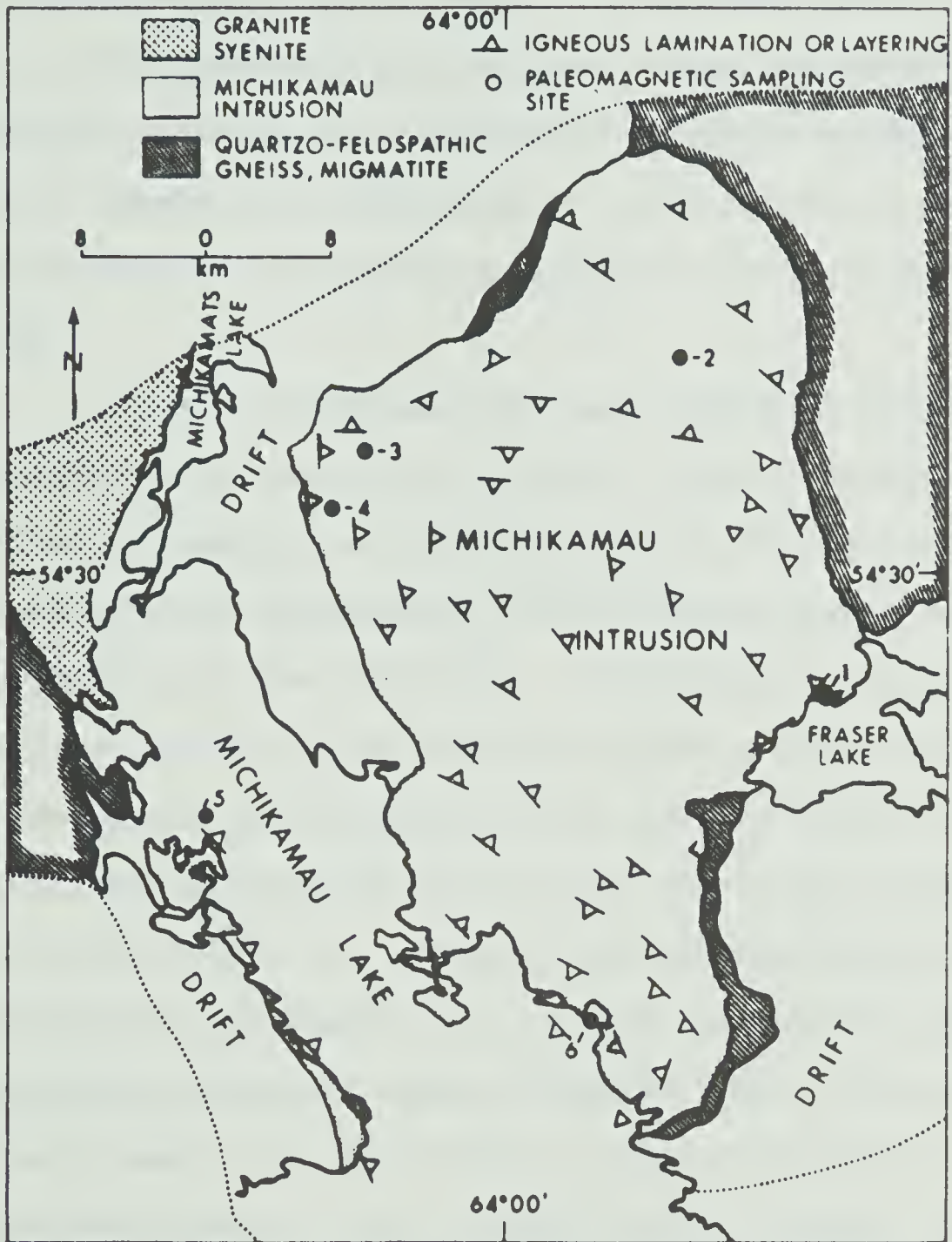


Figure 3.1 Geologic map of the Michikamau Intrusion showing the paleomagnetic sampling sites.



and 80 degrees. These dips are markedly steeper than elsewhere in the intrusion and suggest that the west lake shore area has been separated from the main mass by a fault and tilted steeply to the east. The transgressive relationship of ferrogranodiorite, a later stage differentiate of the intrusion, towards the anorthosite provides evidence that the anorthosite was sufficiently consolidated to fail by fracture while the overlying magma was still essentially liquid.

Three potassium-argon age determinations on biotite are available to date the intrusion (Emslie 1964). The southeastern margin of the intrusion is in contact with paraschists and paragneisses which show evidence of thermal metamorphism by the intrusion. A biotite-rich specimen of paraschist about one km from the contact, which should give a maximum age of the formation, was dated at 1520 ± 80 m.y.. Biotite from leucotroctolite of the intrusion provided an age of 1400 ± 80 m.y.. Granite around Michikamats Lake, which Emslie considered to be related to granite dikes cutting the intrusion, gave an age of 1360 ± 80 m.y.. The 1400 m.y. age of the intrusion is thus bracketed by maximum and minimum ages of 1520 and 1360 million years. Morse (1964) has reported a potassium-argon age determination of 1480 ± 50 m.y. on biotite from possibly rheomorphic granodiorite that cuts the Kiglapait anorthositic intrusion. This intrusion lies some 320 kilometers northeast of Michikamau

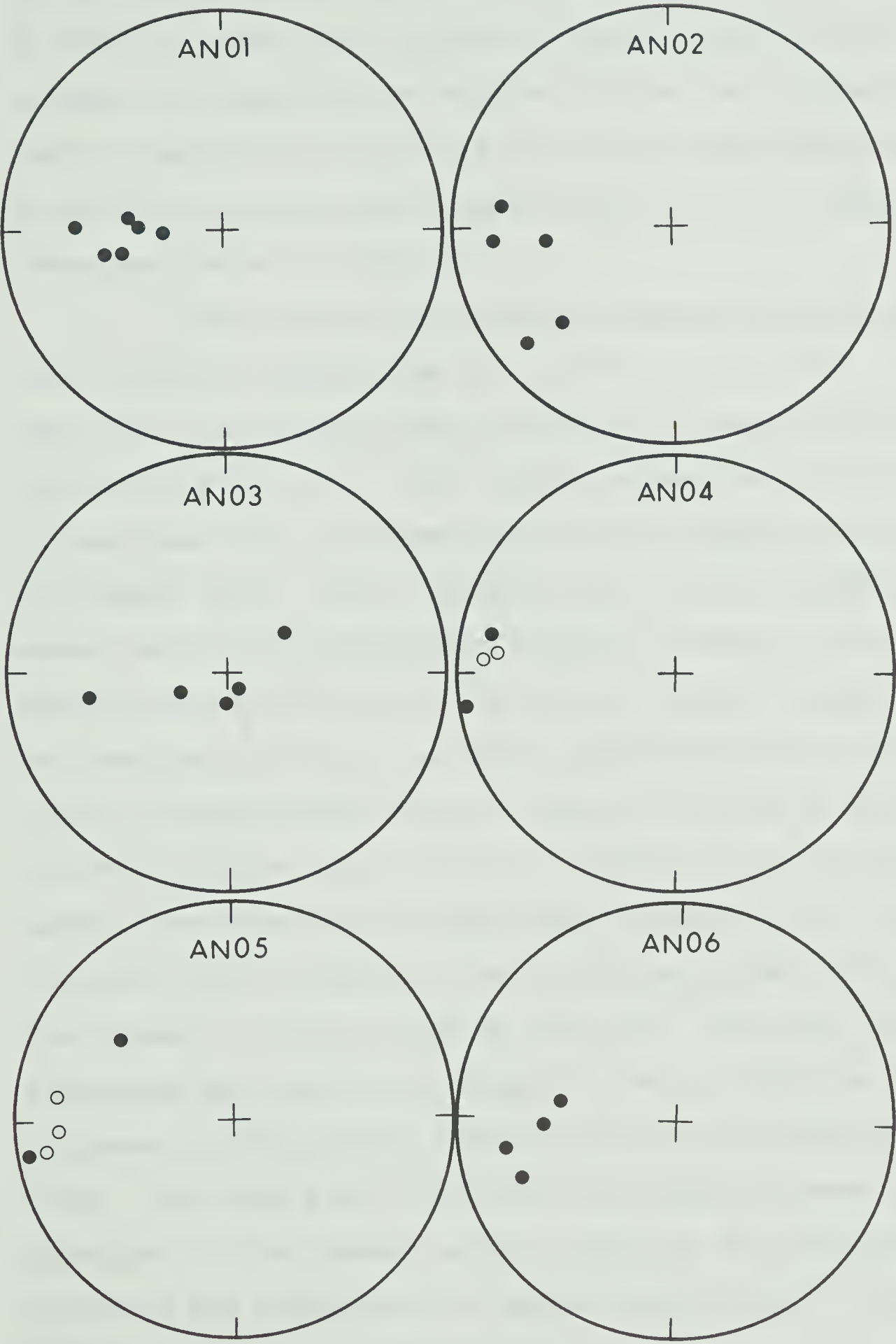
and like the Michikamau intrusion was not involved in the Grenville orogeny. Morse has suggested that the potassium-argon data indicate age equivalence of the two intrusions and gives an approximate age of their primary crystallization.

Samples for paleomagnetic work were made available to the author by Dr. W. F. Fahrig of the Geological Survey of Canada. Twenty-nine drill cores, 3.2 cm in diameter, were collected from six sites whose locations are shown in Figure 3.1. The cores were oriented by means of a solar compass similar to that described by Gough and Opdyke (1963). Values for the strike and dip of the primary layering at each collection site are listed in Table 3.3. These were obtained from Maps 31-1963 and 3-1964 of the Geological Survey of Canada. Site 1, on Fraser Lake, is in rock mapped by Emslie as olivine gabbro of the border group. The remaining five sites are from the anorthosite unit. Two cylindrical specimens, 2.9 cm in length, were cut from each core. Each core is considered to represent an independent sample and in the statistical analyses that follow, the vector sum of unit vectors for the two specimens was taken to be representative of the sample.

3.3 Natural Remanent Magnetization of the Anorthosite Specimens

The natural remanent magnetization of each individual specimen was measured and the results are given in the appendix in Table A1. The specimen magnetization directions were

Figure 3.2 Sample magnetization directions of Michikamau anorthosites: natural remanent magnetization.

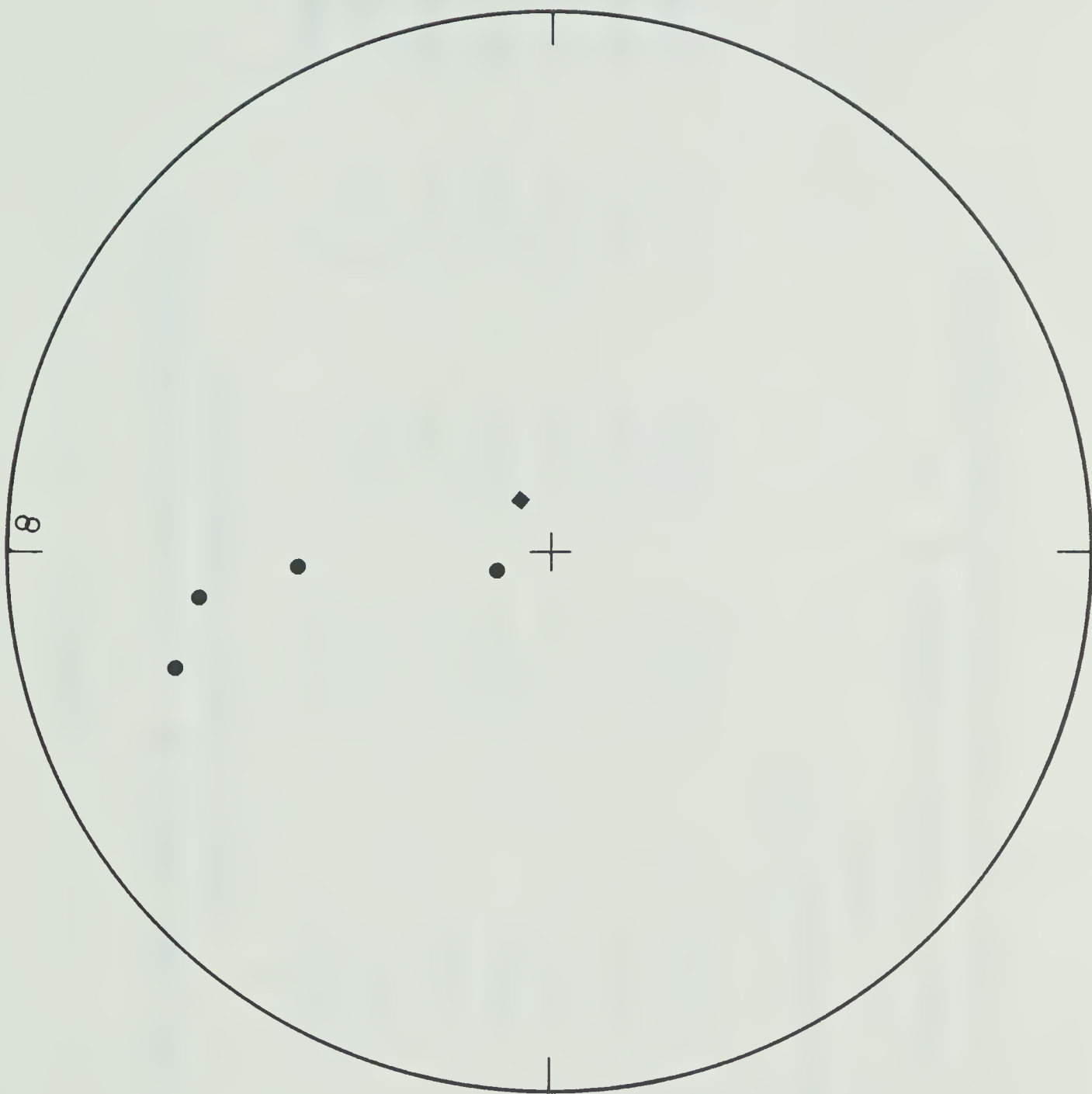


● POSITIVE INCLINATIONS
○ NEGATIVE INCLINATIONS

combined to obtain sample mean directions. These are listed in Table A2 along with values of 'theta' which is the angle between the magnetization vectors for the two specimens. The site mean directions were calculated from sample mean directions by giving each sample direction unit weight. These are listed in Table 3.1.

The specimens are strongly magnetized with magnetic moments ranging from 6.6×10^{-3} to 2.7×10^{-1} gauss cm³. The sample mean directions of magnetization are plotted in Figure 3.2. The initial magnetization directions in specimens from the same sample and in samples from the site agree well. Site 3 (Figure 3.2.3) is an exception where there is a considerable scatter in sample directions. However even at this site, the value of R, the length of the resultant of N unit vectors, indicates that the directions of magnetization are not random on Watson's (1956) criterion (Table 3.1). At site 6 (Figure 3.2.6) the mean sample directions have an approximate great circle distribution whose long axis, when continued, passes through the present or dipole field at the site. The mean site directions are plotted in Figure 3.3 which indicates the influence of the present earth's field on the NRM directions. The mean site directions are smeared between the direction of the present earth's field at the Michikamau intrusion and a direction of magnetization that is approximately horizontal and due west.

Figure 3.3 Mean site directions of Michikamau anorthosites:
natural remanent magnetization.



- POSITIVE INCLINATIONS
- NEGATIVE INCLINATIONS
- ◆ PRESENT EARTH'S FIELD

TABLE 3.1

SITE MEAN DIRECTIONS OF MICHIKAMAU ANORTHOSITES
NATURAL REMANENT MAGNETIZATION

Site	N	Azimuth	Incl.	R	k	Alpha
AN01	6	266.77	40.36	5.8566	34.88	9.68
AN02	5	252.85	18.44	4.7027	13.45	17.07
AN03	5	248.51	78.32	4.1672	4.80	28.57
AN04	4	273.18	- 2.20	3.9197	37.36	11.45
AN05	5	273.24	- 1.21	4.6331	10.90	18.96
AN06	4	263.19	23.82	3.9006	30.19	12.74

N = NUMBER OF CORES FROM EACH SITE

R = RESULTANT OF N UNIT VECTORS

k = ESTIMATE OF FISHER'S PRECISION PARAMETER κ

ALPH = SEMIANGLE OF CONE OF 95% CONFIDENCE FOR MEAN DIRECTION

3.4 Alternating Field Demagnetization

All specimens were subjected to alternating field demagnetization. The procedure adopted in choosing the optimum field was that employed by McElhinny and Gough (1963). At least two, and in many cases three, specimens were selected from each site and were demagnetized progressively in fields up to 700 oersteds. The field at which the vector rotation stops and any further change occurs only in intensity (i.e. the field at which a stable end point in direction is reached) is taken as the optimum field of demagnetization. The rest of the specimens from that site were demagnetized at that field. The changes of direction of remanent magnetization during demagnetization of some typical specimens are shown in Figure 3.4. Table A3 in the appendix gives details of the demagnetization histories of specimens taken through stepwise demagnetization.

The test specimens from sites 1, 2, 5 and 6 behaved in a similar fashion. In fields up to 100 to 150 oersteds a change of direction of magnetization occurred, which varied in magnitude from specimen to specimen but was generally away from the direction of the present earth's field. The directions of magnetization showed little further change during continued demagnetization in fields up to 700 oersteds. The remaining specimens from these sites were then treated in an optimum field for each site,




Figure 3.4 Directional change of anorthosite specimens during a.f. demagnetization.

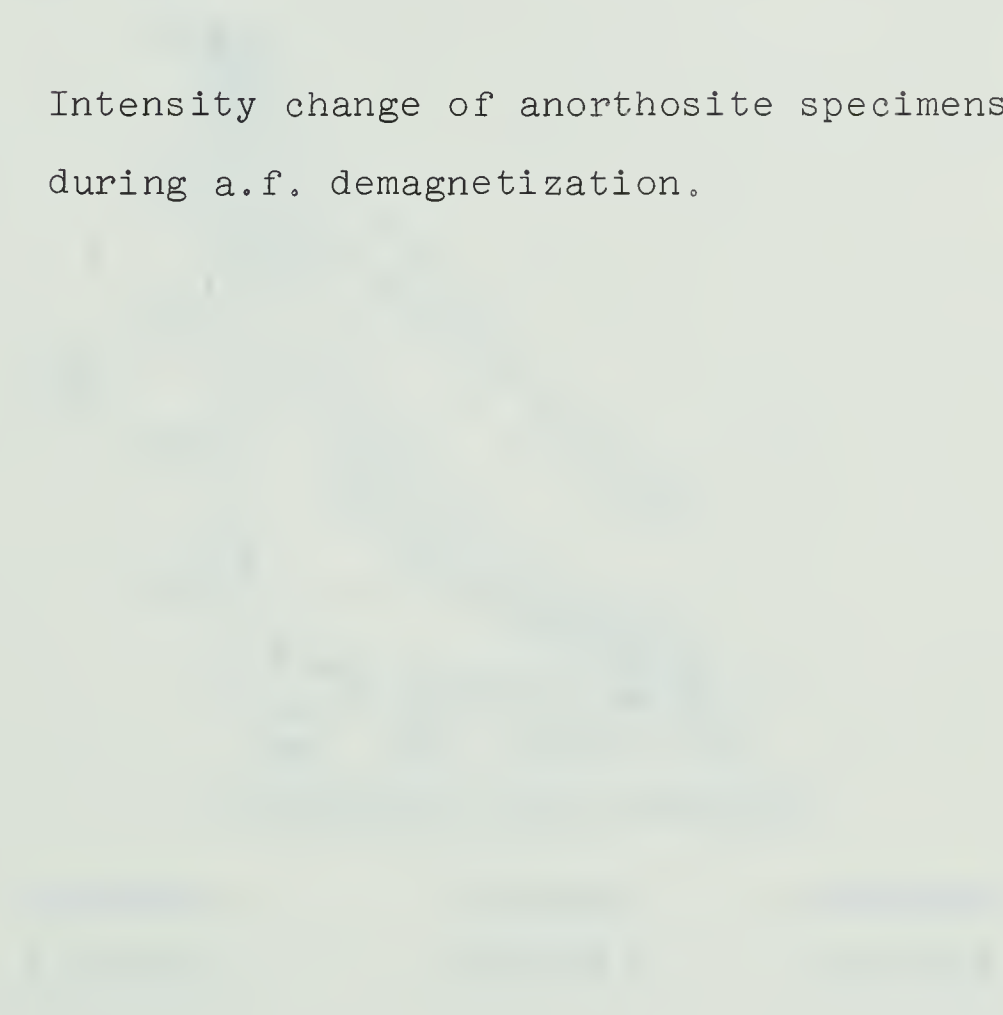
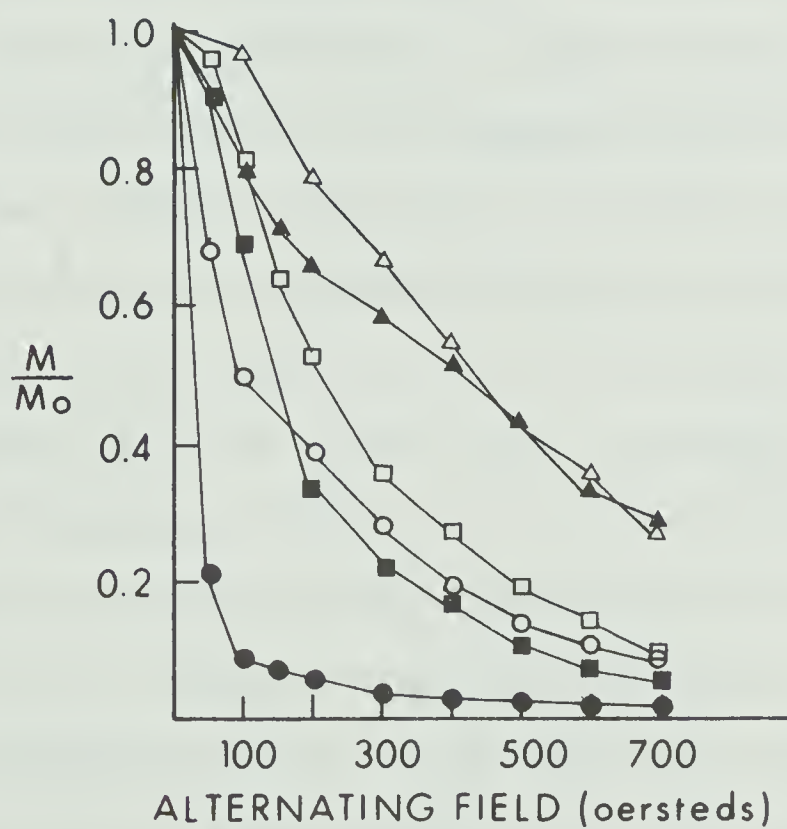
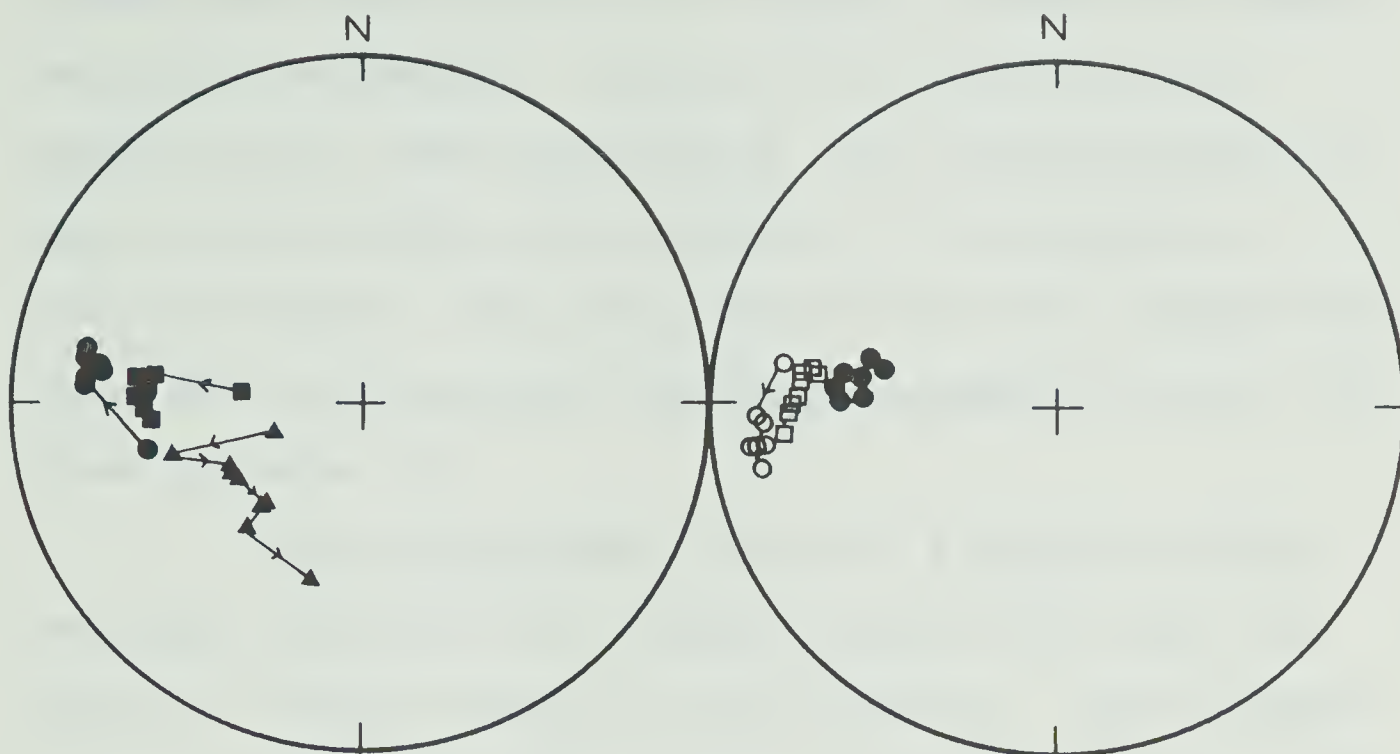


Figure 3.7 Intensity change of anorthosite specimens during a.f. demagnetization.



\blacktriangle AN012A

\triangle AN061A

\square AN053A

\blacksquare AN042A

\bullet AN034B

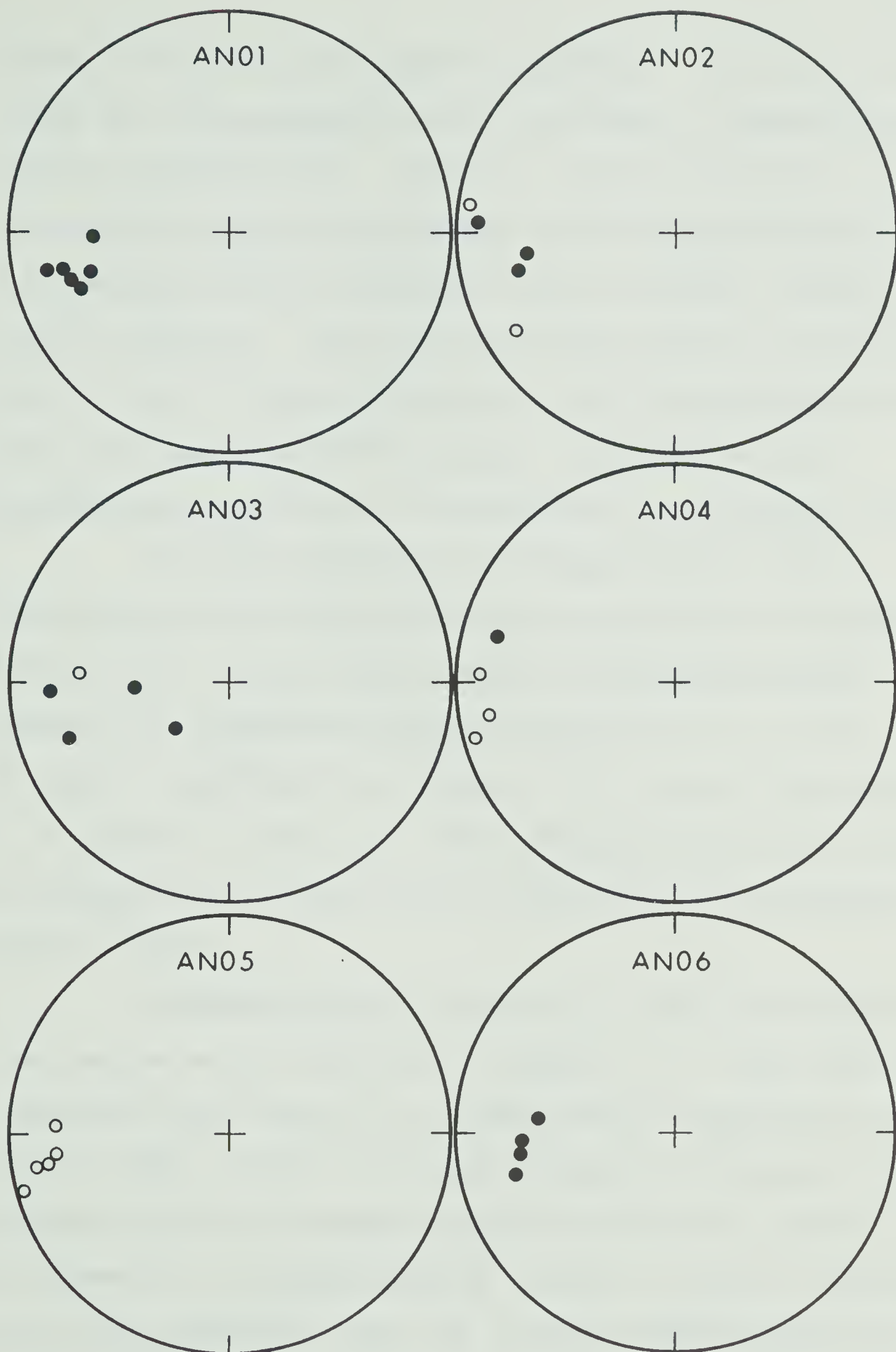
\circ AN023B

chosen from the results of the initial progressive demagnetization procedures. Details of the directions of magnetization, after alternating field demagnetization at each of these sites, are presented in the appendix in Tables A4 and A5. Site mean directions after demagnetization, and the associated virtual paleomagnetic poles, are given in Table 3.2.

One test specimen from site 4 showed a stable end-point from 50 to 700 oersteds whereas the other was stable in fields from 200 to 500 oersteds. The specimens from this site were demagnetized in fields of 200 and 300 oersteds. The mean direction of magnetization of the samples from this site, after demagnetization in these fields, showed little change from the NRM direction. However, the value of k decreased from its NRM value of 37.4 to 25.6 in 200 oersteds and 20.4 in 300 oersteds. These decreases are not significant according to the test devised by McElhinny (1964) and as satisfactory 'end points' were obtained during demagnetization of the test specimens, it is believed that the direction of magnetization after demagnetization in 200 oersteds represents the stable direction of magnetization for this site.

The 'end points' of the directions of magnetization of pilot specimens from site 3 were not as stable as those of the specimens from other sites. The remaining specimens from this site were therefore demagnetized in

Figure 3.5 Sample magnetization directions of Michikamau anorthosites: after optimum demagnetization.



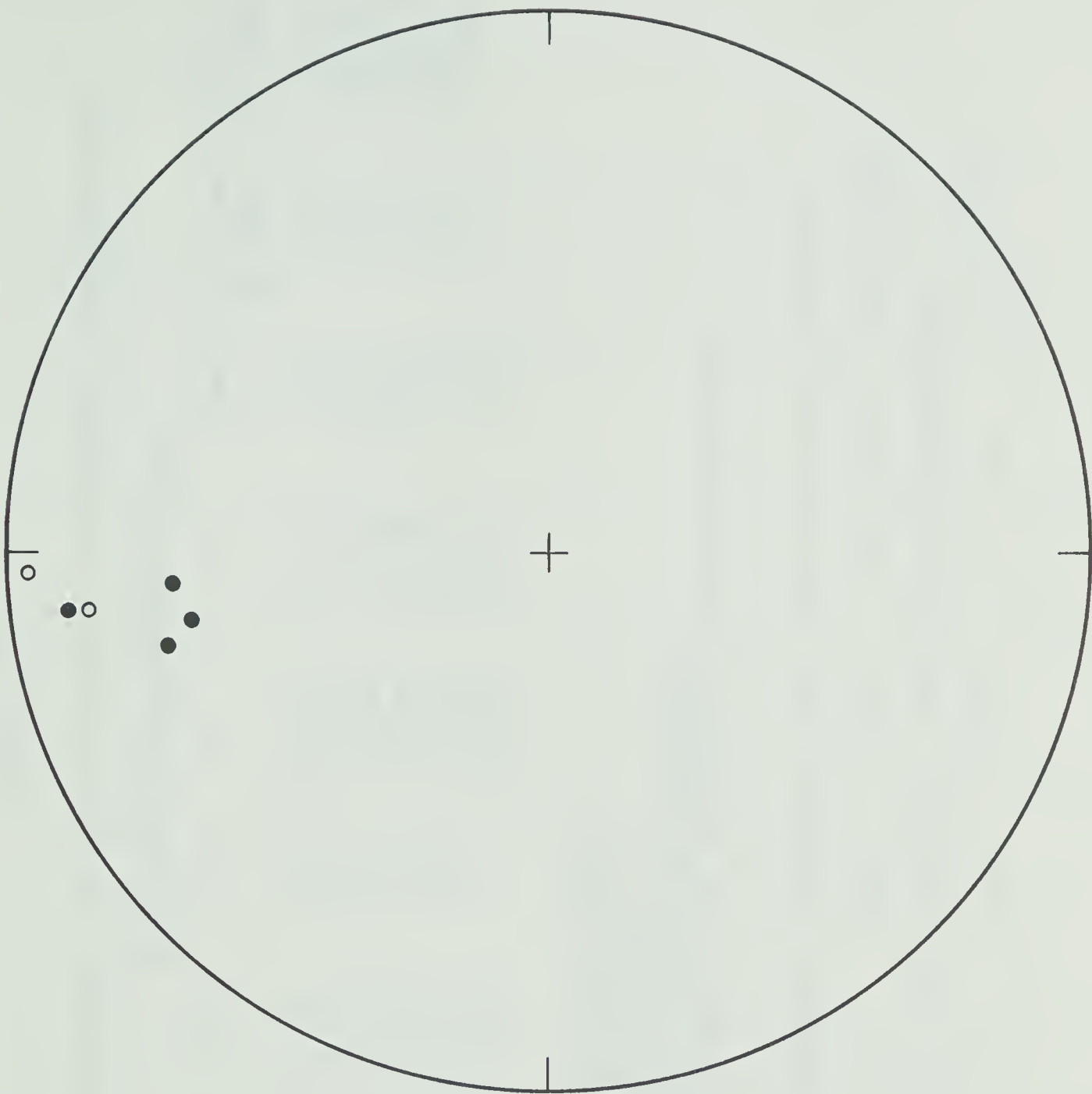
● POSITIVE INCLINATION
○ NEGATIVE INCLINATION

fields of 100, 200, 300 and 400 oersteds. In none of these fields was the grouping of the directions of magnetization improved significantly. However, the mean direction of the samples changed considerably after demagnetization in 100 oersteds and then remained fairly constant between 100 and 700 oersteds. The mean directions quoted in Tables A5 and 3.2 for this site correspond to the demagnetizing field within the range 100-400 oersteds for which the best grouping was observed, as evidenced by the magnitude of k .

The mean directions of magnetization after alternating field demagnetization are plotted in Figures 3.5 and 3.6. At all sites, except 4, demagnetization improved the agreement between observations at a site. This is seen by comparing the lengths of the vector resultants, R , in Tables 3.1 and 3.2. After demagnetization the vectors are grouped well, away from the direction of the present earth's field.

Demagnetization curves for at least one specimen from each site are presented in Figure 3.7. They show an exponential fall typical of thermoremanent magnetization (Nagata 1961). From the stable end-points obtained during alternating field demagnetization and from the typical fall of intensity in demagnetization curves, it may be concluded with high probability that the observed magnetization is thermoremanent in origin and represents the direction of the geomagnetic field at the time of formation of the

Figure 3.6 Mean site directions of anorthosites: after optimum demagnetization.



● POSITIVE INCLINATIONS
○ NEGATIVE INCLINATIONS

TABLE 3.2

SITE MEAN DIRECTIONS AND POLE POSITIONS OF MICHIKAMAU ANORTHOSITES

AFTER OPTIMUM DEMAGNETIZATION

Site	N	Azimuth	Incl.	B	R	k	Alpha	Latitude of Pole	Longitude of Pole
AN01	6	256.18	18.65	300	5.9451	91.10	5.99	-0.09	-136.84
AN02	5	262.68	6.41	300	4.7391	15.33	15.99	-1.58	-145.97
AN03	5	259.29	22.53	300	4.3044	5.75	26.11	3.45	-138.65
AN04	4	267.51	- 2.43	200	3.8826	25.56	13.85	-2.44	-152.78
AN05	5	262.44	- 8.89	300	4.9578	94.74	6.43	-8.03	-150.70
AN06	4	264.90	20.83	300	3.9684	95.03	7.18	5.77	-143.47
Mean	6	262.20	9.60		5.8578	34.9	9.67		

N = NUMBER OF CORES FROM EACH SITE
B = OPTIMUM FIELD OF DEMAGNETIZATION
R = RESULTANT OF N UNIT VECTORS
k = ESTIMATE OF FISHER'S PRECISION PARAMETER
ALPHA = SEMIANGLE OF CONE OF 95% CONFIDENCE FOR MEAN DIRECTION

Mean pole position calculated from formation mean direction

Lat. = -0.60 Long. = -145.55 $\delta p = 4.87$ $\delta m = 9.75$

Mean pole position calculated from site pole positions

Lat. = -0.50 Long. = -144.75 k = 102.7 $A_{95} = 5.64$

Michikamau intrusion.

3.5 Analysis of Data

The site mean directions listed in Table 3.2 have been combined to obtain a mean direction for the Michikamau intrusion. Fisher's analysis was applied to the site means and the parameters of the formation mean direction obtained were

$N = 6$ sites, $D = 262.2^\circ$, $I = 9.6^\circ$, $k = 34.9$, and $\alpha_{95} = 9.7^\circ$.

This direction can be used to calculate the virtual paleomagnetic pole position on the assumption that the magnetizing field was that of an axial geocentric dipole. The calculation places the paleomagnetic pole for the Michikamau intrusion at 0.6°S latitude and 145.6°W longitude with $\delta p = 4.9^\circ$ and $\delta m = 9.8^\circ$. Alternatively the paleomagnetic pole position can be obtained by combining the pole positions calculated from individual site mean directions. Irving (1964) discusses the relative merits of these two methods of calculation. The results of the two calculations, which are listed in Table 3.2 agree essentially with each other.

The precise meaning of the estimates of the mean direction and pole position, and their dispersions, depends on the degree of approximation of the directions used for the analysis to Fisher's distribution. To test this, the statistic χ^2 may be used with a large enough sample.

However, it would be misleading to test the data of the Michikamau intrusion for approximation to Fisher's distribution, as the number of sites is too small to permit such a test.

Graham's fold test may be applied to igneous laminations in the anorthosite to check whether these rocks acquired their magnetization in their present attitudes. If, on rotating the laminations to the horizontal, the value of Fisher's k were to increase significantly from its value before the rotation, it would be reasonable to conclude that the rock had been deformed after it had acquired its remanent magnetization. Stability of the NRM since the time of deformation would also be indicated. If, on the other hand, there were a significant decrease in k after rotation of the laminations to the horizontal, it would be safe to conclude that the rocks had acquired the magnetization in their present attitudes. McElhinny (1964) has devised a statistical test which gives an estimate of the significance of a given increase or decrease in k for a particular value of N . This particular test is applied to the data of the Michikamau anorthosites by correcting them for the appropriate dip of the igneous lamination. The correction makes the lamination horizontal by rotating the rock about the strike direction. The results are shown in Table 3.3. The mean direction for the intrusion changes to $D=268.9^\circ$ and $I=-4.7^\circ$, and k decreases from 34.9 to 7.8. This change in k is significant at the

TABLE 3.3A

APPLICATION OF FOLD TEST TO THE DATA OF ANORTHOSITES

Site	Igneous Layering		Site Mean Directions			
			Before*		After*	
	Strike	Dip	Azim	Incl	Azim	Incl
AN01	34	35 NW	256.0	18.5	258.0	38.7
AN02	126	20 NE	262.5	6.5	266.1	19.9
AN03	86	30 SE	259.5	22.5	248.9	16.2
AN04	138	25 NE	267.5	- 2.5	269.5	16.4
AN05	132	67 NE	262.5	- 9.0	277.8	38.8
AN06	130	27 SW	265.0	21.0	261.3	1.1

TABLE 3.3B

ANORTHOSITE FORMATION MEAN DIRECTIONS

	Azim	Incl	k	Alpha
NRM not corrected for tilt	265.2	25.7	7.1	21.5
NRM corrected for tilt	265.2	9.0	3.8	29.4
After demagnetization not corrected for tilt	262.2	9.6	34.9	9.7
After demagnetization corrected for tilt	268.9	- 4.7	7.8	20.5

* DIRECTIONS BEFORE AND AFTER CORRECTING FOR THE TILT OF
IGNEOUS LAYERING

95% confidence limit, and supports the conclusion that the observed magnetization was acquired with the rocks in their present attitudes.

The angular dispersion $\Delta = 81/\sqrt{k}$ with $k=34.9$ is 13.7° . The use of an F test in the manner outlined by Gough et al. (1964) provides an upper limit for the value of Δ of 23.6° at the 95% confidence level. This is greater than that calculated by Creer (1962) for the present earth's field at low latitudes (approximately 18°). It is possible therefore that the sampling of the Michikamau intrusion has been sufficiently detailed that the paleosecular variation is fully represented in the measurements, but the point cannot be proved one way or the other.

3.6 Comparison with Paleomagnetic Results from Rocks of Similar Age in North America

It is of interest to compare the pole position obtained for the Michikamau intrusion with pole positions determined for Precambrian rock units of North America of similar age. The pole positions are listed in Table 3.4 and plotted in Figure 3.8.

The pole position for the Michikamau intrusion differs greatly from that calculated by Hargraves and Burt (1967) for the Allard Lake anorthosites and also from that given by Fahrig et al. (1965) for the Molson dikes. However, the time of magnetization of the former rocks is uncertain

TABLE 3.4

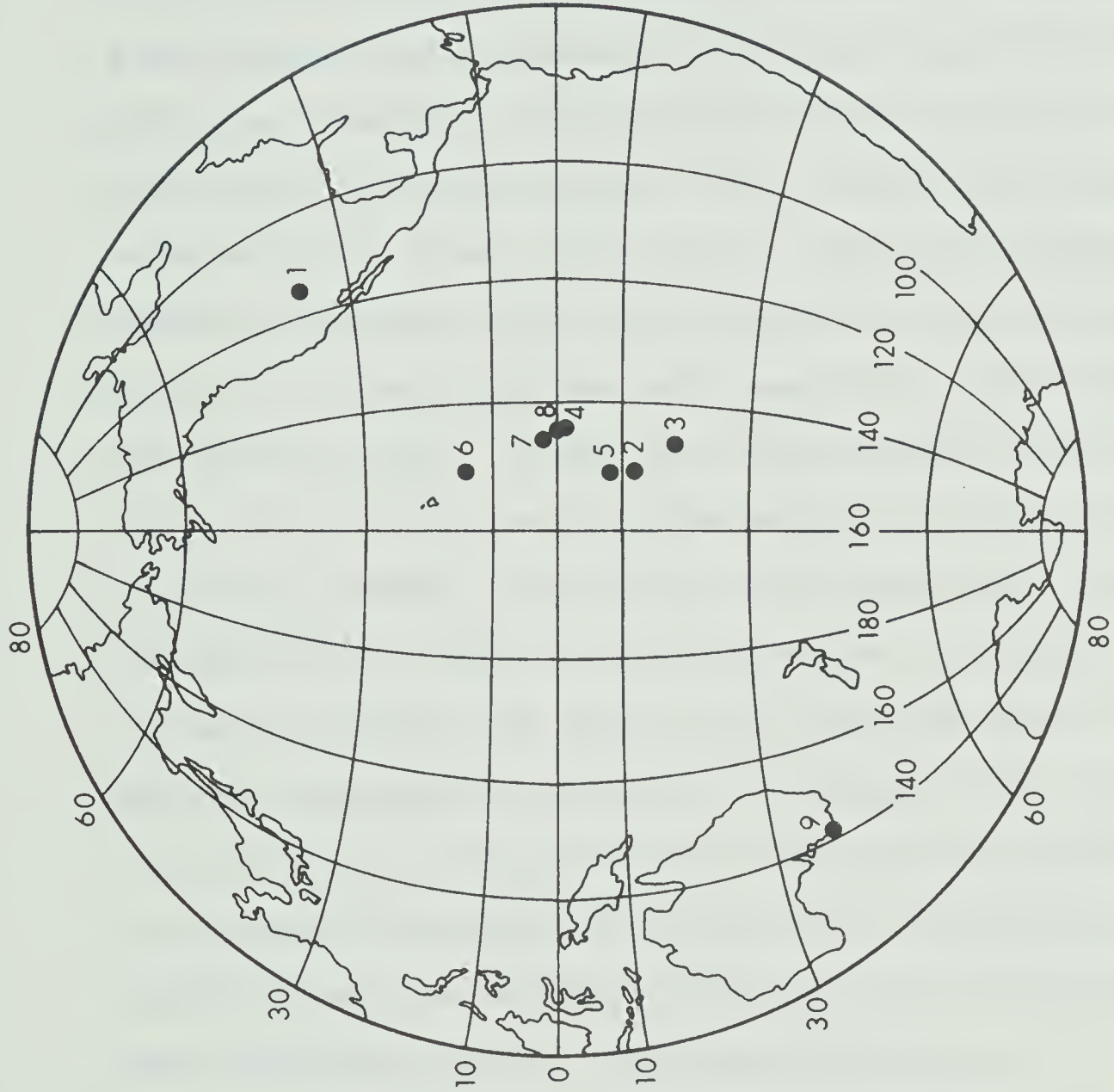
POLE POSITIONS FOR 1400 M.Y. AGE FROM NORTH AMERICAN ROCK UNITS

Rock Unit	Age (M.Y.)	Lat.	Long.	References
Molson Dikes	1445	36.2 N	108.9 W	Fahrig et al. (1965)
Belt Series, Grand Canyon Series and Purcell System	>1100<1600	12.0 S	151.0 W	Irving (1964)
Purcell System, B. C.	>1100<1600	18.0 S	147.0 W	Irving (1964)
St. Francois mountains, Missouri	1300-1550	1.0 S	144.0 W	Hays and Scharon (1966)
Front Range, Colorado-Wyoming	1410±30	8.0 S	151.0 W	Eggler and Larson (1968)
Arbuckle mountains, Oklahoma	1320-1400	17.0 N	150.0 W	Spall (1968)
Croker Island Complex, Ontario	1475±50	5.5 N	143.0 W	Palmer (1969)
Michikamau anorthosite	1400±80	0.5 S	144.7 W	present work

and according to Hargraves and Burt may well lie during the Grenville orogeny. The age reported by Fahrig et al. (1965) for the time of intrusion of the Molson dikes (1445 m.y.) is similar to that of the Michikamau intrusion. However, it is based on a single whole rock potassium-argon age determination on a sample of low potassium content and therefore the age equivalence of these dikes and the Michikamau intrusion cannot be considered established. In addition, the paleomagnetic result from the Molson dikes is based on a very small number of samples.

Irving (1964) calculated a combined pole position for the Belt series of Montana and the Grand Canyon series of Arizona (Collinson and Runcorn 1960) and the Purcell system of British Columbia (Norris and Black 1961), and also a mean pole position for the Purcell System from additional results by Black (1963). These both lie very close to the pole position determined from the Michikamau rocks. In addition Runcorn (1964) has reported further paleomagnetic results from rocks from the Belt series and other Precambrian formations from western United States. The pole positions deduced from the various formations studied by Runcorn (1964) (not recorded in Tables 3.4 and Figure 3.8) again lie in the same general region as the Michikamau pole position. The exact ages of the rocks from western Canada and western United States are however

Figure 3.8 Paleomagnetic poles derived from North American rocks for 1400 million years.



INDEX

- 1 MOLSON DIKES
- 2 BELT SERIES, GRAND CANYON SERIES.
- 3 PURCELL SYSTEM
- 4 ST. FRANCOIS MTNS.
- 5 FRONT RANGE
- 6 ARBUCKLE MTNS.
- 7 CROKER ISLAND
- 8 MICHIKAMAU
- 9 ALLARD LAKE

PRECAMBRIAN POLE POSITIONS FOR N. AMERICA

uncertain, but may lie within the limits 1100 m.y. (Runcorn 1964) to 1600 m.y. (Giletti 1966).

Hays and Scharon (1966) have reported measurements on some Precambrian igneous rocks from the St. Francois Mountains of southeast Missouri. A mean pole position has been calculated from their published data giving unit weight to each of the five rock units from which they obtained results. This calculation provides a pole position almost identical to that of Michikamau rocks. However, the rock units from which they took specimens are subject to uncertainties with regard to their absolute and relative ages. These rock units bracket granite, which did not give useful paleomagnetic results, but whose age probably lies within the range 1300 to 1550 m.y. (Tilton et al. 1962). The differences in times of intrusion between the granite and the rock units that yielded paleomagnetic results is unknown. The combination of directions of magnetization from the rock units of the St. Francois Mountains is, therefore, of uncertain validity, and the striking similarity of the pole positions from Michikamau and St. Francois Mountains is of debatable significance.

Eggler and Larson (1968) have given a paleomagnetic pole position for some igneous Precambrian rocks from the Front Range of Colorado-Wyoming, whose age has

been precisely determined by the rubidium-strontium isochron method as 1410 ± 30 m.y.. The similarity in ages of the Front Range formations and the Michikamau intrusion is paralleled by the similarity in their respective pole positions. Palmer (1969) has calculated a paleomagnetic pole position for the Croker Island Complex of Ontario whose age is estimated by the rubidium-strontium isochron method as 1475 ± 50 m.y. and the location of the paleomagnetic pole is within a few degrees of the Michikamau pole. Spall (1968) computed a paleomagnetic pole position for the basement rocks from the Arbuckle Mountains of Oklahoma which are dated at 1320 ± 1400 m.y. by the lead-lead ages of zircon. The pole position lies at 17°N , 150°W which is in the same general region as that of Michikamau intrusion. The same formation was studied by Ku et al. (1966) who obtained a similar result. Thus, although the magnetizations of some of the formations may span a considerable time and the calculation of a combined pole position may be of doubtful validity, it is a significant fact that the pole positions for 1400 m.y. agree remarkably well.

The following conclusions may be made from the similarity of pole positions listed in Table 3.4:-

1. The paleomagnetic pole position relative to North America for the age of 1400 m.y. is well established to be on the present day equator at 145° W.

2. The agreement of the poles from widely different regions in North America indicates that the field was sensibly dipolar 1400 m.y. ago.
3. The correspondence in paleomagnetic pole positions and the ages of the formations from different regions of North America suggests that there have been no major movements between the sampled regions, separated by several thousand kilometers, since the rocks were formed.
4. The Michikamau anorthosites give useful paleomagnetic results which may be utilized in the study of global tectonics. The importance of paleomagnetic results from massive anorthosite bodies is further discussed in Chapter 9.

3.7 Summary

A paleomagnetic study has been made of the Michikamau anorthositic intrusion in northern Labrador. This formation had been previously dated at 1400 m.y. by the potassium-argon method. Twenty-nine oriented cores were collected from six sites. The stability of magnetization has been well tested and it is concluded that the observed magnetization is thermoremanent and represents the direction of the earth's field at the intrusion at the time of its formation. A fold test was applied to the remanent magnetizations after partial demagnetization in alternating fields. The results

suggest that the magnetization was acquired with the rocks in their present attitudes. The paleomagnetic pole position for the intrusion lies at 0.5°S , 144.7°W with $A_{95}=5.6^{\circ}$. A comparison is made of this result with results from rocks of similar age in North America. The agreement between the pole positions suggests that there have been no large relative movements between this region and the other sampling sites for the last 1400 m.y., and that the geomagnetic field at that time approximated that of a geocentric dipole.

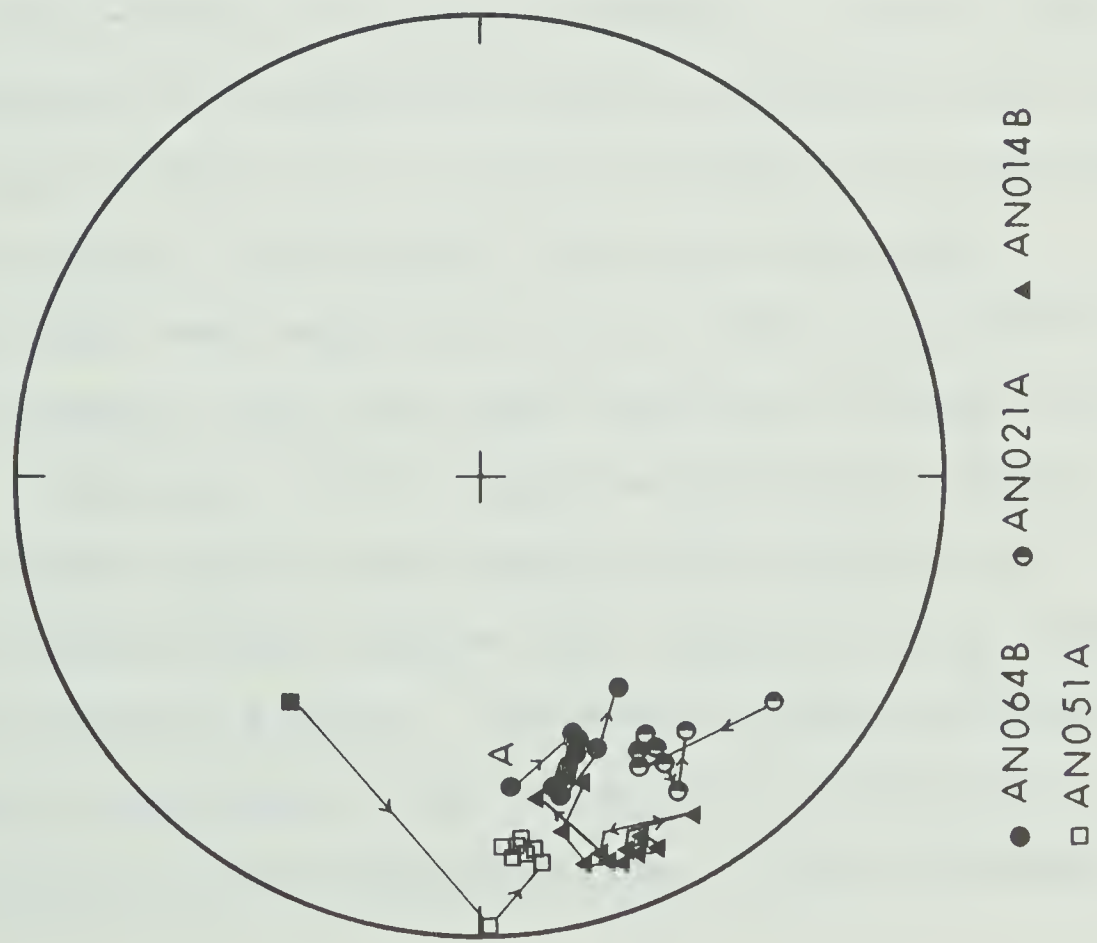
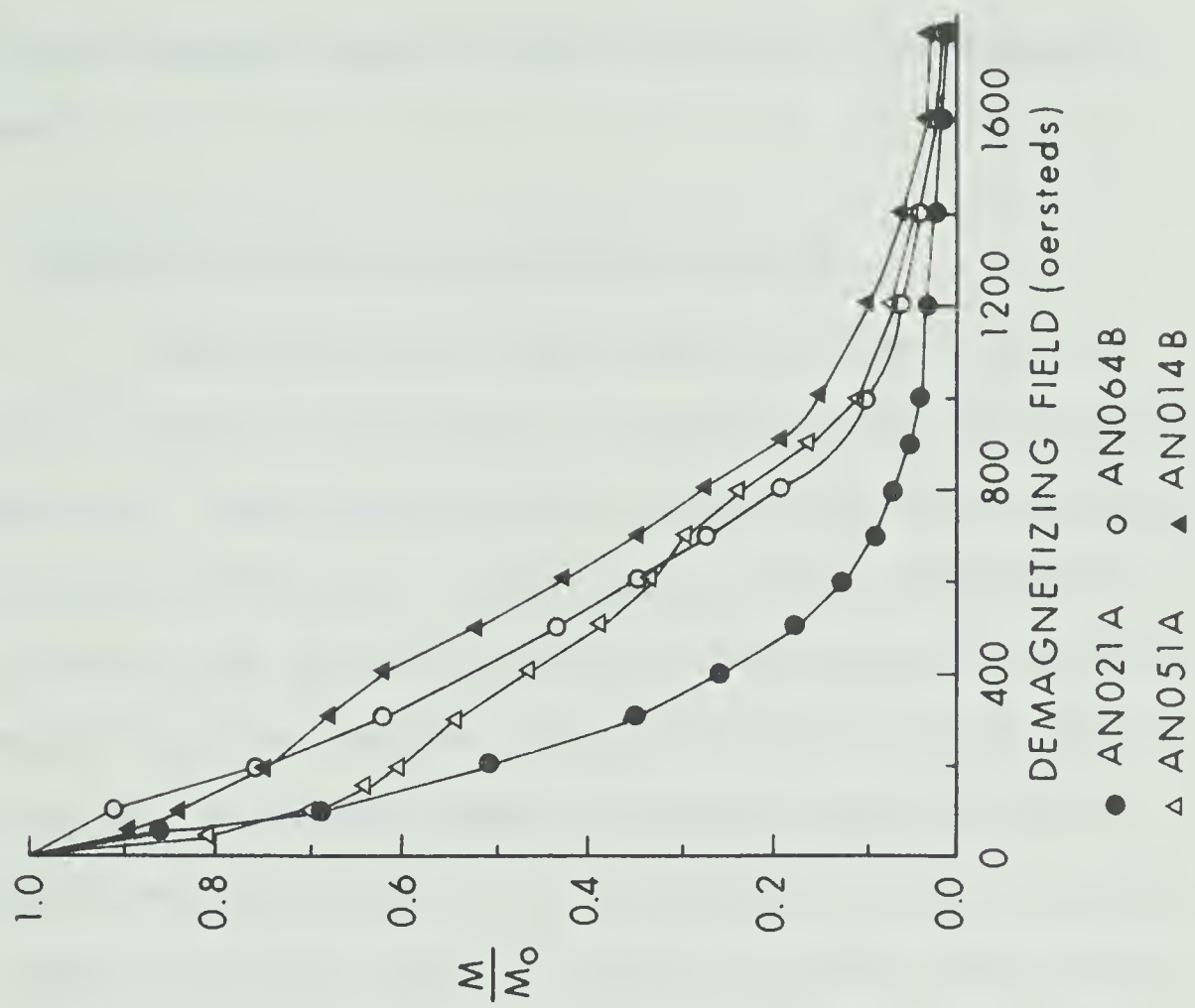
CHAPTER 4

STABILITY OF MAGNETIZATION OF MICHIKAMAU ANORTHOSITES4.1 High Magnetic Stability Exhibited by Michikamau Anorthosites

It was pointed out in Chapter 3 that the anorthosites exhibited extreme resistance to alternating field demagnetization. It would be of interest to find the field at which the magnetization of the specimens vanishes. Hence a systematic demagnetization was conducted of at least one specimen from each site to the highest fields that could be attained with our apparatus. The results are presented in Table B1 of Appendix B and in Figures 4.1 and 4.2. After an initial movement away from the direction of the present earth's field, the directions of magnetization remained unchanged even at 1800 oersteds. This may also be observed from Table B1 where values of 'Psi', which is the angular change in magnetization from the previous demagnetizing step, are tabulated. An exponential drop in intensities is indicated in Figure 4.2. The excellent grouping in directions and the gradational drop in intensity may be explained by postulating the presence of a wide range of coercivities (Graham 1953). According to Stacey (1963), such a broad spectrum of coercivities is possible if there is a large range in

Figure 4.2 Intensity change of anorthosite specimens
during a.f. demagnetization.

Figure 4.1 Directional change of anorthosite specimens
during a.f. demagnetization.



grain and domain sizes of the contained ferromagnetic mineral.

4.2 Magnetic Stability of Igneous Rocks

Explanation of high magnetic stability in igneous rocks has long been a puzzling problem in rock magnetism. High coercivities are usually attributed to the mineral hematite. For igneous rocks, hematite is very rarely the mineral in which the primary component of magnetization resides. The difficulty arises from predictions of theory based on energy considerations. Whereas hematite grains will be single-domained through the range of sizes commonly found in rocks, the theory predicts that roughly spherical magnetite grains will be either multi-domain or superparamagnetic. Stacey (1963) has estimated that spherical hematite grains are expected to be single domain up to 1 mm in size while for spherical magnetite grains the critical size is 0.03 microns. Attempts have been made from time to time to explain why certain igneous rocks have high stability of magnetization.

Verhoogen (1959) suggested that small regions within magnetic grains were magnetically isolated and acted as single domain grains, the isolation being caused by local internal strains. Verhoogen's theory requires stresses of the order of 10^{10} dyne/cm² to account for coercivities of 1500 oersteds or more. It is extremely

unlikely that such large internal stresses can occur in massive anorthosites which cool very slowly and hence are relatively free of internal stresses. This model has been criticized by Dickson et al. (1966) as a physical impossibility because of formation of the closed circuits. According to Uyeda (1962), this model cannot account for stability in fields greater than about 750 oersteds. Examples are numerous in literature where the volcanic rocks have coercive forces of 1000 oersteds or more. Strangway (1961) proposed that powder-like opaque minerals present in silicate grains might be the source of stable magnetism. Carmichael (1961) pointed out that elongated small hematite grains present in an ilmenite-hematite solid solution have high stability of magnetization. Stacey (1963) introduced a model based on pseudo-single-domain behaviour of particles just large enough to contain four domains. High stability of magnetization is explained in this case by Barkhausen discreteness. The domain walls thus have preferred locations in the samples leaving a residual magnetic moment associated with the grain. However Strangway et al. (1968) have pointed out that in Stacey's model the pinning of walls depends upon imperfections or impurities and the resulting TRM should be sensitive to annealing; which should result in a reduced and less stable magnetization after prolonged heating.

However extended heating experiments of unoxidized volcanic rocks tend to produce high TRM and high stability. Evans and McElhinny (1966) have suggested that the high stability of the Modipe gabbro can be explained as due to elongated magnetite particles contained therein. Strangway et al. (1968) proposed a model in which high temperature oxidation produces ilmenite lamellas in the titanomagnetite grains. These lamellas effectively subdivide the large grains into single domain grains that are much larger than the superparamagnetic critical size calculated by Néel theory. The effectiveness of lamella development in increasing magnetic stability was partly anticipated by Powell (1963) and was discussed earlier by Graham (1953).

Thus it is essential to identify the type, shape and amount of the ferromagnetic mineral or minerals in the anorthosites to explain their very high magnetic stability.

4.3 Polished Section Studies of Michikamau Anorthosites

There are various methods by which the primary magnetic mineral of a rock may be identified. Nicholls (1955), Nagata (1967) and others have enumerated methods, based on their magnetic properties, by which these minerals can be identified. However, as paleomagnetic research at the University of Alberta is in the development stage, laboratory facilities are rather limited and

not all methods mentioned by Nagata (1967) can be used to differentiate between the various magnetic minerals.

Study of polished sections under the ore microscope has long been recognized as a useful tool in identifying ore minerals. Ozima and Larson (1967), Watkins (1967) and more recently Larson and Strangway (1969) have used this method successfully to identify various magnetic minerals contained in a rock sample. Towards identification of the primary magnetic mineral contained in Michikamau anorthosites, detailed microscopic study of the anorthosites has been undertaken. Polished sections were initially made out of one sample from each site. A Vicker's microscope with magnification $\times 160$ was used. Estimates were made systematically of Vicker's Hardness Number (VHN) and Reflectivity of the mineral grains. Bowie (1967) has discussed the errors involved in estimating the values of hardness and reflectivity for ore minerals. The method used by the author for estimating reflectivity and hardness is a standard one. A diamond indenter is brought into contact with the mineral surface and a known load is applied. The mean diameter of the impression, which is in the shape of a parallelogram was measured and this value was used in computing the VHN number. The quality of the indentation was noted. The reflectivity estimates were made by comparing the amount of light reflected from the mineral with that from a standard pyrite specimen whose

reflectivity was known as 54.5% under the same conditions. The results of observations are summarized in Table 4.1.

The magnetic mineral occurs essentially in two forms; either as a grain which in section appears as an irregular patch or as fine needles oriented parallel to one another in plagioclase. Both forms are common in all sections with varying abundances. Photomicrographs of the needle shaped grains are presented in Plate 1. Although the needle shaped grains are too small to make exact estimates of VHN number and reflectivities, it may be seen from the values of Table 4.1 that the mineral is magnetite. It is identified from its isotropic character, grey color, VHN values between 500 and 600 and a reflectivity of about 21%. Ilmenite occurs either as lamellas or as intergrowths associated with magnetite. Ilmenite is identified mainly by its optical anisotropy, light brown color and slightly lower values for reflectivity and VHN number. Hematite was very rarely observed. Cameron (1961), Bowie (1967) Battey (1967) and others have listed the values of VHN number and reflectivity for hematite as 1100 and 28 respectively.

The typical size of a needle shaped grain is of the order of 10×0.5 microns while those of irregular shape vary between 70×65 and 140×110 microns. Certain parts of the section contain needle shaped grains with a length to width ratio of twenty-five or more. As may be seen from

TABLE 4.1

SUMMARY OF OBSERVATIONS ON POLISHED SECTIONS
OF MICHIKAMAU ANORTHOSITES

Grain Description	Size (μ)	VHN	Ref1.	Type
Sample No. AN011				
Patch shaped grains more abundant than grains in the shape of needles				
A patch shaped grain in which intergrowth lamellas are observed	112×96	599	20.2	Magnetite with ilmenite lamellas
A patch shaped grain	91×62	570	26.0	Magnetite
A grain with lamellas developed inside	146×101	548	17.4	Magnetite
A rod shaped grain*#	15×0.5	576	19.4	
A rod shaped grain*#	20×01	58	20.2	Magnetite
Sample No. AN024				
Rod shaped grains more abundant than the patch shaped ones				
Patch shaped grain#	102×68	498	20.0	Magnetite
A rod shaped grain*	12×0.5	585	25.5	Magnetite
A rod shaped grain*	18×0.5	632	24.6	Magnetite
Patch shaped grain#	94×86	565	19.6	Magnetite
Sample No. AN032				
A rod shaped grain*	41×02	655	25.0	Magnetite

TABLE 4.1 (CONTD)

Grain Description	Size	VHN	Refl.	Type
Isotropic patch shaped grain#	147×83	586	20.8	Magnetite
Isotropic patch shaped grain#	94×86	615	23.2	Magnetite
A rod shaped grain*	28×01	718	20.5	Magnetite
A plate shaped grain	22×02	458	21.2	Magnetite
Isotropic grain#	215×102	624	26.2	Magnetite

Sample No. AN044

Elongated rod shaped grains more abundant than grains in the form of patches. The typical size of a rod is 20×1.0 micr. rather difficult to get reflectivity and hardness estimates on rod shaped grains

Patch shaped isotropic grain	47×65	509	27.0	Magnetite
	69×28	439	34.2	
	96×72	429	32.8	
A rod shaped grain	20×02	657	19.5	Magnetite
A rod shaped grain	17×01	612	19.0	Magnetite
A rod shaped grain	22×1.5	598	18.5	Magnetite
A rod shaped grain	26×01	571	20.2	Magnetite
A patch shaped grain with an anisotropic part in the middle	78×66	602	20.8	Magnetite
	29×32	565	17.6	Ilmenite

TABLE 4.1 (CONTD)

Grain Description	Size	VHN	Refl.	Type
Sample No. AN053				
Rod shaped grains more abundant than patch shaped grains which are slightly anisotropic				
Isotropic patch shaped grain#	91×63	455	19.4	Magnetite
Isotropic grain	76×51	581	20.0	Magnetite
A rod shaped grain*#	29×02	580	22.8	Magnetite
Sample No. AN061				
A grain in the form of a needle*	27×01	680	23.2	Magnetite
A patch of grain partly anisotropic#	124×86	627	18.2	
An elongated needle shaped grain*#	34×01	594	19.2	Magnetite
A rod shaped grain*	38×02	572	20.8	Magnetite
A rod shaped grain*	26×01	605	21.6	Magnetite
Patch shaped grain#	104×67	597	19.8	Magnetite
A grain in the shape of a needle*#	15×0.5	570	18.6	Magnetite

* A SWARM OF SIMILAR GRAINS ARE OBSERVED

VHN AND REFL. ESTIMATES ARE THE MEAN OF 10 OBSERVATIONS

PLATE 1: PHOTOMICROGRAPHS OF POLISHED SECTIONS OF
ANORTHOSITES SHOWING ELONGATED MAGNETITE
GRAINS IN PLAGIOCLASE



Plate 1, the needle shaped grains occur in swarms and are perfectly oriented. An attempt was made to find a correlation, if any, between the relative abundance of irregular shaped grains over the needle shaped grains and a magnetic stability factor for the site. This attempt was unsuccessful as an exact estimate of the relative amounts of the two types of grains could not be made quantitatively from the polished section.

It was thought possible that the needle shaped grains were in fact sections through plates extended in the third dimension. In order to check this, further polished sections were made from each sample in two perpendicular directions. Mineral grains, both of irregular shape and in the shape of needles, are present in the two orthogonal sections. It was further noticed that by slightly changing the focus of the microscope, different grains may be brought into vision which conclusively proves that the grains are in the form of rods and not plates. It is therefore clear that irregular grains of magnetite, and fine needles of magnetite within plagioclase crystals, are generally distributed in the Michikamau anorthosite, and that one or both types of magnetite grains contribute to the NRM of this rock.

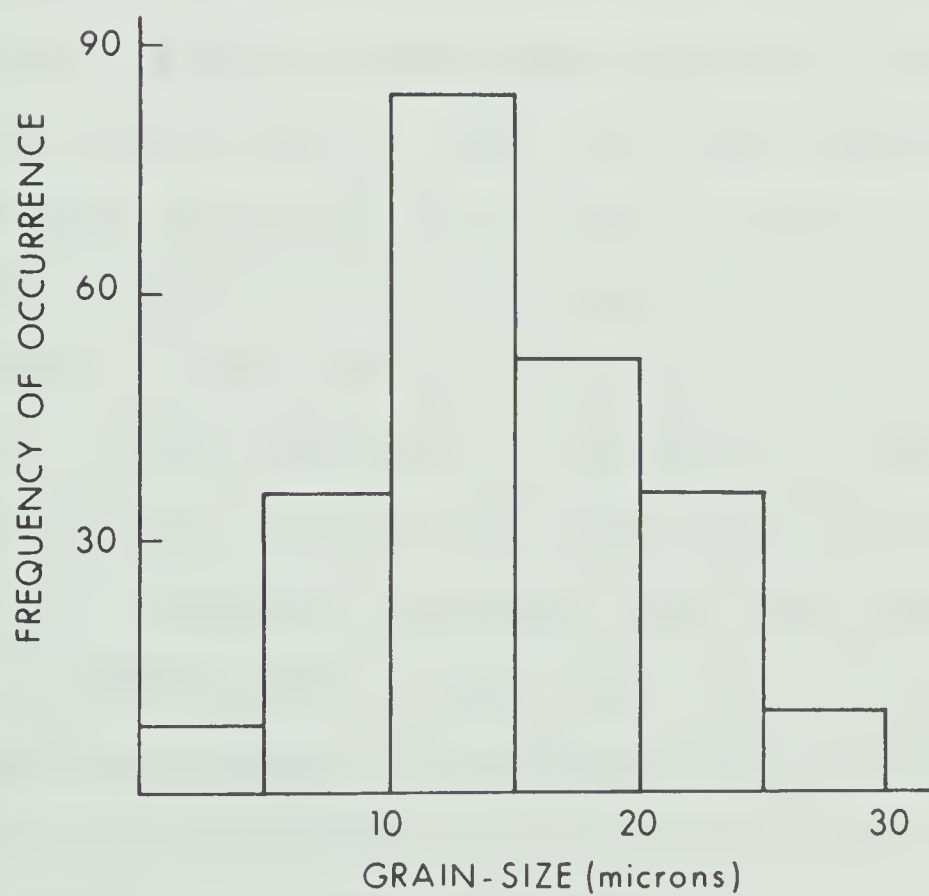
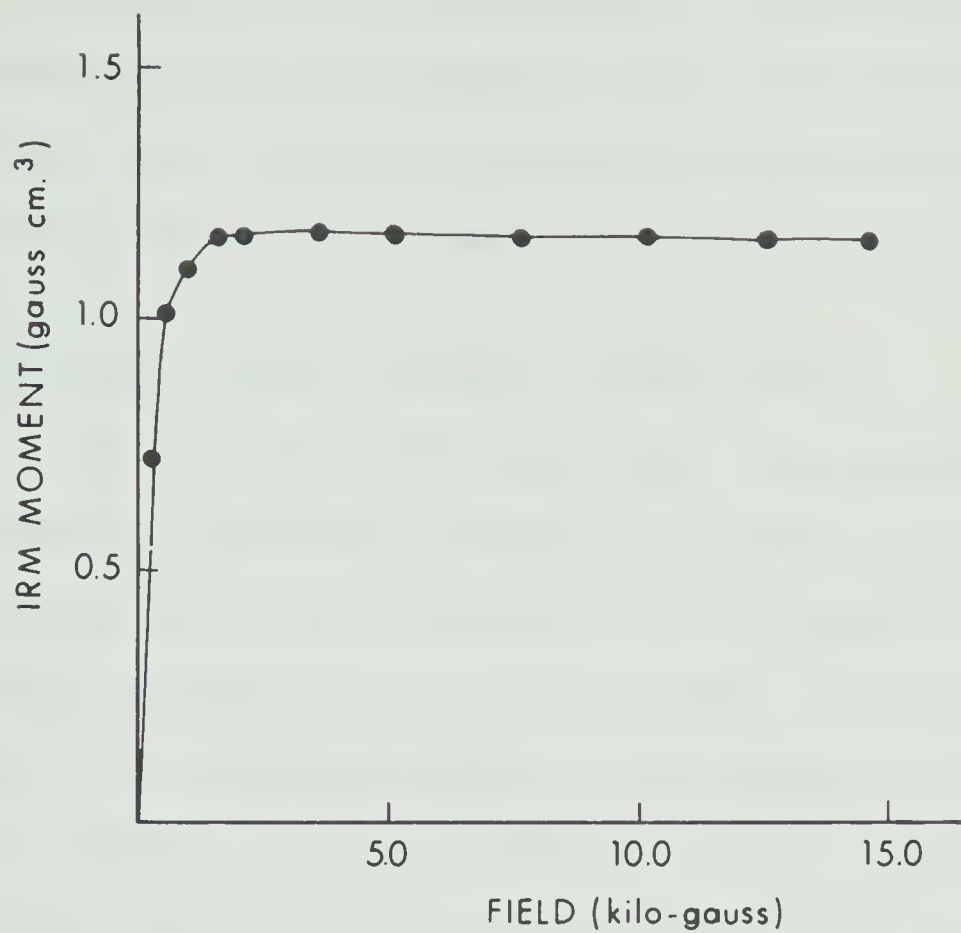
4.4 Studies on Isothermal Remanent Magnetization

Another test that was performed to distinguish the primary magnetic mineral is the study of isothermal remanent magnetization of the samples. Roquet (1954) has studied the IRM of magnetite and hematite of various grain sizes. She reported that magnetite and hematite reach saturation at widely differing magnetic fields; magnetite in a field of 3 kilogauss and hematite in a field of 30 kilogauss. The hematite curve starts to flatten out above 20 kilogauss and the main raise in IRM occurs between 4 and 20 kilogauss. Thus if hematite were present in a substantial quantity, one would see a rise in saturation magnetization between 4 and 20 kilogauss long after magnetite had reached its saturation.

One specimen of Michikamau anorthosite was first demagnetized in a peak field of 1800 oersteds. The specimen was introduced between the poles of an electromagnet and was made to acquire IRM in successively higher fields from 200 gauss to 14.5 kilogauss which was the maximum available field. The IRM intensity was measured after each application of field, care being taken to see that the calibration of the magnetometer remained the same. A plot of the IRM acquired in various fields is shown in Figure 4.3. The specimen was saturated in a field of 3.5 kilogauss and the saturation intensity was main-

Figure 4.3 Saturation IRM of specimen AN041A

Figure 4.4 Histogram of lengths of rod-shaped magnetite grains observed in Michikamau anorthosite.



tained in fields up to 14 kilogauss. Thus the IRM test clearly showed that the mineral being dealt with was magnetite. The results of saturation magnetization studies are tabulated in Table B2 of Appendix B.

4.5 Critical Size of a Single-Domain Grain

It has long been known that the presence of small grains, sufficiently small to contain only a single magnetic domain, accounts for the great stability of remanent magnetization of many rocks. Estimates may be made of the critical size of a particle to behave as a single domain. As the dimensions of the specimen are diminished, the relative contributions of the various energy terms (Chapter 1) to the total energy are changed, and surface energies become more important than volume energies (Kittel 1946). When very small dimensions are reached, there will be a point at which it is favourable energetically to do away with the domain boundaries, so that the whole specimen becomes one domain. If the dimensions of the grain are many times the thickness of a Bloch wall then one should expect the grain to be subdivided by domain walls into more than one domain. Magnetostatic energy could thus be eliminated or made small but domain wall energy would be introduced. However, the wall energy is a function of the thickness of the wall and increases with decreasing thickness.

Hence if the grain size becomes small compared with the normal wall thickness the wall energy may now rise to a comparatively high value, so that walls cannot form in the small grain except by introducing wall energy greater than the magnetostatic energy of the single-domain grain. In these circumstances, the grain remains a single domain with its magnetization in a direction of easy magnetization.

Various estimates have been made of the critical size below which a grain behaves like a single domain (Néel 1947; Stoner and Wohlfarth 1948; Kittel 1946, 1949). By neglecting the magnetocrystalline energy term, the critical radius is given by

$$d = \pi a (N_w / 2N_D)^{\frac{1}{2}} \quad (4.1)$$

where a is the lattice constant, N_w is the Weiss molecular field constant and N_D is the demagnetizing factor in the direction of easy magnetization. For a spherical particle of iron, (4.1) gives $d = 2.9 \times 10^{-2}$ micron. According to the theory of Néel (1955), single-domain spherical grains of magnetite should be no larger than about 0.03 microns. Stacey (1963) has estimated that 0.03 micron is also the critical size for superparamagnetic behaviour of magnetite. Hence according to the latter author, it is unlikely there is a significant range of stable single domains of magnetite.

However it is of more interest to report the estimates of critical sizes for single domain behaviour of particles in the form of prolate spheroids. These estimates were made for magnetic metals by Kittel (1949) and for magnetite and maghemite by Morrish and Yu (1955). The method of Morrish and Yu which closely follows the earlier treatment of Kittel is outlined here. The particle is taken to be in the form of a prolate spheroid with semi-major axis b and semi-minor axis a . This spheroidal particle may be considered to be composed of cylindrical shells which in turn contain a number of rings. Morrish and Yu estimated the exchange energy of the molecules in a ring of radius r and proceeded on to calculate the exchange energy for the prolate spheroid as

$$E_{\text{ex}} = \frac{11}{12} \cdot \frac{I_o^2}{I_{oo}^2} \cdot \frac{4\pi}{9} \cdot \frac{k\theta b}{s} [\log(\frac{2a}{s}) - 1] \quad (4.2)$$

where I_o , I_{oo} are the saturation intensities at room temperature and at absolute zero, k is Boltzmann's constant, θ is the Curie temperature, s is the cell constant of one molecule of magnetite, and a and b are the dimensions of the prolate spheroid. The magnetostatic energy for a saturated single domain configuration of the prolate spheroid is

$$E_{m.s} = \frac{1}{2} I_o^2 D \times \left(\frac{4}{3} \pi a^2 b \right) \quad (4.3)$$

where D is the demagnetizing factor of the particle. The

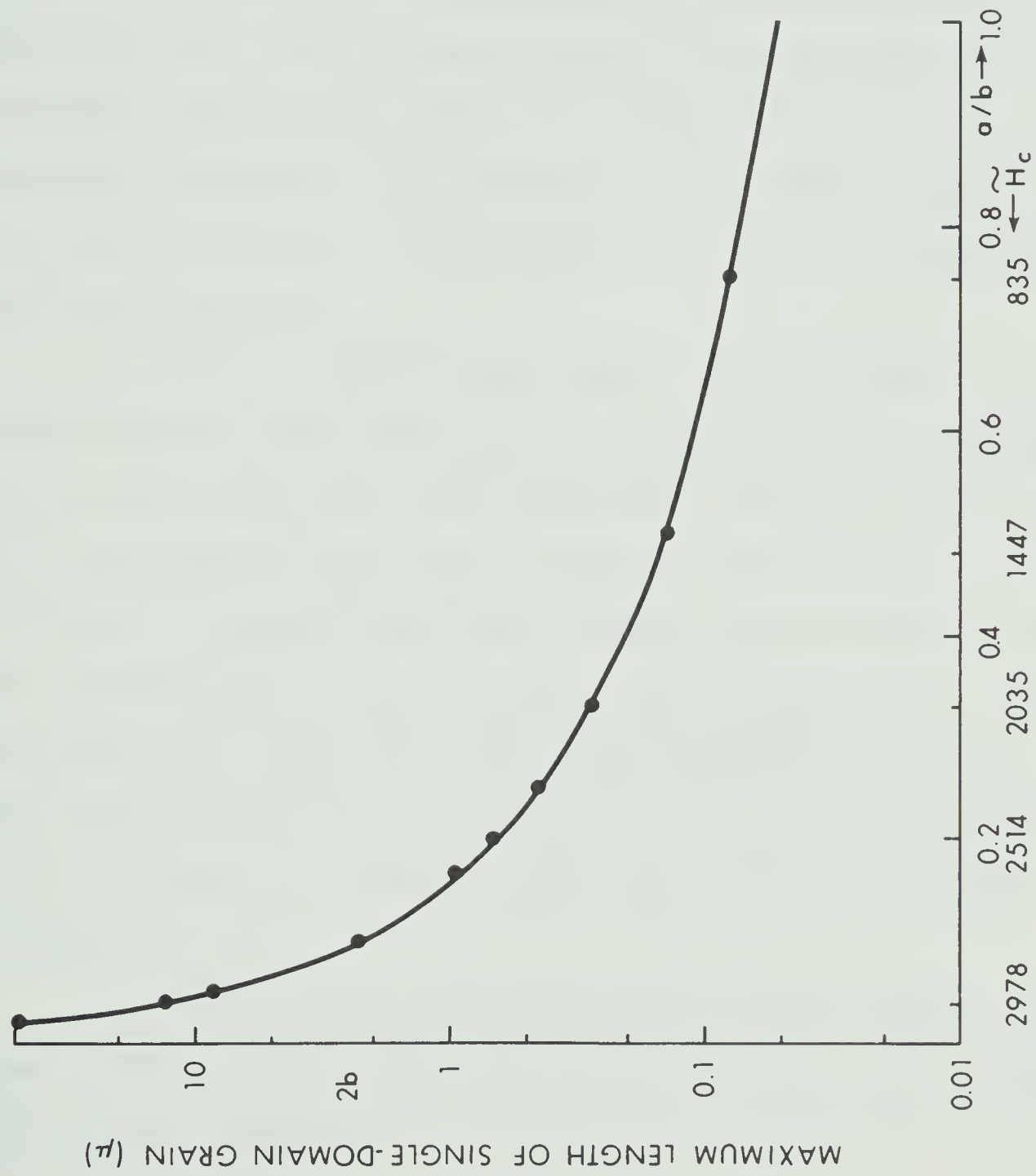
critical size for single domain behaviour is obtained by equating 4.2 and 4.3. The resulting equation (after correcting for a few typographic errors in Morrish and Yu's original) is given by

$$\frac{a^2}{\log(476a10^5)-1} = \frac{6.55 \times 10^{-12}}{D} \quad (4.4)$$

Morrish and Yu plotted the length of the elongated particle (2b) as a function of a/b for magnetite. However they did not estimate the critical sizes for dimensional ratios of more than 10:1. As the observed magnetite grains in Michikamau anorthosites have dimensional ratios of more than 20:1, it is essential to estimate the critical size for dimensional ratios of this order and compare them with the observed values. The calculations showed that grains of dimensional ratios of this order can be as long as 10 microns and still behave as single domains. The results are tabulated in Table B3 of the appendix and are shown in Figure 4.5.

Strangway et al. (1968) have also estimated the critical size for single domain behaviour of long needle shaped grains. Their approach is based on comparing the total wall energy (given by $0.6 \times \text{area of walls}$ to first approximation) to the total free energy ($(\frac{1}{2}N_a J_s^2 + K_1/12) \times \text{volume}$ to a first approximation). Their results essentially agree with those of Morrish and Yu.

Figure 4.5 The critical single-domain size of magnetite as a function of axial ratio. The length of the major axis of the prolate spheroid is shown as a function of minor to major axis ratio.



In the calculations by Morrish and Yu, the anisotropy energy was neglected in comparison with exchange energy; this is justifiable if the critical radius is appreciably smaller than the thickness of a Bloch wall in the material. This follows because the anisotropy and exchange energies are equal in a Bloch wall, but the exchange energy will be dominant if the change in spin direction is forced to take place in a distance less than the wall thickness.

Morrish and Yu state that for $b/a > 7$, the magnetocrystalline energy term is considerable. Strangway et al. have shown that for dimensional ratios of 15:1 and 20:1, the magnetocrystalline energy is the dominant term. Inclusion of magnetocrystalline energy term in Morrish and Yu's calculations would increase the critical size of the particle by at least 50%. Thus the estimates given in Table B3 may be small by a factor of 0.7. That is grains can be as long as 20 microns and still behave as single domains.

Kittel (1949) estimated the critical single domain size by taking anisotropy terms into account. He obtained the critical radius as

$$R_c = 9\sigma_w / 4\pi I_s^2 \quad (4.5)$$

where σ_w is the total wall energy per unit area and I_s the saturation magnetization.

4.6 High Coercive Force of Single-Domain Particles

It has been stated that the formation of domain boundaries is energetically unfavourable in the case of small particles. In the absence of domain boundaries, changes of magnetization cannot proceed by the process of boundary displacement, but must proceed by the process of rotation of the total magnetic moment of the particle. When the possibility of boundary movement is ruled out, large increases in coercive force may be obtained by increasing the effective anisotropy of the specimen (Kittel 1946). Kittel (1949) calculated the coercive force due to anisotropy of particle shape as

$$H_c = (N_t - N_o) J_s$$

where N_t and N_o are the values of the demagnetizing factors in the long direction of the elongated particle and perpendicular to it and J_s the saturation magnetization of the mineral grain. The coercive force was estimated for various axial ratios of the mineral magnetite and plotted along the abscissa in Figure 4.5. This facilitates comparison of observed coercivities with the observed lengths of mineral grains.

4.7 Discussion

It is of interest to check whether the observed high coercivities of Michikamau anorthosites are indeed

due to the considerations discussed above. First one should check whether the needle shaped grains fall in the single domain range. Figure 4.4 is a histogram of the observed lengths of the needle shaped grains. The histogram peaks between 10 and 15 microns with a gradual drop on either side. Strangway et al. (1968) and Evans (1969) have stated that observation of grains between 5 and 0.2 microns (the limit of microscopic resolution) in large numbers makes it probable that smaller grains exist also. From Plate 1 it may be observed that the grains have length to width ratios of at least 20:1 and probably 25:1. Oriented needles of 10 microns long, and dimensional ratio 25:1 fall in the single domain range of Figure 4.5. Thus it is highly probable that many of the observed needles are single domain.

The Michikamau anorthosites are known to have coercivities of at least 2000 oersteds. It is postulated that some of the magnetic mineral in this rock unit may have coercivities close to 3000 oersteds. This is substantiated from Figure 4.5 where it is shown that the grains of interest have theoretical coercivities up to a limit of 2900 oersteds. However this point cannot be proved experimentally with our present apparatus.

There are cases in the literature where the high coercivities of particles have been attributed to their shape anisotropy. Stoner and Wohlfarth (1947) have pointed out that with coercivities in the region of 500 oersteds,

usually some type of magnetic anisotropy was involved and with coercivities appreciably greater than 500 oersteds, there is strong presumptive evidence of some degree of shape anisotropy. Kittel (1949) also showed that the effect of shape anisotropy of an iron particle on the coercive force is to increase it to high values. However both the above works were concerned with a discussion of magnetic metals.

In the subject of rock magnetism only one case was known to the author where appeal was made to the shape of the grains in explaining the observed high coercivities. The exception was the work on Modipe Gabbro of Africa by Evans and McElhinny (1966). In a later paper (Evans et al. 1968), they showed that numerous small magnetite particles in the form of rods were observed within clinopyroxene. The sizes of the opaques they observed were significantly less than those of the Michikamau anorthosites. The needle shaped opaques of the Modipe Gabbro were observed to occur in clinopyroxene. The magnetite needles of the Michikamau anorthosites occur in plagioclase. Hatch et al. (1961), in their classic book on petrology, state that 'regularly oriented plates of dendritic iron ore' were observed in 'hortonolite'. Thus the occurrence of plate or needle shaped magnetite grains may be a more common feature than has been suspected. It is expected that more cases of similar nature will be reported in future, where the high coercivities may be explained by shape of the magnetic mineral.

However the situation is not simple. Inspection of Figure 4.2 shows that about 70 to 80 percent of magnetization is lost in about 1000 oersteds. This shows a coercivity spectrum ranging from low values to very high values. The magnetization lost in fields of 1000 oersteds or less does not reside in single-domain needle shaped grains. It is likely that the coercivities of less than 1000 oersteds of Michikamau anorthosites may be due partly to the patch shaped grains discussed in #4.3, and partly to needles whose dimensions are such that they form two or more domains.

CHAPTER 5

THE PALEOMAGNETISM OF DIABASE DIKES FROM THE
GRENVILLE PROVINCE: EXPERIMENTAL RESULTS5.1 Objectives of the Study

Diabase dike swarms are numerous across the Canadian Shield and are observed in all structural provinces. These dikes were well distributed in time and space and are very informative regarding the tectonic development of the Canadian shield (Fahrig and Wanless 1963). Of particular interest are the diabase dikes in the Grenville structural province. The Grenville province lies on the southeastern edge of the shield and represents a region in which mountain building took place one billion years ago. Extensive aeromagnetic mapping by the Geological Survey of Canada has revealed the presence of these dikes throughout Ontario and Quebec. The aeromagnetic maps show that the dikes strike east-west. The evidence of local geological considerations makes it probable that the time of intrusion of the dikes is related to the mountain building activity of Grenville times (Wilson 1965). Potassium-argon age determinations by the Geological Survey of Canada have given ages ranging from 450 m.y. (65-113) to 974 m.y. (Wanless et al. 1966). In addition to the potassium argon age determinations, the

only other control on the ages of these dikes is the evidence cited by a few geologists (ex: Gill and L'Esperance 1952; Wilson 1965) who noted that the dikes had cut into "Grenville" strata and hence concluded that the dikes were of late Precambrian age. The possibility cannot be ruled out that the dikes were intruded earlier than the Grenville orogeny and that the low apparent ages are caused by leakage of argon during later alteration. However, it is unlikely that the dikes are pre-Grenville as they show no signs of metamorphism either in hand samples or in polished sections.

If the dikes were indeed younger than the Grenville metamorphism and their true age could be established, they would be of special interest because the polar wander curve relative to North America is completely unknown in the age range 1000 to 400 m.y.. However the age of the Grenville dikes must be regarded as uncertain, with a probable relation to the Grenville orogeny.

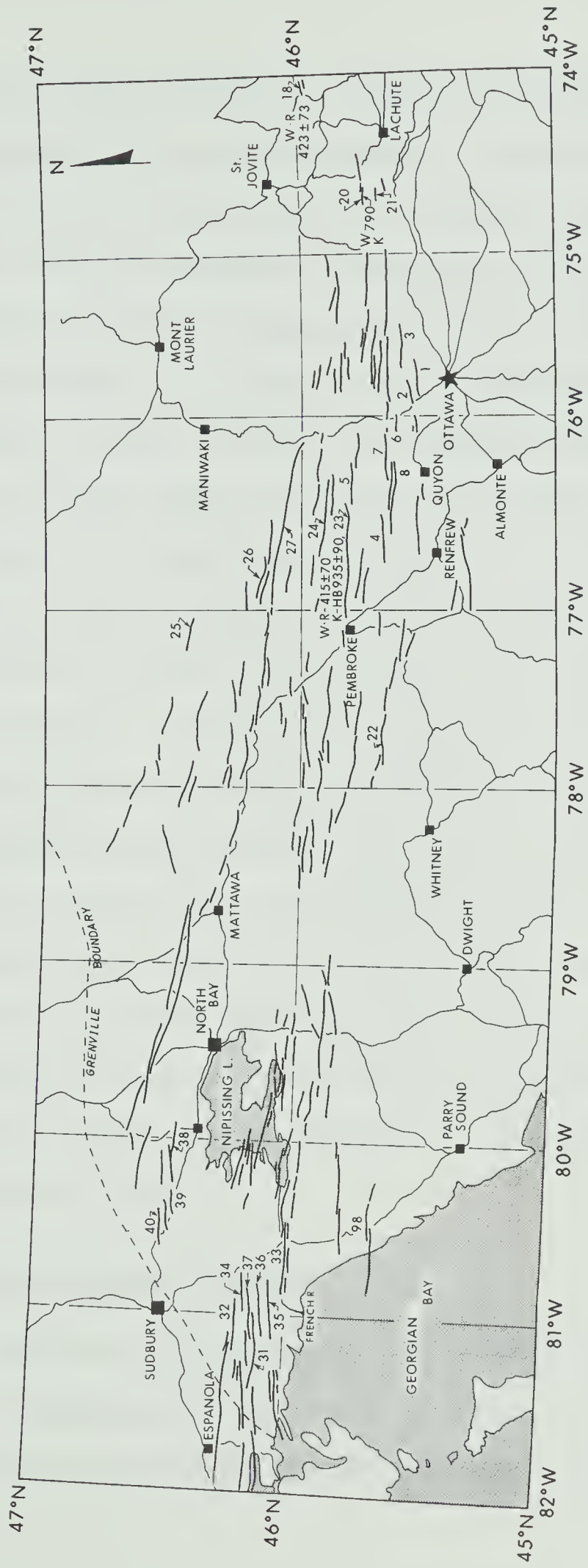
Study of the paleomagnetism of dike swarms is of interest in another aspect. Strangway (1961) studied certain dike swarms of the Canadian Shield and concluded that the stable component of magnetization in dikes tends to lie close to the plane of the dike. In support of his

hypothesis that by some mechanism dikes tend to be magnetized in their plane, he cited results, available at that time, of Graham (1953), Gough (1956) and Bruckshaw and Robertson (1949). Evidence against this hypothesis was later advanced by Fahrig et al. (1965), by Evans (1968) and more recently by Larson and Strangway (1969). In particular, Evans showed by a statistical study that the data available at present provide no reason for supposing that dikes do not become magnetized parallel to the ambient field. Both as a precaution in paleomagnetic study of the dikes and for the inherent interest of the point, it would be a useful corollary to test the data for consistency with Strangway's original hypothesis.

5.2 Geologic Setting and Paleomagnetic Sampling

The dikes intrude throughout the Grenville geological province of Ontario and Quebec. The composition of the rocks is of the quartz diabase type. These dikes are often several hundred miles long (as inferred from aeromagnetic maps) and are usually 20-150 meters wide. Samples were collected from widely spaced dikes throughout the Grenville province. In this study, each dike is taken as representing a site for statistical analysis. Initial sampling of nine dikes was made by Dr. W. F.

Figure 5.1 Location of diabase dikes intruding the
Grenville province of Ontario and Quebec.



Fahrig of the Geological Survey of Canada who kindly made the samples available to the author. In view of the vast area in which these dikes are exposed, samples from nine sites cannot adequately represent this dike swarm. Accordingly further sampling was done by the author, assisted by Mr. A. B. Reid of this Department, during the summer of 1968. In all, 137 samples were collected from 29 sites whose locations are shown in Figure 5.1. Sites 1-28 are from the eastern part of the Grenville province while sites 31-37 are from the western edge of the Grenville Front. Sites 38-40 and 98 are from the region in between. At least five samples were collected from each dike and wherever possible these samples were equally spaced across the width of the dike. The samples were in the form of cylindrical cores 2.58 cm in diameter and about 15 cm in length. Two cylinders 2.58 cm long were cut from each core and used in the paleomagnetic study. The cores were oriented in situ by means of a solar compass similar to that described by Gough and Opdyke (1963).

5.3 Measurement of Magnetization

The direction and intensity of remanent magnetization of each specimen was measured by means of the PAR spinner magnetometer described in Chapter 2. The

results are given in Appendix C. Table C1 lists the direction and intensity of magnetization of each specimen. The vector sum of the two unit vectors representing the magnetizations of two cylinders from a given core was calculated and taken as the mean direction of magnetization for that core. These are summarized in Table C2. If the vectors of magnetization diverge by an angle θ exceeding 23° , Laroche (1966) terms them as 'inhomogeneous' and will not include them in any further analysis. Laroche arrived at this figure of 23° by using a minimum within-core precision of 25. Although the choice of this minimum value of k is arbitrary, this procedure was taken as a test of homogeneity of magnetization of individual cores. It may be noticed that the magnetization of only 72% of the cores is 'homogeneous' before demagnetization. The behaviour of the 'inhomogeneous' cores was followed during alternating field demagnetization. If the angle between specimen magnetizations was greater than 23° after treatment in a.c. fields, these cores were no longer used in the final statistical analysis. The NRM moments average to 1.74×10^{-2} gauss cm^3 and were distributed between 4.5×10^0 and 5.4×10^{-6} gauss cm^3 . The mean direction of magnetization for the dike was taken as the vector sum of N unit vectors representing the N cores from that dike. The results are given in Table 5.1 and plotted in Figure 5.2.

TABLE 5.1

SITE MEAN DIRECTIONS OF GRENVILLE DIKES(NRM)

Site	N	Azimuth	Incl	R	k	Alpha
GR01	5	(335.62)	(55.28)	3.2980	2.35	40.84
GR02	5	67.31	67.48	3.8960	3.62	32.89
GR03	5	297.74	79.39	4.4151	6.84	23.94
GR04	6	(343.39)	(-48.46)	2.7924	1.56	45.78
GR05	5	50.97	66.28	3.6306	2.92	36.63
GR06	5	(26.55)	(61.25)	2.5844	1.66	48.66
GR07	6	338.44	63.24	5.7287	18.43	13.31
GR08	5	(25.74)	(72.10)	2.8777	1.88	45.61
GR18	6	200.40	75.95	5.6879	16.02	14.28
GR20	5	17.24	79.77	4.6921	12.99	17.37
GR21	3	127.74	60.53	2.8194	11.08	24.29
GR22	6	129.44	83.57	5.0267	5.14	25.22
GR23	5	31.74	82.65	4.8474	26.21	12.23
GR24	3	291.49	47.94	2.8633	14.63	21.13
GR25	4	(117.17)	(48.58)	2.8565	2.62	43.22
GR26	4	27.71	72.04	3.9110	33.72	12.06
GR27	3	(32.28)	(10.36)	1.6253	1.45	67.01
GR28	4	(82.26)	(82.10)	2.3291	1.80	52.24
GR31	5	(45.95)	(49.37)	3.4732	2.62	38.68
GR32	5	29.20	73.77	4.7639	16.94	15.21
GR33	5	87.06	57.08	4.8016	20.16	13.95
GR34	5	(329.19)	(24.34)	3.3500	2.42	40.21
GR35	6	(186.24)	(22.27)	0.9034	0.98	57.70
GR36	5	24.14	64.17	4.8449	25.80	12.33
GR37	5	314.74	71.87	4.8273	23.16	13.01
GR38	5	5.23	77.50	4.7456	15.72	15.79
GR39	5	312.74	56.06	4.5059	8.09	22.01
GR98	6	331.49	83.09	5.6486	14.23	15.15

N = NUMBER OF CORES FROM EACH SITE

R = RESULTANT OF N UNIT VECTORS

k = ESTIMATE OF FISHER PRECISION PARAMETER

Figure 5.2 Mean site directions of Grenville dikes:
natural remanent magnetization.



- POSITIVE INCLINATIONS
- NEGATIVE INCLINATIONS
- ▼ PRESENT GEOMAGNETIC FIELD AT SAMPLING LOCALITY

Fisher's statistical parameters k and α_{95} are also listed in Table 5.1. Table C3 in Appendix C gives the mean direction of magnetization of each site computed by giving unit weight to each specimen. Most of the site mean directions are seen to group around the present earth's field. Such a grouping is possible if a strong secondary component, produced by the present geomagnetic field, masks any primary component of magnetization of the dike.

5.4 Alternating Field and Thermal Demagnetization

Systematic demagnetization by alternating fields was carried out in an attempt to isolate a primary component of magnetization. Demagnetization was conducted, by means of the apparatus described in Chapter 2, on two pilot specimens from each site. Not all sites yielded stable end-points of direction during demagnetization; hence it was more difficult to decide on an optimum field than in the study of Michikamau anorthosites. A compromise procedure between those of McElhinny and Gough (1963) and Irving et al. (1961) was adopted. If a stable end point in direction was obtained during demagnetization, the field at which this was achieved was taken as the optimum field for that site. However if no stable end point was observed, which was the case for most of the sites, the specimens were all demagnetized in steps, the precision

parameter k was calculated for each successive step and the field at which the maximum k was obtained was chosen as the optimum field of demagnetization for that site. The optimum field of demagnetization for most of the sites was about 100 oersteds which indicates a magnetic mineral of low coercive force. The behaviour of individual specimens during demagnetization will next be discussed.

Eleven of the twenty-nine sites (GR01, 04, 06, 08, 24, 25, 27, 28, 31, 34, and 35) have random NRM directions, on Watson's (1956) criterion. These are presented within brackets in Table 5.1. The grouping in site GR01 improved to being barely significant after demagnetization. The grouping in sites GR06, 24 and 34 was not improved by demagnetization. During demagnetization, the individual specimen vectors for these sites moved about in a random fashion; large fluctuations in intensity were also noticed. Such behaviour is typical of unstable remanent magnetization. Results from these sites were therefore not included in the final analysis. In the rest of the sites, demagnetization improved the grouping remarkably as may be noticed from increases in the values of k . In general, specimens of the Grenville dikes behaved in three different ways during demagnetization which formed the basis for dividing them into the following three groups for convenience of discussion.

Group 1: For some of the sites which had NRM directions close to the present earth's field, demagnetization improved the grouping but with insignificant changes in the mean direction. No stable end point in direction was observed during demagnetization in successively higher fields. This behaviour indicates either that the primary component of magnetization of these dikes has a direction close to that of the present geomagnetic field or that these dikes do not carry a primary component. If the latter were the case, the observed remanent magnetization would be only a secondary viscous component acquired probably during recent times. Specimens from sites GR02, 03, 05, 07, 18, 20, 23, 25, 26, 27, 98, and 39 behaved in this fashion. These sites are called 'Group 1' sites. Typical directional changes in magnetization for this group of sites are presented in Figure 5.3.1.

Group 2: All specimens from sites GR04, 08, 22 and 28 showed a systematic change in direction during demagnetization. Sites which originally gave directions with large positive inclinations moved systematically in such a way that stable end-points in direction were obtained with steep negative inclinations. It is very probable that these sites carry a primary component with steep negative inclination. Better within-site grouping was observed after demagnetization. In particular site

Figure 5.3 Response of specimens of Grenville diabase to
a.f. demagnetization.

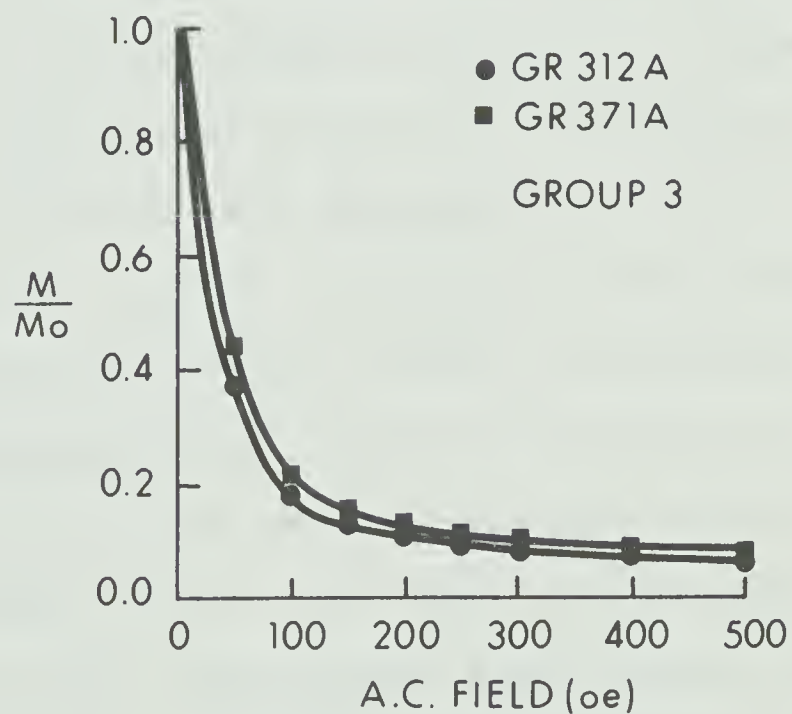
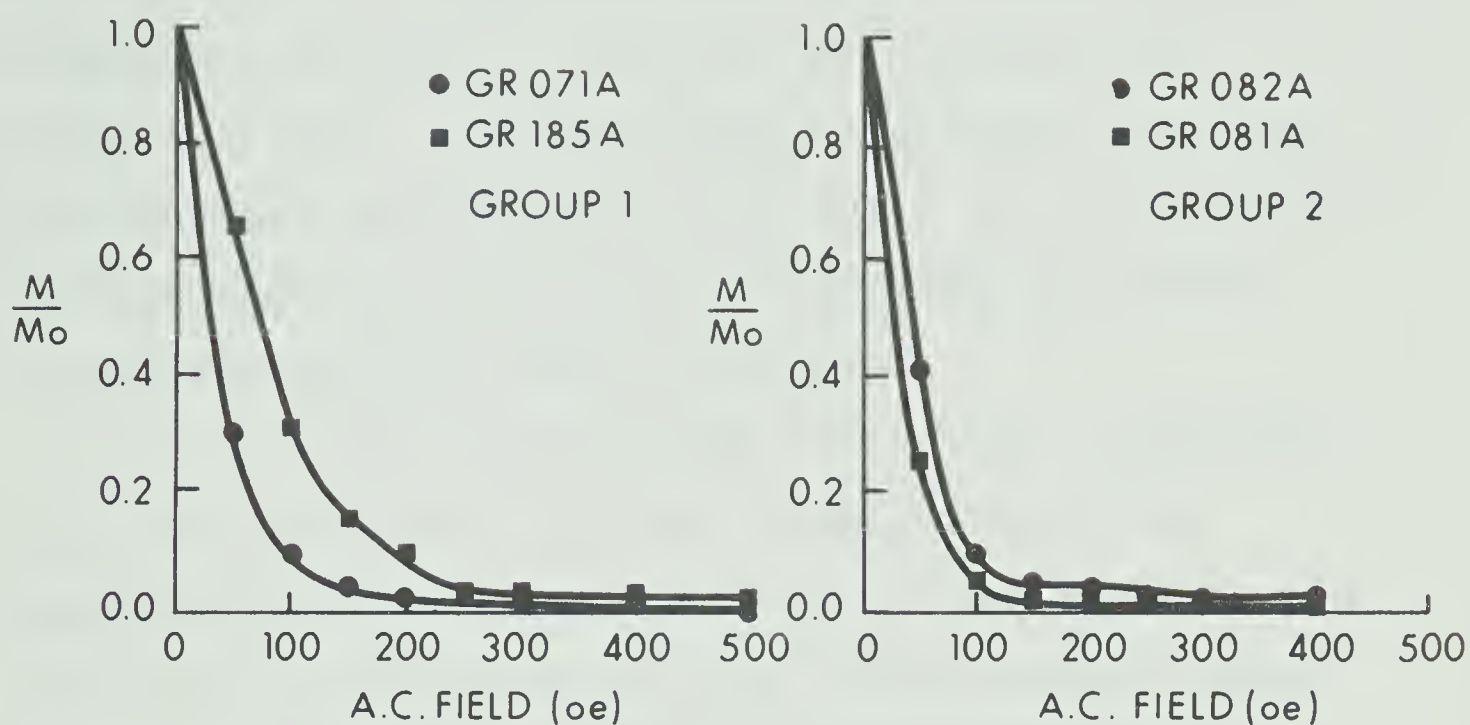


SOLID SYMBOLS : POSITIVE
INCLINATIONS
OPEN SYMBOLS : NEGATIVE
INCLINATIONS

GR04 which was randomly magnetized originally had a significant direction after demagnetization. Changes in directions typical of this group are shown in Figure 5.3.2. Group 3: A more conventional behaviour was observed for specimens from the remaining sites. On demagnetization, specimen magnetization directions were found to move to easterly azimuths and shallower inclinations. Such behaviour is to be expected if a viscous component due to the present geomagnetic field was being eliminated during demagnetization, and a stable component was retained. Typical examples of this directional behaviour are shown in Figure 5.3.3. Sites GR31, 32, 33, 35, 36, and 37 belong to 'Group 3'. Curves of normalized intensity plotted versus demagnetizing field for two specimens from each group of sites are shown in Figure 5.4. It will be seen that there is no marked difference between the curves in Figure 5.4 for the three groups selected on their directional changes, except that the Group 3 specimens retain a larger fraction of their initial moment to 500 oersteds.

The directions and intensities of magnetization of individual specimens after treatment in alternating fields are listed in Table C5 of the appendix. The computed mean sample directions are given in Table C6. Figure 5.5 illustrates the site mean directions after demagnetization. The directions have better groupings as evidenced by the

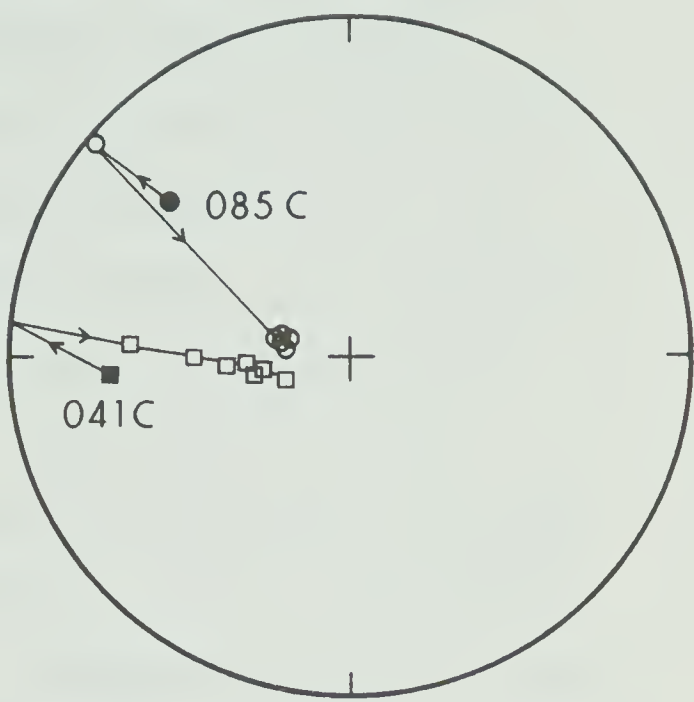
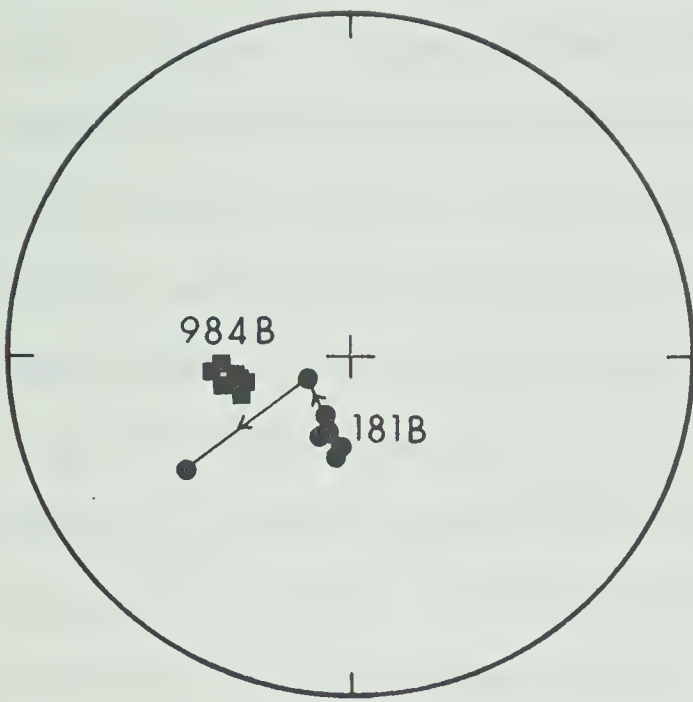
Figure 5.4 Intensity change of specimens of Grenville diabase during a.f. demagnetization.



values of k in Table 5.2 which lists the site mean directions after demagnetization. For convenience in discussion, the data of Table 5.2 are arranged into Groups 1, 2 and 3. Grouping within individual cores was also improved as evidenced by the values of θ in Table C6. The site mean directions obtained by giving unit weight to each specimen are listed in Table C7.

In view of the different responses of specimens from the three groups of sites to alternating field demagnetization, a second stability test was applied. The behaviour of specimens was studied during thermal demagnetization (Chapter 1). Thermal demagnetization was conducted at the Southwest Center for Advanced Studies, Dallas, Texas, at the invitation of Drs. A. L. Hales and C. E. Helsley. The apparatus used was a non-inductively wound furnace similar to that described by Irving et al. (1961) and Robertson (1963). Annulment of the geomagnetic field at the specimen is very critical for thermal work and this is accomplished by placing the furnace in a magnetically shielded room which gave cancellation of the field to an accuracy of 10γ . At least one specimen from each site, and in some cases three, were selected for thermal treatment. The specimens were heated in air to successively higher temperatures of 150, 200...510°C and cooled in field-free space. Heating of the specimens in

Figure 5.6 Response of specimens of Grenville diabase
to thermal demagnetization.

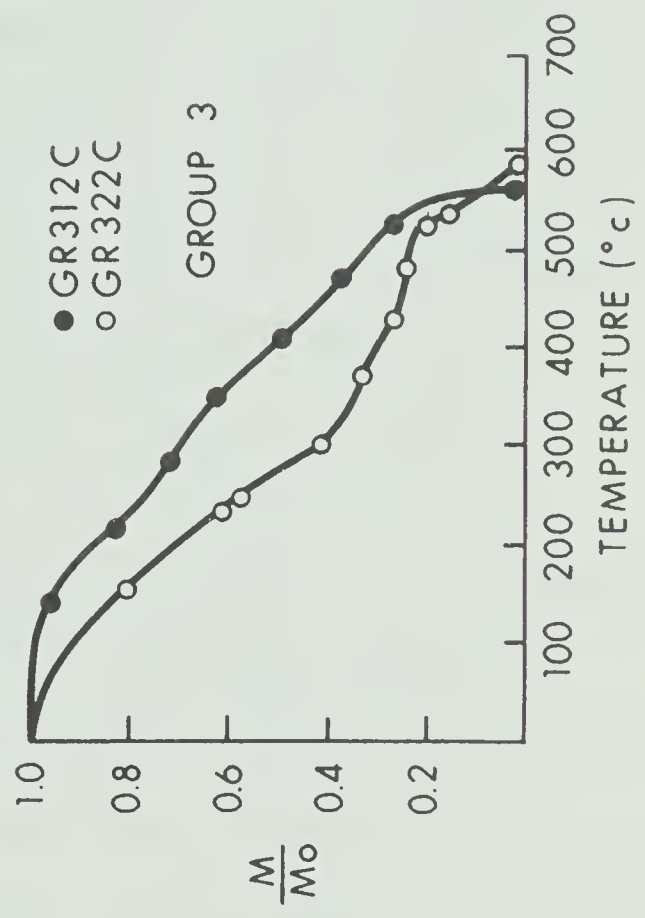
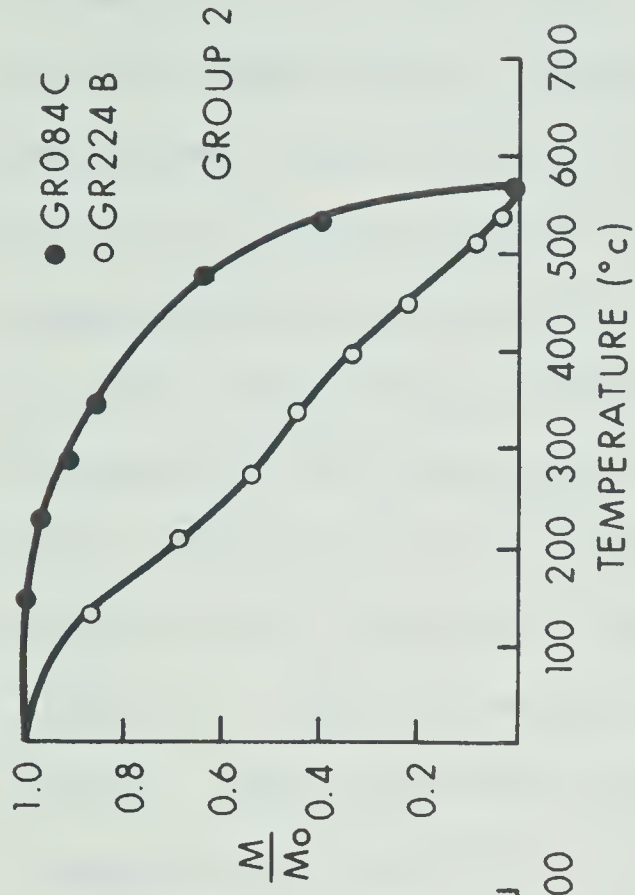
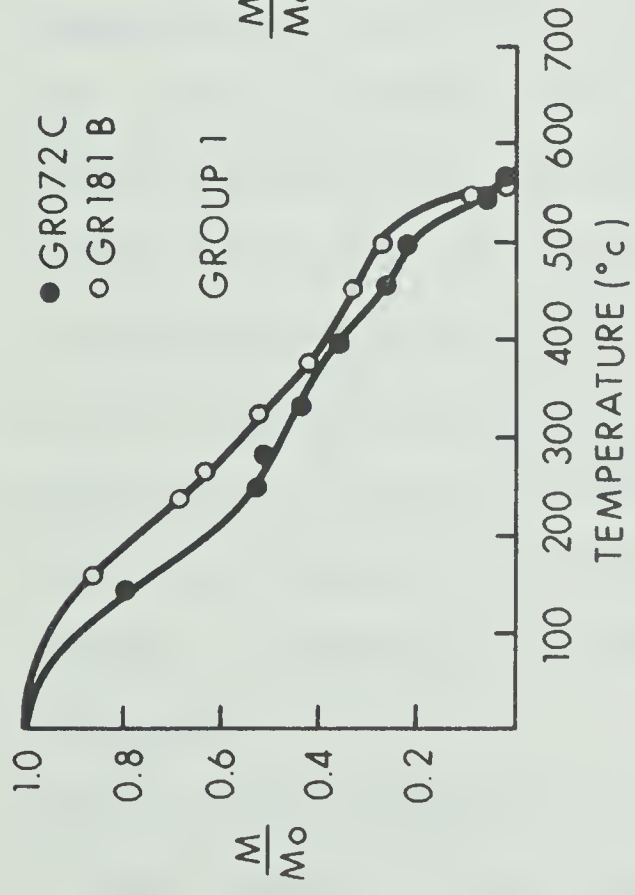


SOLID SYMBOLS : POSITIVE
INCLINATIONS
OPEN SYMBOLS: NEGATIVE
INCLINATIONS

air involves the risk of oxidation. But no excessive color change of specimen was noticed after heating, indicating no extensive oxidation of the specimens took place during heating. The maximum temperature in each run was maintained for about five minutes. The remanent magnetization was measured after each heating by means of a PAR spinner magnetometer. The results of this stepwise thermal demagnetization of individual specimens are given in Table C8 of Appendix C. It was found that specimens behaved under thermal demagnetization in three distinct ways, and that the sites grouped together on the basis of response to alternating-field demagnetization also gave similar responses when heated. It is thus reasonable to discuss the thermal studies under the same groups as before.

Group 1: The response of four specimens from site GR18 was studied. There is a stable end point in direction during thermal demagnetization. A similar response was noticed of specimens from sites GR02, 03, 05, 07, 23 and 98. There was very little change in the direction of magnetization. The stable directions were maintained in temperatures up to 550°C after which large movements in direction were noticed, with abrupt changes in intensity. It was apparent that these 'wild' changes in magnetization were due to a viscous component acquired by the specimen

Figure 5.7 Intensity change of specimens of Grenville
diabase during thermal demagnetization.



while its magnetization was being measured. This was evidenced by the fact that continuous change in the spinner magnetometer readings was observed while a measurement was carried out. Such an effect is possible if the viscous component is considerably higher than the magnetization remaining in the specimen after heating. The very small changes in magnetization during heating are reflected in the generally low values of 'Psi' for these sites (Table C8 of the appendix). Psi is the change in magnetization direction from the previous step of demagnetization. Thus low values of psi indicate stable end points. Some specimens exhibited a range of blocking temperatures from 500° to 580°C. The significance of this observation will be discussed in terms of the mineralogical composition in Chapter 7. The mean directions obtained for these sites after thermal demagnetization are not significantly different from those obtained after alternating field demagnetization. The changes in direction and decay in intensity during thermal demagnetization are plotted in Figures 5.6.1 and 5.7.1 respectively. The changes in magnetization are typical of a stable primary component.

Group 2: The response of specimens from sites GR08 and 28 is very similar to that under a.f. demagnetization. A similar systematic change in direction was observed

from positive to negative inclinations. An increase in intensity during thermal demagnetization was noticed, which is to be expected when a secondary component of opposite direction was being eliminated. A similar response to both alternating field and thermal demagnetization experiments makes it conclusive that these sites carry a primary component which has high negative inclinations. The change in magnetization for this group of sites is shown in Figures 5.6.2 and 5.7.2.

Group 3: The response of specimens from site GR32 is typical of those from sites GR31, 32, 33, 35, 36 and 37. An eastward movement of directions was noticed, the movement being very similar to that caused by alternating field demagnetization. The directional changes in magnetization after each heating are shown in Figure 5.6.3. Curves of normalized intensity plotted versus temperature are given in Figure 5.7.3.

Thus thermal demagnetization studies confirm the conclusions drawn from the observations of alternating field demagnetization. It is very likely that the specimens from the three groups of sites carry primary components of magnetization. The paleomagnetic pole positions, calculated from the site mean directions are listed in Table 5.3 and are presented in Figure 5.8. The data from alternating field demagnetization are analysed in Chapter 7

TABLE 5.2

SITE MEAN DIRECTIONS OF GRENVILLE DIKES AFTER
OPTIMUM DEMAGNETIZATION

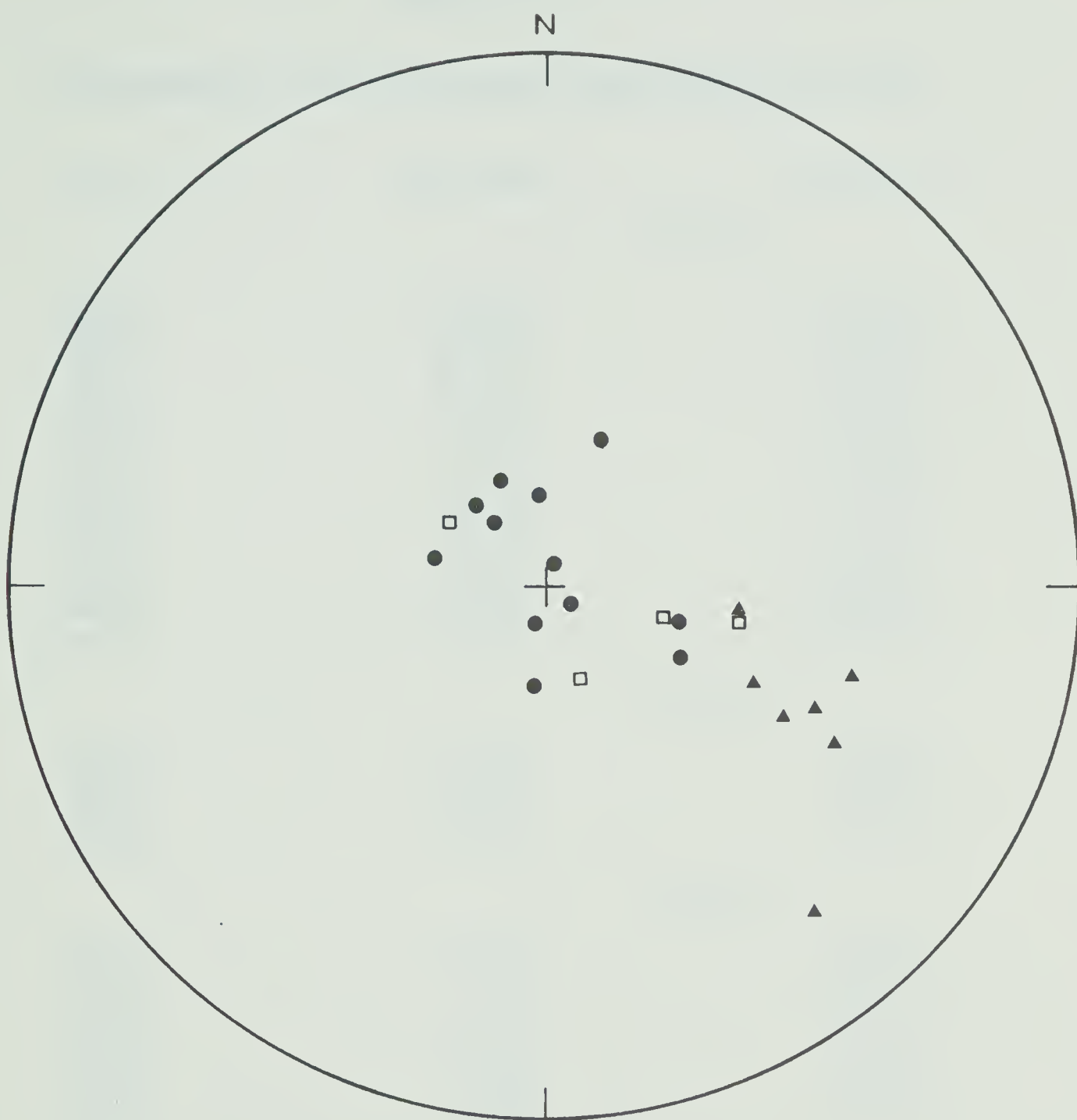
Site	N	Azimuth	Incl	R	k	Alpha	Treat
Group 1							
GR02	5	103.23	61.71	4.8025	20.25	13.91	100
GR03	5	2.72	85.32	4.7924	19.27	14.26	50
GR05	5	349.38	77.77	4.8793	33.14	10.88	100
GR07	6	327.19	76.71	5.7378	19.07	13.09	100
GR18	6	199.25	82.30	5.8088	26.15	11.20	150
GR20	5	182.82	65.07	4.7482	15.88	15.71	150
GR23	5	123.67	83.33	4.7044	13.53	17.02	100
GR25	4	118.44	58.28	3.9367	47.37	10.17	250
GR26	4	20.72	57.28	3.7460	11.81	20.37	100
GR27	3	337.05	66.55	2.8832	17.13	19.53	300
GR39	5	319.86	68.31	4.0238	4.10	30.93	100
GR98	6	284.60	66.65	5.4206	8.63	19.50	100
Group 2							
GR04	6	296.18	-61.34	5.7714	21.87	12.22	150
GR08	5	106.96	-44.51	4.7128	13.93	16.78	200
GR22	6	167.48	-57.58	5.1130	5.64	24.07	300
GR28	3	104.35	-63.71	2.6984	6.63	31.39	150
Group 3							
GR21	3	139.74	13.82	2.9183	24.49	16.33	150
GR31	5	114.40	44.39	4.0013	4.01	31.29	200
GR32	5	117.63	27.33	4.9240	52.65	8.63	250
GR33	5	97.37	49.87	4.5906	9.77	20.03	100
GR35	6	113.99	33.02	4.4167	3.16	32.16	400
GR36	5	106.35	29.17	4.9866	298.57	3.62	200
GR37	5	118.98	35.90	4.9714	140.03	5.29	300

N = NUMBER OF CORES FROM EACH SITE

R = RESULTANT OF N UNIT VECTORS

k = ESTIMATE OF FISHER PRECISION PARAMETER

Figure 5.5 Mean site directions of Grenville dikes:
after optimum demagnetization.



- GROUP 1 SITES (ALL POSITIVE INCLINATIONS)
 - GROUP 2 SITES (ALL NEGATIVE INCLINATIONS)
 - ▲ GROUP 3 SITES (ALL POSITIVE INCLINATIONS)
- (FOR EXPLANATION OF GROUPS, SEE TEXT)

TABLE 5.3

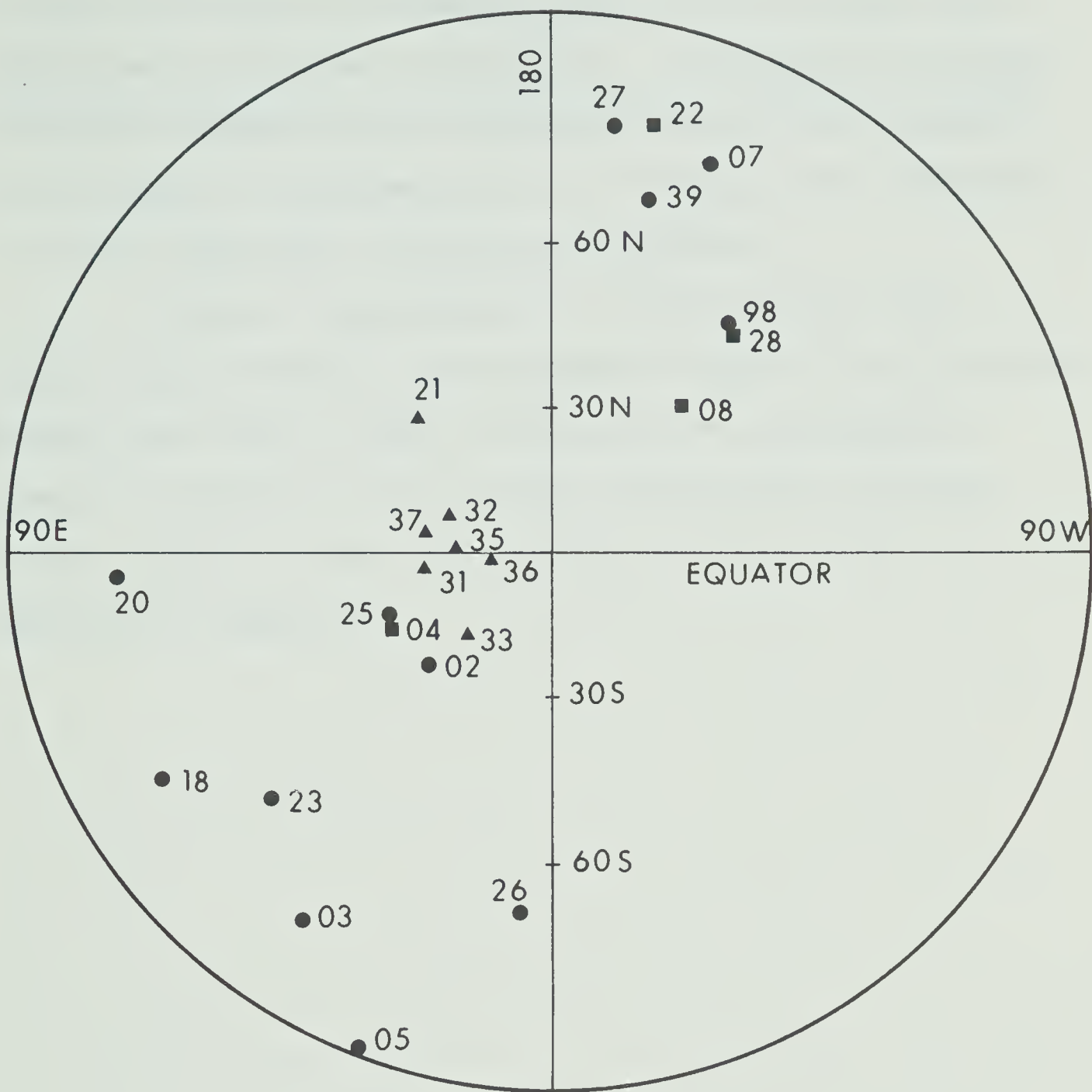
PALEOMAGNETIC POLE POSITIONS FOR GRENVILLE DIKES

Site	Latitude	Longitude
Group 1		
GR02	21.59	- 25.71
GR03	54.84	- 75.04
GR05	68.48	- 87.88
GR07	63.79	-107.61
GR18	31.46	- 79.82
GR20	2.87	- 76.67
GR23	37.69	- 62.82
GR25	11.44	- 32.77
GR26	65.80	- 13.33
GR27	74.30	-147.40
GR39	63.59	-144.94
GR98	41.13	-137.86
Group 2		
GR04	-14.82	146.63
GR08	-29.89	21.86
GR22	-78.08	-20.17
GR28	-39.06	42.73
Group 3		
GR21	-26.28	-28.98
GR31	3.47	-26.17
GR32	- 7.48	-21.30
GR33	16.97	-18.10
GR35	- 2.56	-20.77
GR36	0.36	-13.64
GR37	- 4.00	-25.65

-VE LATITUDE REFERS TO SOUTH OF EQUATOR

-VE LONGITUDE REFERS TO WEST OF GREENWICH

Figure 5.8 Paleomagnetic pole positions for Grenville dikes.



- GROUP 1 SITES
- GROUP 2 SITES
- ▲ GROUP 3 SITES

to find out whether the three groups of sites carry three significantly different directions. A statistical analysis of thermal demagnetization results alone was not attempted as the number of specimens treated thermally was inadequate to obtain meaningful statistical parameters.

Before a paleomagnetic interpretation of the results was attempted, a petrographic study of the Grenville diabase was made in order to identify the ferromagnetic minerals contained in it and make quantitative estimates of the content of each. The results of this study are reported in Chapter 6.

CHAPTER 6

STUDIES ON STABILITY OF MAGNETIZATION OF GRENVILLE DIABASE6.1 Objectives of the Study

The magnetic properties of Grenville diabase were described in Chapter 5. The specimens exhibited varying degrees of stability and were shown to behave differently under both alternating field and thermal demagnetization. In particular during alternating field demagnetization, most of the specimens did not show stable end-points of direction. It was observed that the magnetization directions of certain specimens made random movements after treatment in 200 oersteds. These movements indicate that the magnetization resides in minerals of low magnetic stability. Examples are specimens from sites GR02, 03, 18 and 98. On the other hand, specimens from certain other sites yielded stable end-points of direction on demagnetization in fields up to 500 oersteds. One might expect such a marked contrast in magnetic properties to be related to the state of alteration of the magnetic mineral, since the magnetic behaviour generally depends on the type of magnetic mineral, its grain-size and its alteration state.

There are numerous examples in the literature of the correlation of magnetic properties with the opaque

petrological parameters. Akimoto and Kushiro (1960) investigated the magnetic and petrological properties of certain dolerite sheets of Japan and concluded that the alteration of titanomagnetite to titanomaghemite greatly reduced the bulk coercivity of the rock. Watkins (1967) observed unstable magnetic components in some basaltic rocks and concluded that their instability was the result of their titanomaghemite content. Larson and Strangway (1969) showed that the magnetic stability of the Spanish Peak dike swarm was correlatable with the presence of small grains observed microscopically. They also found that there was no relation between the presence of maghemite in their rocks and the degree of magnetic stability. Ade-Hall et al. (1968) and Ade-Hall and Wilson (1969) showed that the stability of remanence, as determined by a.f. partial demagnetization, was related to two opaque petrological properties; titanomagnetite high temperature oxidation, and titanomagnetite granulation. They defined two artificial quantities, the magnetite oxidation number M , and the magnetite granulation number G , and showed that the stability of magnetization could be correlated with the product MG . Larson et al. (1969) showed that a relation existed between the distribution of grain-size and the spectrum of coercivities. Petrographic studies of Grenville diabase were undertaken with a view to seeking these or

other relations between magnetic and opaque petrological properties.

6.2 Opaque Petrological Properties of the Grenville Diabase

Polished sections were made of one sample of known remanence from each of six dikes, to study the relations of the iron-titanium phases. All polished sections were observed under an ore microscope at magnification $\times 160$ (#4.3). Systematic measurements were made of VHN number, reflectivity and grain-sizes of the opaque minerals. Table 6.1 lists some representative values of VHN number, reflectivities and sizes of the opaques in these sections.

Microscopic observations yielded valuable information on general features of the magnetic minerals. Two types of minerals were identified (named A and B in Table 6.1). The mineral of A type was grey in color, isotropic and was usually present in larger grains than the B type. A had consistently lower values of VHN number and reflectivity than B. The B type mineral was slightly bluish grey in color, had higher values of VHN number and reflectivity and was often anisotropic. Mineral A has been identified as titanomagnetite and mineral B as titanomaghemite. Hematite was absent or present only as traces in the samples. They were specially abundant in samples GR231 and GR181 and were very rare in samples

TABLE 6.1

SUMMARY OF OBSERVATIONS ON POLISHED SECTIONS

OF GRENVILLE DIABASE DIKES

Grain Size (μ)	VHN	Refl.	Lamellas	Description
Sample GR181				
75 × 118	562	18.0	Abundant	Isotropic grain with
64 × 48	602	20.3		anisotropic lamellas
122 × 65	617	24.8		
48 × 173	611	20.2	Present	A and B minerals co-
41 × 39	1022	24.8		existing in same grain
53 × 101	605	21.3	Present	Isotropic
49 × 59	1115	25.3		Anisotropic
71 × 156	551	22.8		A and B minerals co-
58 × 39	1085	27.8		existing in same grain
98 × 112	476	23.2	Few	Titanomagnetite
70 × 94	512	19.6		
152 × 49	564	23.8		
101 × 72	581	22.0		
Sample GR231				
64 × 37	495	19.1	Present	A and B minerals co-
51 × 29	947	22.8		existing in same grain
77 × 46	603	21.7	Abundant	
23 × 36	572	21.2	Present	Isotropic
19 × 28	1012	25.6		Anisotropic
82 × 106	612	20.7		Low temperature altera-
27 × 35	1054	26.2		tion is evident
65 × 99	597	20.0		Isotropic
46 × 41	985	26.7		Anisotropic
117 × 49	542	19.7		
48 × 62	995	25.6		
24 × 96	562	21.2		
56 × 48	571	20.6		
79 × 76	498	21.8		
56 × 64	956	23.7		
Sample GR221				
95 × 105	737	26.0		Titanomaghemite
75 × 58	579	22.2	Present	Titanomagnetite
52 × 67	848	24.0		Anisotropic

TABLE 6.1 (CONTD)

Grain Size	VHN	Refl.	Lamellas	Description
102 × 112	612	19.8		Isotropic
128 × 98	540	21.6		
65 × 101	885	24.8		Anisotropic
48 × 84	651	20.8	Present	Isotropic
75 × 92	524	19.7		Isotropic
58 × 76	1021	25.6		Anisotropic
68 × 64	492	23.8		
94 × 61	595	22.9		
Sample GR081				
85 × 112	865	23.4		Extensive lamellas are present in more than 25% of grains
76 × 165	738	24.2	Abundant	Low temperature alteration is evident
78 × 92	561	20.7	Present	Isotropic
62 × 70	982	25.3		Anisotropic
90 × 76	662	19.6	Present	
66 × 60	1012	24.2		
60 × 98	572	18.8	Present	Isotropic
46 × 80	985	23.6		Anisotropic
101 × 84	668	22.6	Present	
94 × 45	954	23.6		
98 × 48	542	21.2	Few	
45 × 68	869	26.7		
86 × 76	560	20.8	Present	Isotropic
72 × 64	885	25.4		Anisotropic
Sample GR364				
19 × 37	572	19.2	None	A & B minerals co-existing in the same grain
7 × 21	953	22.8		
20 × 42	602	20.6	None	Isotropic
32 × 46	650	25.5	Few	
18 × 53	582	19.7		
22 × 41	658	21.6	Rare	Isotropic
12 × 22	976	26.7		Slightly anisotropic
28 × 52	566	20.8	Few	
16 × 39	984	27.6		
32 × 48	644	19.9	None	Isotropic
18 × 28	1012	24.9		
26 × 46	485	20.6	Few	
44 × 29	512	21.2	Few	

TABLE 6.1 (CONTD)

Grain Size	VHN	Refl.	Lamellas	Description
Sampel GR374				
135 × 106	555	22.3	Few	Slightly anisotropic
38 × 102	452	20.8	Few	
47 × 52	607	19.0	None	Isotropic
29 × 40	590	19.2	None	A & B minerals co-
17 × 13	1077	25.8		existing in the same grain
48 × 34	548	23.4	None	
55 × 38	605	20.5	None	A & B minerals co-
16 × 24	1055	26.4		existing in the same grain
70 × 45	581	21.2	Few	A & B minerals co-
41 × 20	1032	20.0		existing in the same grain
50 × 28	647	22.7	Few	
21 × 17	988	26.8		
68 × 73	581	21.8	None	
26 × 48	1025	25.9		
19 × 37	572	19.2	None	A and B minerals co-
7 × 21	953	22.8		existing in the same grain

GR363 and GR374.

The principal result of the polished-section work is the observation of the presence of both titanomagnetite and titanomaghemite in all samples, with varying abundance. Titanomaghemite is probably formed by low-temperature oxidation of titanomagnetite. Typical example is shown in Plate 3 where alteration of original titanomagnetite to titanomaghemite may be clearly seen. The two minerals often coexist in the same grain. Plates 4 and 5 contain photomicrographs of polished sections showing typical titanomagnetite and titanomaghemite grains. Samples GR364 and GR374 are characterized by smaller grains and grey titanomagnetites.

For each sample an average value of grain-size and the relative abundance of titanomagnetite to titanomaghemite were estimated from the observations and are listed in Table 6.2. Also listed in Table 6.2 are values of the magnetite oxidation number M for each sample. M is defined by Ade-Hall et al. (1968) as

$$M = \frac{\sum(n \times \text{percentage of total magnetite area represented by class } n)}{\text{total area}} \quad (6.1)$$

Here n is an integer between 1 and 6 and is largest for the highest oxygen content. Ade-Hall et al. defined six classes of oxidation as a slight modification of an earlier

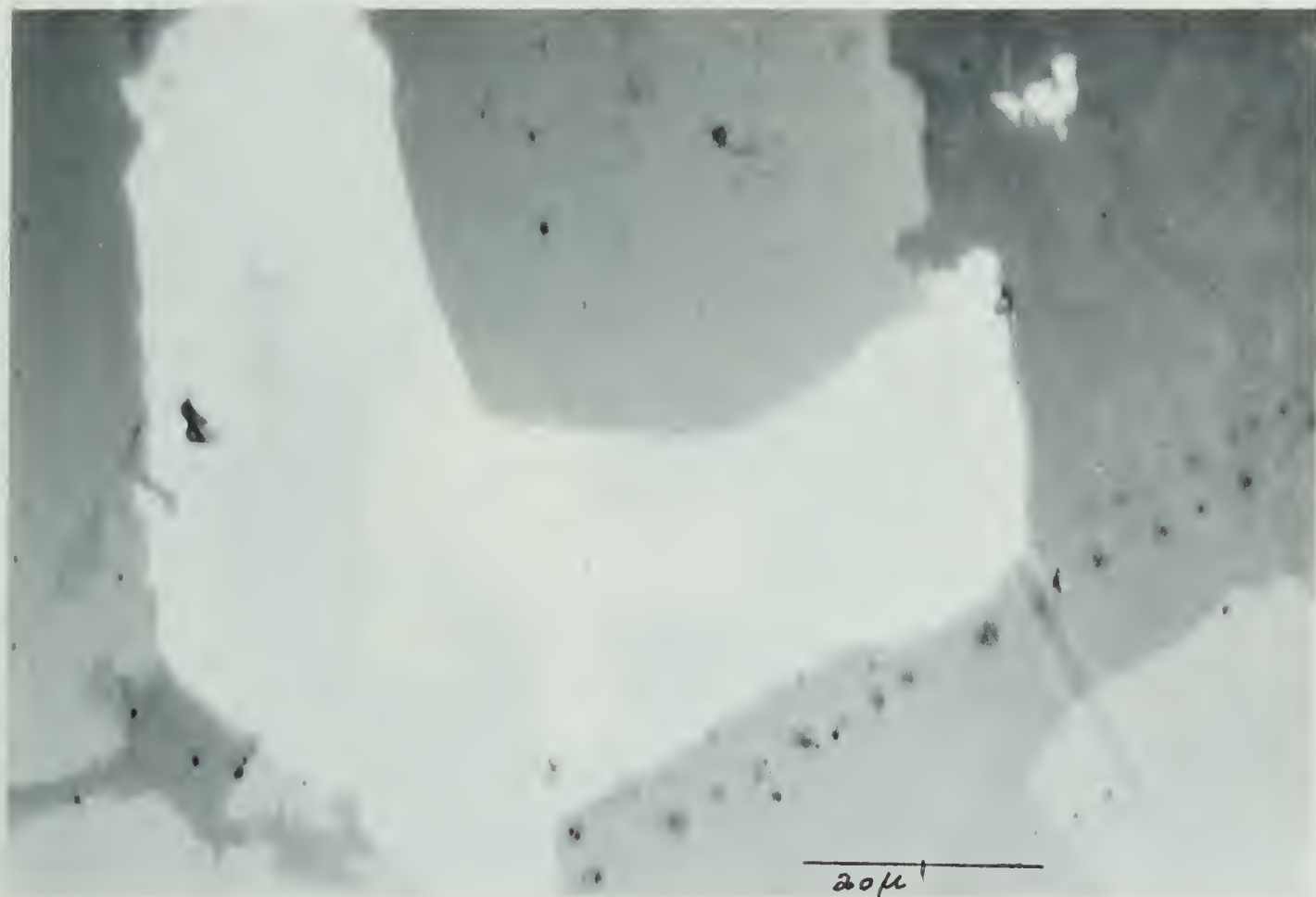
PHOTOMICROGRAPHS OF POLISHED SECTIONS OF GRENVILLE DIABASE
SHOWING

PLATE 2: LAMELLAE DEVELOPMENT IN GR221

PLATE 3: ALTERATION OF TITANOMAGNETITE TO TITANOMAGHEMITE
IN GR181

PLATE 4: A TITANOMAGNETITE GRAIN IN GR364

PLATE 5: A TITANOMAGHEMITE GRAIN IN GR231



classification by Wilson and Watkins (1967). These classes were described in detail by Ade-Hall and his co-workers.

Each sample of diabase contained grains representing several classes of oxidation. Thus the procedure in calculating M involved the following: classification of each part of the grain into one of the six classes; measurement of percentage of total magnetite area represented by that class and fitting these values in (6.1). An average number of one hundred opaque grains from each sample, well spread over the polished section, was taken as a representative sample for estimation of the magnetite oxidation number for that sample.

An attempt was made to estimate the value of magnetite granulation number G. Ade-Hall et al. defined G as

$$G = (P/20) + 1 \quad (6.2)$$

where P is the mean area percentage of granulation for 50 titanomagnetite grains per section. G varies between 1.00 (granulation absent) and 6.00 (every grain completely granulated). However, this attempt was unsuccessful as it was not possible to obtain P reliably. Thus, values of G are not listed in Table 6.2.

TABLE 6.2

MAGNETIC AND PETROLOGIC PARAMETERS OF GRENVILLE DIABASE

Sample No	Grain-size (μ)	B/A	M	k	SF	S ₂₀₀	Theta
GR081	90-100	0.459	2.87	13.9	0.187	0.453	89.6°
GR181	80-90	0.372	2.38	26.2	0.816	0.899	43.9°
GR221	60-70	0.520	2.44	5.6	0.261	0.425	69.6°
GR231	70-80	0.465	3.11	13.5	0.119	0.914	38.1°
GR364	20-30	0.108	1.28	298.6	7.430	0.613	18.6°
GR374	40-50	0.197	1.73	140.0	1.360	0.639	9.2°

6.3 Correlation between Petrological Properties and Magnetic Stability Factor

The petrological data of Table 6.2 may be used to make some quantitative correlations between magnetic properties and petrological parameters. Of particular interest in paleomagnetism is a factor representing the magnetic stability of the sample. Magnetic stability has a different meaning to different groups of workers. Hence it is debatable which parameter to choose as representative of the stability of magnetization. An ideal magnetic stability factor should be representative of the changes in direction as well as intensity of magnetization of the sample. This is particularly important in correlations between petrologic and magnetic parameters. Ade-Hall et al. (1968), following an earlier suggestion by Wilson et al. (1968), used a stability factor S_{200} . They defined S_{200} as $R_{200}/(R_{200}+r)$ where R_{200} is the length of the remanent magnetization vector after demagnetization in 200 oersteds and r is the vector change between 0 and 200 oersteds treatment. Thus a rock with stable magnetization, according to this definition, will have S_{200} approaching 1.0 while rocks with unstable magnetization will often have S_{200} less than 0.5. This definition of stability factor has the disadvantage, in the opinion of the author,

in that it is affected by the divergence of the direction of magnetization of the secondary component from the primary component and by the nature of the secondary magnetization. For example if an isothermal remanent magnetization making a large angle with the primary is superposed on TRM of the sample, the value of S_{200} depends on the angle between the IRM and TRM vectors.

Larson and Strangway's (1969) tabulation of values of k implies their choice of the Fisher precision parameter as a stability factor. k here is the Fisher precision parameter for the sample magnetization directions for that site. k reflects the tightness of grouping of the directions of magnetization alone, and takes no account of magnetization magnitudes; this choice has also limitations.

Tarling and Symons (1967) introduced a stability index SI which they defined as

$$SI = \max [(R)^{\frac{1}{2}} / \theta_{63}^0] \quad (6.3)$$

where θ_{63} is the circular standard deviation of the directions of a specimen's remanence taken within a range R of alternating field or temperature. SI too has the limitation that it is related only to remanence directions.

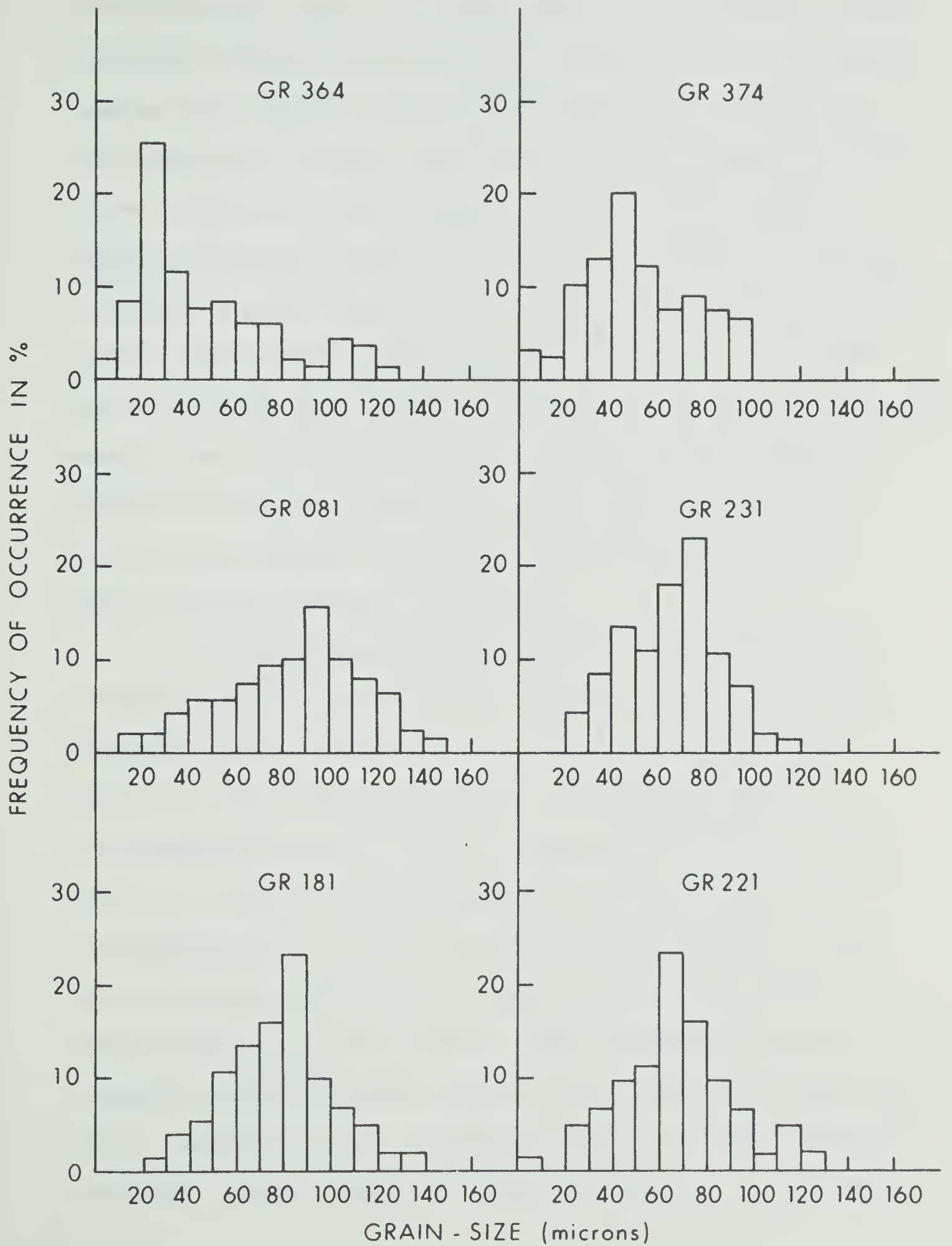
An alternative stability factor has been introduced in this study for purposes of correlation. It is defined as

$$SF = \left(\frac{M_{opt}}{M_0} \right) / \theta_{63}^0 \quad (6.4)$$

where M_{opt} and M_0 are the values of remanence intensity at optimum field of demagnetization and at zero field (NRM) and θ_{63} is the circular standard deviation of the directions taken by the magnetization between zero field and the optimum field. θ_{63} was chosen as representative of the directional change of remanence because it is the least sensitive to the number of included directions of the most commonly used measures of spherical distribution (Tarling and Symons 1967). The factor SF may reflect better the stability of magnetization as the directional and intensity changes are both incorporated in this artificial number. The various magnetic stability factors discussed above are listed in Table 6.2. Also listed in Table 6.2 is 'Theta' which is the angle between the mean magnetization vector of that site and the mean direction for the Grenville dikes.

It will be of interest to study the relation between grain-size and the various stability factors. Figure 6.1 represents a grain-size spectrum of the titanomagnetites observed for each sample. Titanomaghemite grains were not included in preparing these histograms. It is obvious that samples GR364 and GR374 have grain sizes smaller than the other four. A mean grain size was obtained

Figure 6.1 Histogram of grain-sizes of titanomagnetites
observed in Grenville diabase.



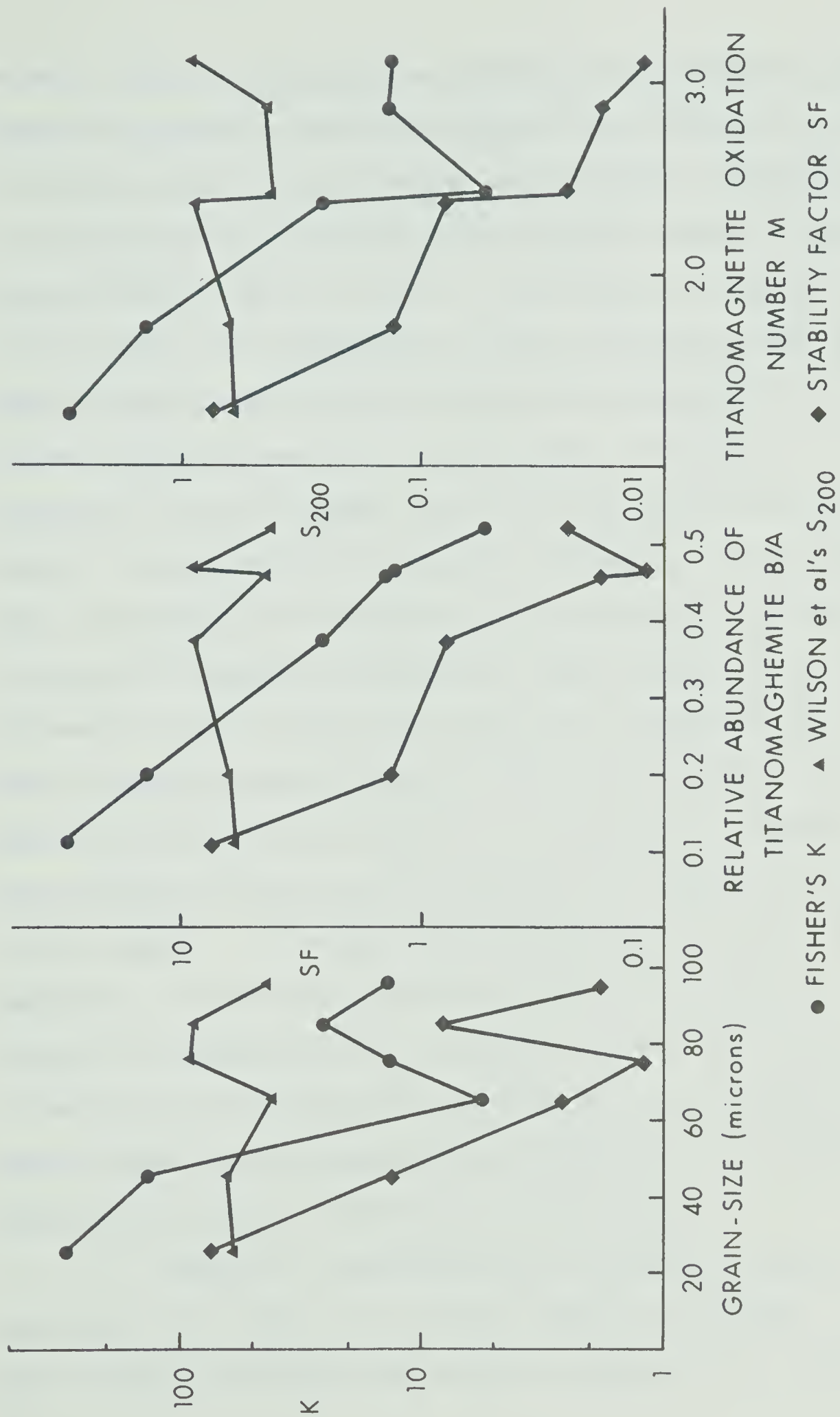
for each sample and this value was plotted against various stability factors for that site in Figure 6.2. In general samples with smaller grain sizes had higher values for all stability factors. All the stability parameters were found to fall off with increase in grain size until a minimum value was reached at about 70 microns. A further increase in grain size was associated with slight increases in the value of stability parameters. The observations indicated that high values of the stability factors were not merely due to small grain sizes. However the number of samples in the study was not large enough to make any further conclusions regarding the correlation between grain-size and magnetic stability.

A second point of interest is the correlation between relative amounts of titanomagnetite and titanomaghemite and the stability factors. In the data of Table 6.2, the grain volumes of titanomagnetite and titanomaghemite were used in computing B/A which is the ratio of volume of titanomaghemite to the volume of titanomagnetite. In this estimate, the average of the two observed directions is taken as the value for the third dimension of the grain. This procedure assumes a roughly spherical grain, which is an acceptable approximation. Ade-Hall et al. estimated the grain areas instead of grain volumes unlike the previous workers (ex: Wilson

Figure 6.2 Grain-size versus magnetic stability.

Figure 6.3 Relative abundance of titanomaghemite versus magnetic stability.

Figure 6.4 Titanomagnetite oxidation number versus magnetic stability.



et al. 1968). Although the procedure of Ade-Hall et al. avoids assumptions about the shape of the grain, use of the grain areas in correlation with magnetic properties is inappropriate in dealing with magnetic moment which is proportional to grain volume. Furthermore in quantitative correlations, the difference in the use of area and volume may be significant as they differ by an exponent of $2/3$ of the linear dimension. A mean value of B/A was estimated for each sample and this value was plotted in Figure 6.3 against the stability parameters. An extremely good correlation was obtained with an exponential drop in values of magnetic parameters (particularly k) as B/A increased. This observation was not in agreement with that of Larson and Strangway (1969) who concluded that grain size and not the amount of oxidation the mineral had undergone controlled the stability of magnetization of the sample. It seems that the presence of titanomaghemite is definitely associated with the observed scatter of magnetization in certain sites. This factor is taken into consideration in Chapter 7 in attempting to select dikes whose magnetization represents the magnetic field at the time of intrusion of the dikes.

Finally a correlation was attempted between the parameter M in Table 6.2 and the stability factors. A plot of this variation was shown in Figure 6.4. A fairly

systematic variation of all magnetic parameters with the magnetite oxidation number was noticed. The significance of this result is not known at present since stability is expected to be related to MG and not to M alone (Ade-Hall et al. 1968).

The petrographic studies indicated clearly that maghemitization is strongly associated with instability of magnetization of the Grenville diabase. Magnetic minerals with large grain sizes do generally have smaller values of the magnetic stability factors. Since there is a tendency for larger grains to show greater maghemitization, it is difficult to associate the stability with either of these properties alone. There is also a correlation between magnetic stability and magnetite oxidation number. The relative contribution of these factors in reducing the bulk coercivity of the sample is not known at present. Moreover most of the magnetic stability factors discussed above are statistical functions of the variation of intensity and direction of magnetization of the sample and do not represent a physical property of the mineral. Thus the above correlations do not demonstrate a physical mechanism but only represent an empirical relation between the magnetic and petrological observations.

6.4 Possible Causes for the Occurrence of Titanomaghemite

Few workers have reported the occurrence of titanomaghemite in their samples. In their early classic work Akimoto and Kushiro (1960) recognized titanomaghemite in certain dolerite sheets of Japan. They attributed the unstable magnetization of these sheets to this mineral. Watkins (1967) and Ozima and Larson (1967) also observed varying amounts of titanomaghemitites in certain Miocene lavas of Oregon and of andesitic rocks of Japan respectively. However titanomaghemite is very rarely the original magnetic mineral of a rock and almost invariably is formed by the alteration of titanomagnetite. Nagata (1961) suggested a possible origin of unstable magnetization in rocks containing titanomaghemite. The primary magnetic mineral was titanomagnetite. The titanomagnetite was altered probably by hydrothermal solutions, and titanomaghemite was formed by secondary oxidation of titanomagnetite. Thus the TRM of the original titanomagnetite, acquired at the time of formation of the rock, disappears as the oxidation of titanomagnetite proceeds to titanomaghemite. This oxidation probably takes place below the Curie point of titanomaghemite so that no new TRM is acquired. Further, if the oxygen supply is at a rapid rate, the titanomaghemite nuclei grow to multidomain size so that any CRM of the titanomaghemite disappears.

Thus the titanomaghemite retains only a viscous IRM. Katsura and Kushiro (1961) also suggested a similar origin for titanomaghemite.

A similar process may have altered the magnetization of some of the diabase dikes in the Grenville province. The most probable time of oxidation of the titanomagnetites would be very recent after weathering had exposed the outcrops.

In conclusion it may be said that microscopic examination of polished samples is generally effective in identifying titanomaghemite coexisting with titanomagnetite. Further as Wright (1968) has pointed out, petrographic examination should be made of paleomagnetic specimens in order to explain their magnetic behaviour in terms of petrology before any implications of global tectonics may be made of the results.

CHAPTER 7

PALEOMAGNETISM OF THE DIABASE DIKES FROM THE GRENVILLE
PROVINCE: INTERPRETATION AND CONCLUSIONS7.1 Analysis of Data

Paleomagnetic and petrologic observations of the Grenville diabase dikes were reported in Chapters 5 and 6. It appears from these results that the magnetizations of some of these dikes has been affected by alteration of the primary magnetic mineral to titanomaghemite. As pointed out in Chapter 6, the alteration probably took place recently, so that the primary and secondary magnetizations were acquired at different times. Hence it would be meaningless to compute a mean pole position for all Grenville dikes. In order to obtain a pole position representative of the time of intrusion of Grenville dikes, certain dikes have to be excluded whose magnetization is likely to have been affected by the alteration.

Paleomagnetic pole positions, calculated from the site mean directions, are listed in Table 7.1. These site magnetizations have been tested for the possible presence of more than one concentration of directions. The procedure was after McElhinny (1963). The test showed

that while Group 3 was significantly different from the other two, the data of Groups 1 and 2 gave no reason to assert that the two vectors were different. However there was considerable overlap in directions for the three groups of sites. The reversed directions of sites GR08 and 28 were not significantly different from the Group 1 sites. Directions for sites GR02, 04, 20, and 25 were not significantly different from Group 3 sites. Thus the previous grouping, based on response of specimens to alternating field demagnetization, yields no clear basis for selection of sites. It is possible that the response to a.f. demagnetization depends on the oxidation state, and this in turn on the position of the dike in the Grenville province. A suggestive point is that all Group 3 sites were collected from the western edge of the Grenville province.

An alternative grouping, based on the remanent magnetization directions, is suggested as follows:

Group A: sites GR02, 04, 20, 21, 25, 31, 32, 33,
35, 36, 37

Group B: sites GR03, 05, 07, 08, 18, 22, 23, 26,
27, 28, 39, 98

This grouping is supported by petrological studies reported in Chapter 6. The petrological parameter B/A (#6.3) is listed in Table 7.1 for purposes of comparison. In Group B

TABLE 7.1

MAGNETIZATION DIRECTIONS AND PARAMETER B/A FOR
GRENVILLE DIKES

Site	Mag. Directions		Pole Positions		k	B/A
	D	I	Lat.	Long.		
GR02	103.2	61.7	21.6N	25.7W	20.2	
GR03	2.7	85.3	54.8N	75.0W	19.2	
GR05	349.4	77.8	68.5N	87.8W	33.1	
GR07	327.2	76.7	63.8N	107.6W	19.0	
GR18	199.2	82.3	31.5N	79.8W	26.2	0.372
GR20	182.8	65.1	2.8N	76.7W	15.8	
GR23	123.4	83.3	37.7N	62.8W	13.5	0.465
GR25	118.4	58.3	11.4N	32.7W	47.4	
GR26	20.7	57.3	65.8N	13.3W	11.8	
GR27	337.0	66.5	74.3N	147.4W	17.1	
GR39	319.9	68.3	63.6N	144.9W	4.1	
GR98	284.6	66.6	41.1N	137.8W	8.6	
GR04	296.2	-61.3	14.8S	146.6E	21.8	
GR08	106.9	-44.5	29.9S	21.8E	13.9	0.459
GR22	167.5	-57.6	78.0S	20.2W	5.6	0.520
GR28	104.4	-63.7	39.0S	42.7E	6.6	
GR21	139.7	13.8	26.3S	28.9W	24.5	
GR31	114.4	44.4	3.5N	26.2W	4.0	
GR32	117.6	27.3	7.5S	21.3W	52.6	
GR33	97.4	49.9	17.0N	18.1W	9.8	
GR35	114.0	33.0	2.6S	20.8W	3.1	
GR36	106.4	29.2	0.4N	13.6W	298.6	0.108
GR37	118.9	35.9	4.0S	25.6W	140.0	0.197

sites, high B/A values suggest that the primary magnetization has been partly destroyed by recent oxidation of the magnetic mineral to titanomaghemite. Mean directions and pole positions for the two groups of sites are

	N	D	I	k	α_{95}	Lat.	Long.	A_{95}
Group A	11	118.9	45.2	14.03	11.3	3.0N	29.0W	11.0
Group B	12	315.6	75.3	20.7	8.9	61.6N	110.1W	14.5

These two directions are significantly different at the 95 percent level according to an F-test (McElhinny 1963).

7.2 Discussion

Of the two groups of poles discussed above, the mean Group A pole is believed to be representative of the geomagnetic field at the time of intrusion of the dikes. While the age of the Grenville dikes is uncertain, this pole position is consistent with other paleomagnetic data from North American rock units which may be of similar age. Paleomagnetism of the Keweenawan volcanics and sediments has been studied by DuBois (1962), Vincenz (1968), Palmer (1968) and Beck and Lindsley (1969) and these formations are slightly older than the Grenville dike swarm. All these workers reported considerable scatter in the paleomagnetic pole positions. DuBois (1962) carried out a chronological correlation of rock units based on

their paleomagnetic pole positions. The results of his investigations yielded paleomagnetic poles located in the central Pacific. In particular he reported paleomagnetic results from granite gneisses in the Township of Digby and from syenitic gneisses in Wakefield County both in the Grenville province. The pole position he obtained was at 7.0°S and 162.0°E which he termed the Grenville pole in his report. This pole position is essentially at the antipodes of the mean pole from the Group A sites of this study. DuBois' results suggest that the pole moved through higher 'latitudes' relatively rapidly in late Precambrian. This topic is discussed in more detail in Chapter 8. Palmer (1968) made a study of Keweenawan volcanics of the Lake Superior region and observed poles of both normal and reversed polarity grouped about positions which were not exactly opposed. He attributed this asymmetry to the effects of secondary magnetization. His results gave mean positions for poles of opposite polarities at 34°N , 177°W and 50°N , 148°W respectively. Beck and Lindsley (1969) have obtained a middle Keweenawan pole for the Beaver Bay complex of Minnesota. These authors observed a tight cluster of normal magnetic poles centered at 30°N , 172°W and a widely scattered group of poles of reversed polarity. However they discounted the possibility of secondary magnetization and explained their results in

terms of differences of age for normally and reversely polarized rock units with rocks of reversed polarity being older. The point of interest however was that scatter in late Precambrian pole positions was also observed by these authors. Thus considerable scatter of pole positions seems to be a rule rather than an exception in data from rocks of Keweenawan age.

If a polar wander curve is drawn for the late Precambrian relative to North America (Chapter 8), the pole for the Grenville dikes lies at the younger end of this curve. Fahrig (personal communication) has recently obtained paleomagnetic results for Baffin dikes and Bathurst sheets which were dated at 690 million years. The pole is located at 15°N , 166°E . The closeness of this pole to the pole for the Grenville dikes, in conjunction with the K-Ar age determinations, suggests that the Grenville dikes were intruded during post-Grenville times. Any further conclusions of paleomagnetic results should wait until more data are available on the ages of these dikes.

CHAPTER 8

REVIEW OF PRECAMBRIAN PALEOMAGNETISM OF NORTH AMERICA8.1 Preliminary Remarks

The importance of Precambrian paleomagnetic results was stressed in Chapter 1. There are very few reliable results for the Precambrian of North America. This is partly because there has thus far been little coordination between paleomagnetic work and radiometric age determinations. For some of the rock units which have been studied paleomagnetically, no geochronologic control was available, so that the value of the paleomagnetic results is reduced. However, over the last few years, a program of systematic radiometric dating has been initiated, mainly by the Geological Survey of Canada. The recent conference on Precambrian stratigraphy held at the University of Alberta revealed a wealth of data on ages of many rock units, some of which had been paleomagnetically studied previously. A good number of new paleomagnetic results have been published during the last two years. Thus a compilation and review of all Precambrian results for North America may be timely and helpful in establishing a provisional polar wander curve for this period relative to this continent.

This review has been modelled after similar reviews in the literature (Irving 1959, 1964; McElhinny et al. 1968) and the notation is taken from McElhinny et al. The data presented in Table 8.1 are inhomogeneous since the details of sampling, analysis, reliability of age of the rock unit and demagnetization tests of stability of NRM vary from one study to the other. Hence the table is supplemented by explanatory notes at the end to help the reader evaluate each result.

Column 1 contains reference pole number prefixed with letter P. This reference number is used in any further discussion of this pole. Column 2 specifies the rock unit, its locality and description. Column 3 gives the age of the rock unit studied. If radiometric age determinations are available, the estimates are indicated by an asterisk.

Columns 4 and 5 give the mean direction of magnetization specified by the azimuth D and inclination I. These results have been corrected for the tilt of the formation wherever applicable. The procedure of McElhinny et al. is adopted in calculating the mean directions. If results contain poles of both polarities, the estimate of mean direction is made irrespective of sign, i.e. reversals are assumed.

Columns 6 and 7 contain estimates of Fisher's precision parameter k and semiangle of the cone of 95%

confidence α_{95} for the mean direction. For the data of columns 4-7, different authors have chosen to give different weighting to sampling levels. Thus some mean directions, quoted in the literature, were calculated giving unit weight to individual specimens. Wherever complete data were available, mean directions and statistical parameters have been recalculated giving unit weight to individual sites.

The angular dispersion parameter $\Delta = 81/\sqrt{k}$, corresponding for large k to the standard deviation, is given in column 8 as a quantity related to paleosecular variation. This value is calculated only for those studies where sampling is believed to have been adequate to obtain an adequate record of paleosecular variation.

Columns 9 and 10 give the latitude and longitude of the paleomagnetic pole calculated from the direction specified in columns 4 and 5. No attempt has been made to give the polarity of the calculated pole as this term is rather arbitrary for the Precambrian with a majority of poles lying near the present day equator.

Columns 11, 12 and 13 are the estimates of confidence for the mean pole position. If the pole was calculated by a Fisher analysis of the site poles, A_{95} is given. If the pole was calculated from the mean rock unit direction, semiaxes of the oval of confidence δp and

TABLE 8.1

PALEOMAGNETIC RESULTS FOR THE PRECAMBRAIN OF NORTH AMERICA

Ref	Rock Unit	Age (M.Y.)	D	I	k	α_{95}	Δ	Lat	Long	$\delta p, \delta m$
P1	Stillwater complex	3100±200*	160	-40	23	11	17	62S	292	8,13
P2	Matachewan dikes	2485*	17 212 186	42 -06 -03	6 4 7	18 12 19		63S 37S 46S	241 239 279	13,22 6,13 5,10
P3	Cobalt group	2605*	35	-74	15	15		22N	262	24,26
	Caland and Steeprock mines Ontario									
P4	Ore zone goethite	2700	261	53	6	15		19N	152	10,14
P5	Hanging wall ashrock		243	14	10	15		12S	156	5,09
P6	Basic extrusions		341	35	2	41		57N	235	21,36
P7	Nipissing diabase	2095*	29	-45	38	7		12S	254	6,09
P8	Marathon dikes	1810	268	60	25	11		29N	213	12,16
P9	Abitibi dike swarm	1230*	264 354 221 258 268	61 -32 19 -48 65	102 39 13 35	5 19 7	8	27N 24N 21S 29N 32N	226 107 238 359 228	7,06 17,27 9,11
P10										
P11										
P12	Sudbury nickel	1200-1800	300 310	78 73				53N 47N	245 253	

TABLE 8.1 (CONTD)

Ref	Rock Unit	Age(M.Y.)	D	I	k	α_{95}	Δ	Lat	Long	$\delta p, \delta m$
P13	Blackhead sst.		232	51	25	10		2N	264	9,13
P14	Signal Hill sst.		283	20	21	11		16N	215	6,12
P15	Front Range Colorado Wyoming	1410 \pm 30*	52	-44	80	4	9	8S	209	4,06
P16	St. Francois Mountain Missouri	1400	245	46	65	10		1S	216	9,09
P17	Precambrian rocks of Missouri	1300-1400	243	41	11	6		1S	219	8,12
P18	Purcell System B.C.		33	-32	21	14		18S	213	9,16
P19	Belt series Grand Canyon series Purcell system	1100-1600						12S	213	13,13
P20	Arbuckle Mountains							17N	210	7,11
P21	Croker Island Complex	1475 \pm 50*	252	42	12	9	23	5N	217	7,10
P22	Molson dikes	1445	210	80	28	15		36N	251	28,27
P23	Michikamau anor- thosite	1400*	262	10	35	10	14	1S	215	6
P24	Belt series Montana McNamara formation Miller peak formation Spokane shale (1) Spokane shale (2) Grinnel formation Appekunny formation		26 234 232 206 225 223	-43 30 55 39 48 29	30 20 18 10 15 15	4 7 4 8 6 6		14S 11S 5N 16S 2S 15S	222 194 208 221 208 204	3,05 4,08 4,06 6,10 5,08 4,07

TABLE 8.1 (CONTD)

Ref	Rock Unit	Age(M.Y.)	D	I	k	α_{95}	Δ	Lat	Long	$\delta p, \delta m$
P42	Allard Lake anorthosite	950						38N	320	
P43	Grenville gneisses		286	-44				7S	162	
P44	Dikes of North Michigan		82	-86				45N	261	18,20
P45	Grenville dikes		119	45	14	11		3S	151	11

δm are given.

8.2 Discussion

All the Precambrian pole positions available up to early 1969 are listed in Table 8.1. The results P15.. P24 fix the position of the paleomagnetic pole for 1400 m.y. at 0°N , 147°W . Results P25.. P27 from Coppermine volcanics, Sudbury and McKenzie dike swarms confirm the position of the paleomagnetic pole for 1200 m.y. at 1°N , 175°W . A single paleomagnetic result is available for each of the ages 3100, 2500, 2100, 1800 and 900 million years.

Period 3100-1450 m.y.

An extremely tentative polar wander path may be drawn for this period as shown in Section AE of Figure 8.1. The results suggest minimum polar movement by 28° between 3100 and 2600 m.y., by 34° between 2600 and 2100 m.y., by 46° between 2100 and 1800 m.y., by 32° between 1800 and 1450 m.y.; i.e. a minimum average rate of polar movement by $0.1^{\circ}/\text{m.y.}$ relative to North America between 3100 and 1450 million years. This rate is considerably less than that suggested by McElhinny et al. from southern African data. They inferred a polar movement by 150° between 2700 and 2100 m.y. and by 180° between 1950 and 1300 m.y. i.e. at a rate of $0.25^{\circ}/\text{m.y.}$ However, the

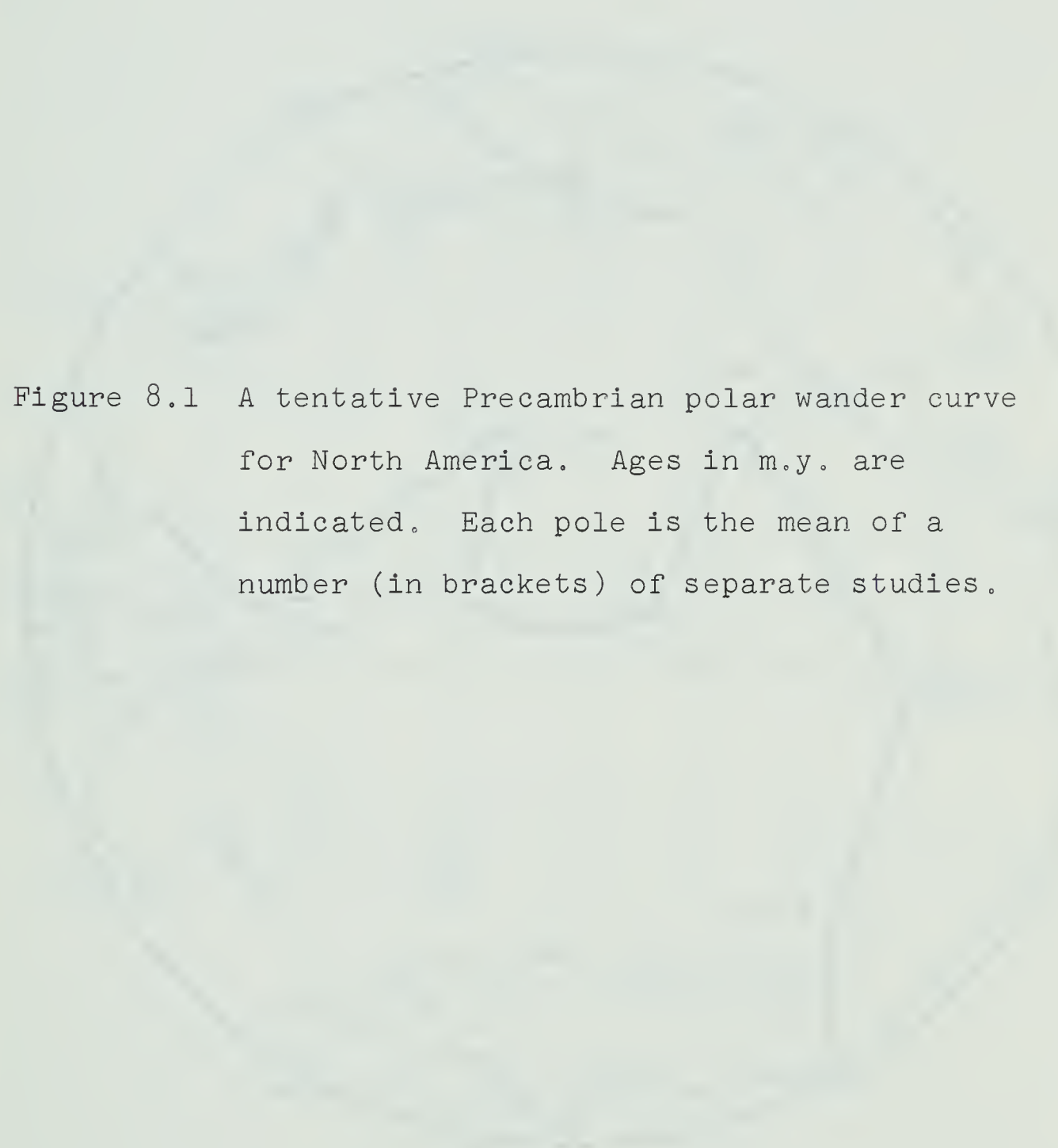
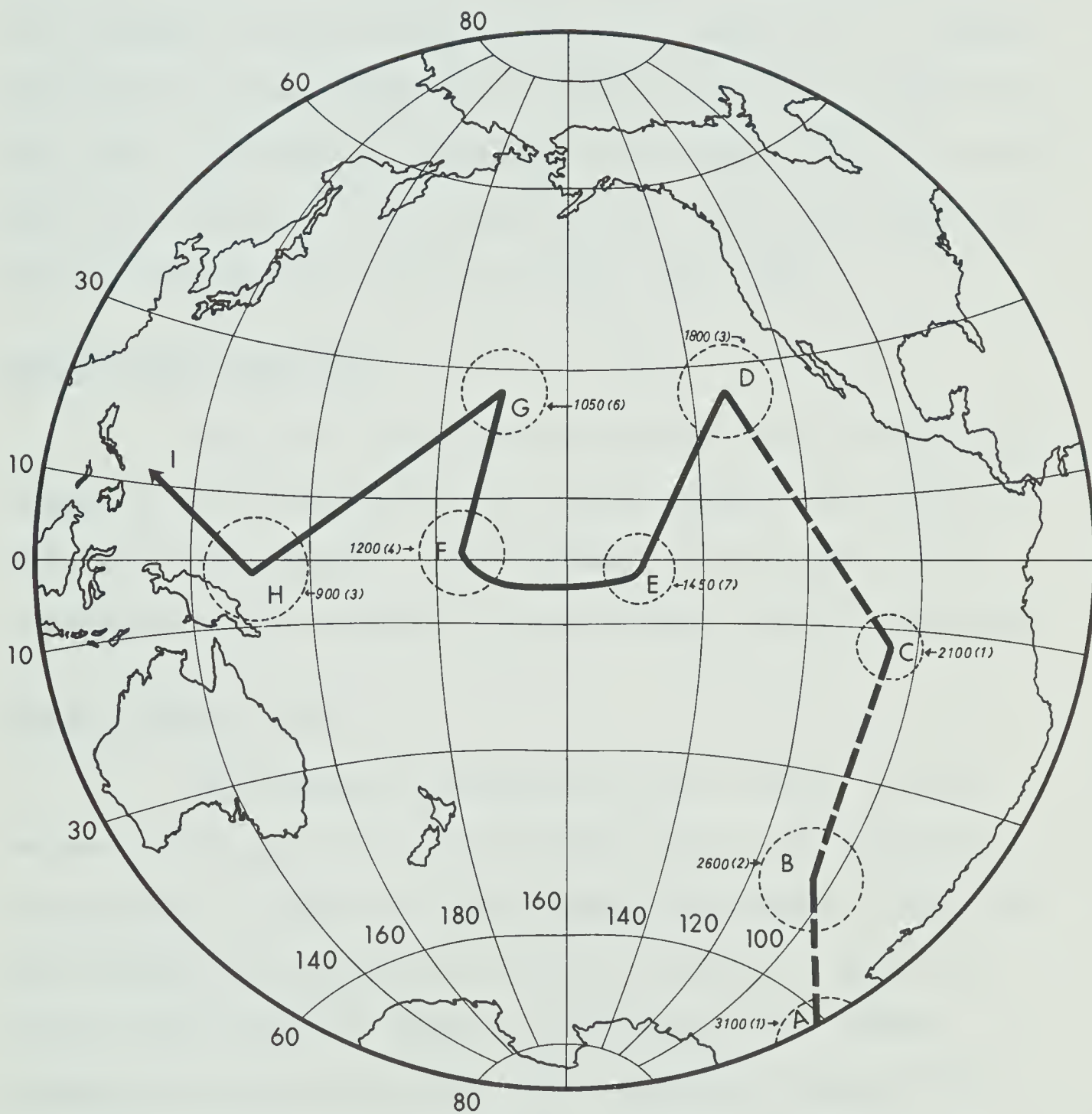


Figure 8.1 A tentative Precambrian polar wander curve for North America. Ages in m.y. are indicated. Each pole is the mean of a number (in brackets) of separate studies.



observation of Jones and McElhinny (1967) of a rapid migration of the pole by 120° during the deposition of Waterberg System between 1750 and 2000 m.y. may correspond to the 46° movement between poles C and D of Figure 8.1. However the African Precambrian polar wander curve has become more and more complicated, and longer and longer, as new results have been added. It is suspected the same will happen to North American curve as new results are added.

Period 1450-1200 m.y.

The polar wander path between 1450 and 1200 m.y. (segment EF of Figure 8.1) is rather better known as its ends are well located. This segment of the curve also suggests a polar movement at an average rate of $0.10^\circ/\text{m.y.}$.

Period 1200-younger

Paleomagnetic results for rock units of ages between 1200 and 900 million years seem to be the most complicated. Many of the paleomagnetic results come from the sediments and volcanics of the Keweenaw peninsula of the Lake Superior region. Tentative polar wander curves for this period have been suggested among others by DuBois (1962), Black (1963) and DuBois (1964). The Grenville dikes discussed earlier in this thesis probably fall at the younger end of this time span. Results from Duluth gabbro, Portage Lake lavas and Beaver Bay Complex

suggest a position for the pole in higher 'latitudes'. The results from the Grenville gneisses studied by DuBois (1962), the Bancroft Intrusives studied by Hood (1958) and of the Grenville dikes reported earlier suggest the pole was close to the present day equator at 155°E longitude 900 million years ago. Thus the uniformity of the movement of the pole suggests the joining of points F and H in Figure 8.1 by the shortest route. This joining is also consistent with the rate of 0.10°m.y. suggested earlier. However the data from Keweenawan results is so compelling as to suggest a rapid excursion of the pole through higher 'latitudes' between 1200 and 900 million years. The hypothesis of an episode of rapid polar wander is not inconsistent with the results from other continents. Unfortunately there were no results available for rock units of comparable age from the southern African shield.

There are no published paleomagnetic results for Precambrian rock units younger than 900 million years. Unpublished paleomagnetic data by Dr. W. F. Fahrig of Bathurst sheets and Baffin dykes reveals the location of the pole at 15°N and 166°E , 690 million years ago.

Thus a tentative polar wander curve for the Precambrian of North America may be as shown in Figure 8.1 with a general movement towards north and west with a

general uniform rate of $0.10^\circ/\text{m.y.}$. Keweenawan results suggest an episode of rapid polar wander between 1200 and 900 million years, and the addition of new results may well add large excursions of the pole at times which cannot be predicted from the existing data. The curve shown in Figure 8.1 summarizes the existing state of knowledge on Precambrian polar wander relative to North America. Even if all the existing pole positions are correct, the true polar wander curve is probably much more complicated than that sketched.

CHAPTER 9

SUMMARY AND CONCLUSIONS

A paleomagnetic investigation of some Precambrian rock units of the Canadian shield was initiated. The Michikamau anorthosite body from the Ungava Province, which had been reliably dated at 1400 m.y., was studied 1) to obtain a reliable paleomagnetic pole for this time relative to the Canadian Shield and 2) to investigate the usefulness of anorthosite bodies for paleomagnetic study. Twenty-nine oriented cores from six sites were supplied to the writer, and their stability of magnetization has been well tested. Evidence is given that the observed magnetization is thermoremanent in origin and represents the direction of the earth's field at the intrusion at the time of its formation. Results of a fold test indicated that the magnetization was acquired with the rocks in their present attitudes. The computed paleomagnetic pole for this rock unit lies at 0.5°S , 144.7°W with $A_{95} = 5.6^{\circ}$. Comparison of this result with results for rock units of similar age in North America suggests that there have been no large relative movements between this region and the other sampling sites for the last 1400 million years. It further suggests that the geomagnetic field 1400 million years ago approximated that of a geocentric dipole. These anortho-

sites, in spite of their coarse grained texture, are found to be extremely useful for paleomagnetic work in that they retain the primary component of magnetization reliably.

Michikamau anorthosites were shown to possess extremely high coercivities of the order of 1800 oersteds. In order to find out the nature of the contained magnetic mineral, petrographic studies were made. Systematic estimates were made of the Vicker's hardness number and reflectivity of the magnetic minerals. The contained magnetic mineral was shown to be magnetite occurring in plagioclase feldspar, in the form of extremely elongated rods of length to width ratio of at least 20:1 and of typical length 12 microns. Theoretical estimates showed that grains in the shape of rods of axial ratio 20:1 and more can be as long as 10 microns and still behave as single domains. Some of the magnetite grains in Michikamau anorthosites were thus shown to be in the single domain range. The observed high coercivity can then be explained in terms of the shape anisotropy of the magnetite rods. It was pointed out that a similar phenomenon may be able to explain some of the high coercivities observed in volcanic rocks.

The diabase dikes intruded in the Grenville Province of the Canadian Shield were studied paleo-

magnetically. Age determinations by the Geological Survey of Canada suggested a K-Ar age between 437 and 970 m.y. for these dikes. A total of 137 cores were collected from 29 dikes. The stability of magnetization was tested both by alternating field and thermal demagnetization. While the response of the specimens to both demagnetizations were similar, most of the sites have varying degrees of stability represented by a large range in coercive forces. Microscopic studies of polished sections of the Grenville diabase were undertaken in order to find a correlation between magnetic and petrological properties. All polished sections contain titanomagnetite and titanomaghemite in varying abundances. A correlation was attempted between the petrological parameters grain-size, relative abundance of titanomaghemite to titanomagnetite, the magnetite oxidation number M and magnetic stability represented by various stability factors. While samples with higher stability do have smaller grain-sizes, a good correlation was obtained between the relative abundance of titanomaghemite and the Fisher precision parameter k . It was shown that low-temperature oxidation of titanomagnetite to titanomaghemite may be responsible for the observed drop in magnetic stability in certain dikes.

Petrological observations were taken into

consideration in excluding certain dikes whose magnetization was affected by secondary alteration. Thus a total of eleven dikes were found to be carrying a stable magnetization believed to be representative of the magnetic field at the time of intrusion of the dikes. The mean paleomagnetic pole for the Grenville diabase dikes lies at 3.0°N , 29.0°W .

This pole position is consistent with other paleomagnetic poles from North American rock units which may be of comparable age. The paleomagnetic results of the Grenville diabase dikes suggest that the dikes were intruded after the Grenville orogeny, perhaps about 700-900 million years ago.

A review has been made of all the Precambrian paleomagnetic results of North America and a tentative polar wander curve is suggested. It is concluded that the Precambrian polar wander curve for North America generally moves north and west with a general minimum average rate of $0.1^{\circ}/\text{m.y.}$. There may have been an episode of rapid polar wander between 1200 and 950 million years.

Suggestions for Further Work

The Michikamau anorthosites have yielded promising paleomagnetic results for the age of 1400 million years. Herz (1969) has stated that all known massive

anorthosite bodies of the world were intruded 1400 million years ago. If this were the case it would be of interest to study the paleomagnetism of other massive anorthosites in the northern hemisphere. The paleomagnetism of massive anorthosite bodies might provide an additional control to the reconstruction of northern Atlantic suggested by Bullard and others (1965).

It was pointed out in Chapter 4 that magnetite grains in the form of rods of axial ratio 20:1 or more can be 10 microns long and still behave as single domain grains. It was further suggested that this phenomenon results in high coercivities of the rocks containing these minerals. Only two practical cases are known where this point is proved. In one (Evans and McElhinny 1966) the rods occur in clinopyroxene, in the other case (present work) they occur in plagioclase. It will be of interest to find out what other silicate crystals can accommodate similar rod shaped grains of magnetite.

During the paleomagnetic study of the diabase dikes from the Grenville province, it was noticed that certain dikes of this swarm do not carry a primary component of magnetization representative of the time of intrusion of the dikes. It was shown to be probable that alteration of original titanomagnetite to titanomaghemite was responsible for destroying the primary component of magnetization. However it was not

clear why only certain dikes were altered while the others remained relatively fresh. The extent of alteration might have been decided either by the relative position of the dike in the Grenville province or by the width of the dike and hence of the rate of cooling. It would be of interest to make a quantitative correlation between these parameters and the extent of alteration.

Finally it would be of interest to compare paleomagnetic results from different Precambrian shields of the world. However many more results from the Canadian Shield are necessary before such comparisons are expected to yield significant results.

REFERENCES

- Ade-Hall, J.M., M.A. Khan, P. Dagley and R.L. Wilson (1968): A detailed opaque petrological and magnetic investigation of a single Tertiary lava flow from Skye, Scotland; *Geophys. J. Royal Astr. Soc.*, 16, p. 375-415
- Ade-Hall, J.M. and R.L. Wilson (1969): Opaque petrology and natural remanence polarity in Mull (Scotland) dykes; *Trans. Amer. Geophys. Union*, 50, p. 132
- Akimoto, S. and I. Kushiro (1960): Natural occurrence of titanomaghemite and its relevance to the unstable magnetization of rocks; *J. Geomag. Geoelec.*, 11, p. 94-110
- As, J.A. and J.D.A. Zijderfeld (1958): Magnetic cleaning of rocks in palaeomagnetic research; *Geophys. J. Royal Astr. Soc.*, 1, p. 308-319
- Balsley, J.R. and A.F. Buddington (1958): Iron-titanium oxide minerals, rocks and aeromagnetic anomalies of the Adirondack area, New York; *Econ. Geol.*, 53, p. 777-805
- Bathey, M.H. (1967): The identification of the opaque oxide minerals by optical and X-ray methods; in *Methods in Palaeomagnetism*, Elsevier Publ. Co., Amsterdam, p. 485-495
- Beck, M.E.Jr. and N.C. Lindsley (1969): Paleomagnetism of the Beaver Bay Complex, Minnesota; *J. Geophys. Res.*, 74, p. 2002-2013
- Bergh, H.W. (1968): Paleomagnetism of the Stillwater Complex, Montana; in press
- Bitter, F. (1931): On inhomogeneities in the magnetization of ferromagnetic materials; *Phys. Rev.*, 38, p. 1903-1905
- Black, R.F. (1963): Palaeomagnetism of part of the Purcell System in Southwestern Alberta and Southeastern British Columbia; *Geol. Survey Canada Bull.*, 83, 31 p.
- Blackett, P.M.S. (1952): A negative experiment relating to magnetism and the earth's rotation; *Phil. Trans. Royal Soc. London, ser. A*, 245, p. 303-370

- Books, K.G., W.S. White and M.E. Beck Jr. (1966): Magnetization of Keweenawan gabbro in Northern Wisconsin and its relation to time of intrusion; in Geological Survey Research 1966, U. S. Geol. Survey Profess. Paper, 550D, D117-D124
- Bowie, S.H.U. (1967): Microscopy: Reflected Light; in Physical Methods in Determinative Mineralogy, ed by J. Zussman, Academic Press, New York, p. 103-159
- Bozorth, R.M. (1951): Ferromagnetism; 817 p., D. Van Nostrand Co., New York
- Brailsford, F. (1960): Magnetic Materials; 188 p., Methuen, London
- Brailsford, F. (1966): Physical Principles of Magnetism; 274 p., D. Van Nostrand Co., London
- Bruckshaw, J.M. and E.I. Robertson (1949): The magnetic properties of the tholeiite dykes of north England; Mon. Not. Royal Astr. Soc., Geophys. Supp., 5, p. 308-320
- Brynjólfsson, A. (1957): Studies of remanent magnetism and viscous magnetism in the basalts of Iceland; Phil. Mag., 6, p. 247-254
- Bullard, E., J.E. Everett and A. Gilbert Smith (1965): The fit of the continents around the Atlantic; Phil. Trans. Royal Soc. A, 258, p. 41-51
- Cameron, E.N. (1961): Ore Microscopy; John Wiley & Sons, New York
- Campbell, F.A. (1962): Age of mineralization at Quemont and Horne mines; Canadian Min. Metallurgical Bull., 55, p. 627
- Carmichael, C.M. (1961): The magnetic properties of ilmenite-hematite crystals; Proc. Royal Soc. London, A, 263, p. 508-530
- Chamalaun, F.H. and K.M. Creer (1963): A revised Devonian pole for Britain; Nature, 198, p. 375
- Chamalaun, F.H. and K.M. Creer (1964): Thermal demagnetization studies on the Old Red sandstone of the Anglo-Welsh cuvette; J. Geophys. Res., 69, p. 1607-1616

- Chevallier, R. (1925): L'aimantation des laves de l'Etna et l'orientation du champ terrestre en Sicile du XII^e au XVII^e siècle; Ann. Phys., 4, p. 5-162
- Chikazumi, S. (1964): Physics of Magnetism; 554 p., John Wiley, New York
- Collinson, D.W. and S.K. Runcorn (1960): Polar wandering and continental drift: evidence from paleomagnetic observations in the United States; Bull. Geol. Soc. Amer., 71, p. 915-958
- Cook, R.M. and J.C. Belshé (1958): Archaeomagnetism: a preliminary report from Britain; Antiquity, 32, p. 167-178
- Cox, A. and R.R. Doell (1960): Review of paleomagnetism; Geol. Soc. Amer. Bull., 71, p. 645-768
- Cox, A., R.R. Doell and G.B. Dalrymple (1963): Geomagnetic polarity epochs and Pleistocene geochronometry; Nature, 198, p. 1049-1051
- Creer, K.M. (1959): A.C. demagnetization of unstable Triassic Keuper Marls from S.W. England; Geophys. J. Royal Astr. Soc., 2, p. 261-275
- Creer, K.M. (1961): Superparamagnetism in red sandstones; Geophys. J. Royal Astr. Soc., 5, p. 16-28
- Creer, K.M. (1962): The dispersion of the geomagnetic field due to secular variation and its determination for remote times from paleomagnetic data; J. Geophys. Res., 67, p. 3461-3476
- Deutsch, E.R. (1965): Polar wandering and continental drift: an evaluation of recent evidence; in Polar Wandering and Continental Drift, AAPG publication, p. 1-46
- Dickson, G.O., C.W.F. Everitt, L.G. Parry and F.D. Stacey (1966): Origin of thermoremanent magnetization; Earth Planetary Sci. Letters, 1, p. 222-224
- Doell, R.R. and A. Cox (1967): Analysis of alternating field demagnetization equipment; in Methods in Palaeomagnetism, Elsevier Publishing Co., Amsterdam, p. 241-253

- Doell, R.R. and A. Cox (1967): Palaeomagnetic sampling with a portable coring drill; in *Methods in Palaeomagnetism*, Elsevier Publishing Company, Amsterdam, p. 21-25
- DuBois, P.M. (1962): Palaeomagnetism and correlation of Keweenawan rocks; *Geol. Survey Canada Bull.* 71, 75 p.
- DuBois, R.L. (1964): Virtual geomagnetic pole positions for North America and their suggested paleolatitudes; *Arizona Geol. Survey Digest*, VII, p. 35-51
- Dunlop, D.J. (1968): Monodomain theory: experimental verification; *Science*, 162, p. 256-258
- Eggler, D.H. and E.E. Larson (1968): Palaeomagnetic study of dated Precambrian rocks of the Front Range, Colorado-Wyoming; *Geophys. J. Royal Astr. Soc.*, 14, p. 497-504
- Emslie, R.F. (1964): Potassium-argon age of the Michikamau anorthositic intrusion, Labrador; *Nature*, 202, p. 172-173
- Emslie, R.F. (1965): The Michikamau anorthositic intrusion, Labrador; *Canadian J. Earth Sci.*, 2, p. 385-399
- Evans, M.E. (1968): Magnetization of dikes: a study of the paleomagnetism of the Widgiemooltha dike suite, Western Australia; *J. Geophys. Res.*, 73, p. 3261-3270
- Evans, M.E. (1969): Precambrian palaeomagnetism of Australia and Africa; Ph.D. thesis, Australian National University
- Evans, M.E. and M.W. McElhinny (1966): The paleomagnetism of the Modipe gabbro; *J. Geophys. Res.*, 71, p. 6053-6063
- Evans M.E., M.W. McElhinny and A.C. Gifford (1968): Single domain magnetite and high coercivities in a gabbroic intrusion; *Earth Planetary Sci. Letters*, 4, p. 142-146
- Fahrig, W.F., E.H. Gaucher and A. Larochelle (1965): Palaeomagnetism of diabase dykes of the Canadian shield; *Canadian J. Earth Sci.*, 2, p. 278-298

- Fahrig, W.F. and D.L. Jones (1969): Paleomagnetic evidence for the extent of McKenzie igneous events; Canadian J. Earth Sci., 6, p. 679-688
- Fahrig, W.F. and R.K. Wanless (1963): Age and significance of diabase dyke swarms of the Canadian shield; Nature, 200, p. 934
- Fisher, R.A. (1953): Dispersion on a sphere; Proc. Royal Soc. London, ser. A, 217, p. 295-305
- Giletti, B.J. (1966): Isotopic ages from Southwestern Montana; J. Geophys. Res., 71, p. 4029-4036
- Giletti, B.J. (1968): Isotopic geochronology of Montana and Wyoming; in Radiometric Dating for Geologists, ed. E. I. Hamilton and R.M. Farquhar, Interscience, New York
- Gill, J.E. and R. L'Esperance (1952): Diabase dikes in the Canadian shield; Trans. Royal Soc. Canada, XLVI, p. 25-36
- Gough, D.I. (1956): A study of the palaeomagnetism of the Pilansberg dykes; Mon. Not. Royal Astr. Soc., Geophys. Supp., 7, p. 196-213
- Gough, D.I. (1964): A spinner magnetometer; J. Geophys. Res., 69, p. 2455-2463
- Gough, D.I. (1967): Notes on rock magnetic sampling for palaeomagnetic research; in Methods in Palaeomagnetism, Elsevier Publishing Company, Amsterdam, p. 3-7
- Gough, D.I. and N.D. Opdyke (1963): The palaeomagnetism of the Lupata alkaline volcanics; Geophys. J. Royal Astr. Soc., 7, p. 457-468
- Gough, D.I., N.D. Opdyke and M.W. McElhinny (1964): The significance of paleomagnetic results from Africa; J. Geophys. Res., 69, p. 2509-2519
- Graham, J.W. (1949): The stability and significance of magnetism in sedimentary rocks; J. Geophys. Res., 54, p. 131-167
- Graham, J.W. (1953): Changes of ferromagnetic minerals and their bearing on ferromagnetic properties of rocks; J. Geophys. Res., 58, p. 243-260

- Graham, K.W.T. (1961): The re-magnetization of a surface outcrop by lightning currents; *Geophys. J. Royal Astr. Soc.*, 6, p. 85-102
- Hargraves, R.B. and D.M. Burt (1967): Paleomagnetism of the Allard Lake anorthosite suite; *Canadian J. Earth Sci.*, 4, p. 357-369
- Harrison, J.M. (1963): The Canadian shield mainland; in *Geology and Economic Minerals of Canada*, C.H. Stockwell editor, *Geol. Surv. Canada Econ. Geol. ser. 1*
- Hatch, F.H., A.K. Wells and M.K. Wells (1961): Petrology of the igneous rocks; 515 p., Thomas Murby and Co., London
- Hays, W.W. and L. Scharon (1966): A paleomagnetic investigation of some of the Precambrian igneous rocks of Southeast Missouri; *J. Geophys. Res.*, 71, p. 553-560
- Helsley, C.E. (1967): Advantages of field-drilling of samples for palaeomagnetic studies; in *Methods in Palaeomagnetism*, Elsevier Publishing Co., Amsterdam, p. 26-30
- Herz, N. (1969): Anorthosite belts, Continental Drift, and the Anorthosite event; *Science*, 164, p. 944-947
- Hood, P.J. (1958): Quoted in Cox and Doell (1960)
- Hood, P.J. (1961): Paleomagnetic study of the Sudbury basin; *J. Geophys. Res.*, 66, p. 1235-1241
- Hospers, J. (1955): Rock magnetism and polar wandering; *J. Geology*, 63, p. 59-74
- Hsu, I-Chi, R.E. Anderson and L. Scharon (1966): Paleomagnetic properties of some of the Precambrian rocks of Missouri; *J. Geophys. Res.*, 71, p. 2645-2650
- Hutchings, A. (1967): Computations of the behaviour of two- and three- axis rotation systems; in *Methods in Palaeomagnetism*, Elsevier Publishing Co., Amsterdam, p. 224-236
- Irving, E. (1959): Palaeomagnetic pole positions: a survey and analysis; *Geophys. J. Royal Astr. Soc.*, 2, p. 51-79
- Irving, E. (1964): Paleomagnetism and its Application to Geological and Geophysical Problems; 399 p., John Wiley, New York

- Irving, E., W.A. Robertson, P.M. Stott, D.H. Tarling and M.A. Ward (1961): Treatment of partially stable sedimentary rocks showing planar distribution of directions of magnetization; J. Geophys. Res., 66, p. 1927-1933
- Irving, E., P.M. Stott and M.A. Ward (1961): Demagnetization of igneous rocks by alternating magnetic fields; Phil. Mag., 6, p. 225-241
- Johnson, E.A. and A.G. McNish (1938): An alternating-current apparatus for measuring small magnetic moments; Terr. Magn. Atmos. Elec., 43, p. 393-399
- Johnson, E.A. and W.F. Steiner (1937): An astatic magnetometer for measuring susceptibility; Rev. Sci. Instr., 8, p. 236-238
- Jones, D.L. and M.W. McElhinny (1967): Stratigraphic interpretation of paleomagnetic measurements on the Waterberg redbeds of South Africa; J. Geophys. Res., 72, p. 4171-4179
- Katsura, T. and I. Kushiro (1961): Titanomagnetite in igneous rocks; Amer. Miner., 46, p. 134-145
- Kittel, C. (1946): Theory of the structure of ferromagnetic domains in films and small particles; Phys. Rev., 70, p. 965-971
- Kittel, C. (1949): Physical theory of ferromagnetic domains; Rev. Mod. Phys., 21, p. 541-583
- Koenigsberger, J.G. (1930): Grossenverhältnis von remanentem zu induziertem magnetismus in gesteinen; grosse und richtung des remanenten magnetismus; Z. Geophys., 6, p. 190-207
- Ku, C.C., S. Sun, H. Soffel and L. Scharon (1967): Paleomagnetism of the basement rocks, Wichita mountains, Oklahoma; J. Geophys. Res., 72, p. 731-737
- Larochelle, A. (1966): Palaeomagnetism of the Abitibi dyke swarm; Canadian J. Earth Sci., 3, p. 671-683
- Larochelle, A. (1967): The palaeomagnetism of the Sudbury diabase dyke swarm; Canadian J. Earth Sci., 4, p. 323-332

- Larson, E., M. Ozima, M. Ozima, T. Nagata and D. Strangway (1969): Stability of remanent magnetization of igneous rocks; *Geophys. J. Royal Astr. Soc.*, 17, p. 263-292
- Larson, E.E. and D. W. Strangway (1969): Magnetization of the Spanish Peaks dike swarm, Colorado, and Shiprock dike, New Mexico; *J. Geophys. Res.*, 74, p. 1505-1514
- Li, Yin-Yuan (1956): Domain walls in antiferromagnets and the weak ferromagnetism of $\alpha\text{Fe}_2\text{O}_3\text{-FeO}$; *Phys. Rev.*, 101, p. 1450-1454
- McElhinny, M.W. (1963): Rock magnetism data reduction; Princeton Univ. Dept. Geol. Engg Report 63-3
- McElhinny, M.W. (1964): Statistical significance of the fold test in palaeomagnetism; *Geophys. J. Royal Astr. Soc.*, 8, p. 338-340
- McElhinny, M.W. (1966): An improved method for demagnetizing rocks in alternating magnetic fields; *Geophys. J. Royal Astr. Soc.*, 10, p. 369-374
- McElhinny, M.W. (1968): Palaeomagnetic directions and pole positions-VIII pole numbers 8/1 to 8/186; *Geophys. J. Royal Astr. Soc.*, 15, p. 409-430
- McElhinny, M.W. (1968): Palaeomagnetic directions and pole positions-IX pole numbers 9/1 to 9/159; *Geophys. J. Royal Astr. Soc.*, 16, p. 207-224
- McElhinny, M.W., J.C. Briden, D.L. Jones and A. Brock (1968): Geological and geophysical implications of paleomagnetic results from Africa; *Rev. Geophys.*, 6, p. 201-238
- McElhinny, M.W. and D.I. Gough (1963): The palaeomagnetism of the Great dyke of Southern Rhodesia; *Geophys. J. Royal Astr. Soc.*, 7, p. 287-303
- McElhinny, M.W. and T.J. Neal (1967): Portable field sampling equipment; in *Methods in Palaeomagnetism*, Elsevier Publishing Co., Amsterdam, p. 36-40
- Moriya, Toru (1960): Anisotropic superexchange interaction and weak ferromagnetism; *Phys. Rev.*, 120, p. 91-98
- Morrish, A.H. (1965): *The Physical Principles of Magnetism*; 680 p., John Wiley, New York

- Morrish, A.H. and S.P. Yu (1955): Dependence of the coercive force on the density of some iron oxide powders; J. Appl. Phys., 26, p. 1049-1055
- Morse, S.A. (1964): Age of Labrador anorthosites; Nature, 203, p. 509-510
- Nagata T. (1940): On the natural remanent magnetization of the lava composing the central cone of volcano Mihara; Bull. Earthquake Res. Instt., 17, p. 281-287
- Nagata, T. (1943): The natural remanent magnetism of volcanic rocks and its relation to geomagnetic phenomena; Bull. Earthquake Res. Instt., 21, p. 1-192
- Nagata, T. (1953): Rock Magnetism; 225 p. Maruzen Co., Tokyo
- Nagata, T. (1961): Rock Magnetism; 350 p., Maruzen Co., Tokyo
- Nagata, T. (1967): Identification of magnetic minerals in rocks using methods based on their magnetic properties; in Methods in Palaeomagnetism, Elsevier Publishing Co., Amsterdam, p. 501-513
- Nairn, A.E.M., D.V. Frost and B.G. Light (1959): Palaeomagnetism of certain rocks from Newfoundland; Nature, 183, p. 596-597
- Néel, L. (1947): Propriétés d'un ferromagnétique cubique en grains fins; C. R. Acad. Sci. Paris, 224, p. 1488-1490
- Néel, Louis (1949): Essai d'interprétation des propriétés magnétiques du sesquioxyde de fer rhomboédrique; Ann. Phys., 41, p. 249-268
- Néel, L. (1949): Théorie du trainage magnétique des ferromagnétiques au grains fins avec applications aux terres cuites; Ann. Geophys., 5, p. 99-136
- Néel, L. (1951): L'inversion de l'aimantation permanente des roches; Ann. Geophys., 7, p. 90-102
- Néel, Louis (1953): Some new results on antiferromagnetism and ferromagnetism; Rev. Mod. Phys., 25, p. 58-63
- Néel, Louis (1955): Some theoretical aspects of rock magnetism; Phil. Mag. Supp. Adv. Phys., 4, p. 191-243

- Nicholls, G.D. (1955): The mineralogy of rock magnetism; Phil. Mag. Supp. Adv. Phys., 4, p. 113-190
- Norris, D.K. and R.F. Black (1961): Application of palaeomagnetism to thrust mechanics; Nature, 192, p. 933-935
- Obradovich, J.D. and Z.E. Peterman (1968): Geochronology of the Belt Series, Montana; Canadian J. Earth Sci., 5, p. 737-747
- Opdyke, N.D. (1967): A large sampling drill; in Methods in Palaeomagnetism, Elsevier Publishing Co., Amsterdam, p. 41-43
- Ozima, M. and E.E. Larson (1967): Study on irreversible change of magnetic properties of some ferromagnetic materials; J. Geomag. Geoelec., 19, p. 117-128
- Ozima, M. and M. Ozima (1965): Origin of thermoremanent magnetization; J. Geophys. Res., 70, p. 1363-1369
- Palmer, H.C. (1968): Paleomagnetism of Keweenawan volcanic rocks from the Lake Superior region; Trans. Amer. Geophys. Union, 49, p. 130-131
- Palmer, H.C. (1969): The paleomagnetism of the Croker Island Complex, Ontario, Canada; Canadian J. Earth Sci., 6, p. 213-218
- Powell, K.W. (1963): Significance of differences in magnetization along certain dolerite dikes; Nature, 199, p. 674-676
- Robertson, W.A. (1963): Construction of non-magnetic oven; in Summary of Activities-Office and Laboratory, Geol. Survey Canada Paper 64-2, p. 51-52
- Robertson, W.A. (1964): Palaeomagnetic results from northern Canada suggesting a tropical Proterozoic climate; Nature, 204, p. 66-67
- Roche, A. (1960): Sur l'aimantation de laves Miocenes d'Auvergne; C. R. Acad. Sci. Paris, 246, p. 3364-3366
- Roquet, J. (1954): Sur les remanences des oxydes de fer et leur interet en geomagnetisme; Ann. Geophys., 10, p. 226-247

- Runcorn, S.K. (1964): Paleomagnetic results from Precambrian sedimentary rocks in the western United States; Geol. Soc. Amer. Bull., 75, p. 687-704
- Sopher, S.R. (1963): Palaeomagnetic study of the Sudbury Irruptive; Geol. Survey Canada Bull., 90, 34 p.
- Spall, H. (1968): Paleomagnetism of basement granites of southern Oklahoma and its implications; progress report; Okl. Geol. Survey Notes, 28, p. 65-80
- Stacey, F.D. (1963): The physical theory of rock magnetism; Phil. Mag. Supp. Adv. Phys., 12, p. 46-133
- Stoner, E.C. and E.P. Wohlfarth (1947): Interpretation of high coercivity in ferromagnetic materials; Nature, 160, p. 650-651
- Stoner, E.C. and E.P. Wohlfarth (1948): A mechanism of magnetic hysteresis in heterogeneous alloys; Phil. Trans. Royal Soc., ser. A, 240, p. 599-642
- Strangway, D.W. (1961): Magnetic properties of diabase dikes; J. Geophys. Res., 66, p. 3021-3032
- Strangway, D.W. (1964): Rock magnetism and dike classification; J. Geol., 72, p. 648-663
- Strangway, D.W. (1967): Field tests for stability; in Methods in Palaeomagnetism, Elsevier Publishing Co., Amsterdam, p. 209-216
- Strangway, D.W., E.E. Larson and M. Goldstein (1968): A possible cause of high magnetic stability in volcanic rocks; J. Geophys. Res., 73, p. 3787-3795
- Symons, D.T.A. (1967): Paleomagnetic evidence on the origin of the Marquette and Steep Rock hard hematite and goethite deposits; Canadian J. Earth Sci., 4, p. 1-20
- Symons, D.T.A. (1967): Paleomagnetism of Pre-Cambrian rocks near Cobalt, Ontario; Canadian J. Earth Sci., 4, p. 1161-1169
- Tarling, D.H. and D.T.A. Symons (1967): A stability index of remanence in palaeomagnetism; Geophys. J. Royal Astr. Soc., 12, p. 443-448
- Theillier, E. (1938): Thesis, University of Paris

- Thellier, E. (1966): Methods and apparatus for alternating current and thermal demagnetization; in *Methods and Techniques in Geophysics*, Vol. 2, p. 205-247
- Thellier, E. and F. Rimbart (1954): Sur l'analyse d'aimantations fossiles par action de champs magnetiques alternatifs; *C. R. Acad. Sci., Paris*, 239, p. 1399-1401
- Tilton, G.R., G.W. Wetherill and G.L. Davis (1962): Mineral ages from the Wichita and Arbuckle Mountains, Oklahoma, and the St. Francois Mountains, Missouri; *J. Geophys. Res.*, 67, p. 4011-4019
- Uyeda, S. (1958): Thermoremanent magnetism as a medium of paleomagnetism, with special reference to reverse thermoremanent magnetism; *Japan. J. Geophys.*, 2, p. 1-123
- Uyeda, S. (1962): Thermoremanent magnetism and reverse thermoremanent magnetism; in *Proceedings of the Benedum Earth Magnetism Symposium*, ed. T. Nagata, p. 87-106, University of Pittsburgh Press
- Verhoogen, J. (1959): The origin of thermoremanent magnetization; *J. Geophys. Res.*, 64, p. 2441-2450
- Vincenz, S.A. (1968): Phenomenon of partial self-reversal in Keweenawan rocks, 1. Magnetization of Portage Lake lavas; *J. Geophys. Res.*, 73, p. 2729-2752
- Vine, F.J. and D.H. Matthews (1963): Magnetic anomalies over ocean ridges; *Nature*, 199, p. 947-949
- Wanless, R.K., R.D. Stevens, G.R. Lachance and C.M. Edmonds (1967): Age determinations and geological studies: K-Ar Isotopic ages, report 7; *Geol. Surv. Canada Paper* 66-17
- Wanless, R.K., R.D. Stevens, G.R. Lachance and R.Y. Rimsaite (1965): Age determinations and geologic studies; *Geol. Survey Canada Paper* 64-17
- Watkins, N.D. (1967): Unstable components and paleomagnetic evidence for a geomagnetic polarity transition; *J. Geomag. Geoelec.*, 19, p. 63-76

- Watson, G.S. (1956): Analysis of dispersion on a sphere; Mon. Not. Royal Astr. Soc., Geophys. Supp., 7, p. 153-159
- Watson, G.S. and E. Irving (1957): Statistical methods in rock magnetism; Mon. Not. Royal Astr. Soc. Geophys. Supp., 7, p. 289-300
- Weiss, P. (1907): L'hypothese du champ moleculaire et la propriete ferromagnetique; J. de Physique, 6, p. 661
- Wilson, M.E. (1965): The Precambrian of Canada; the Canadian Shield; in the Geologic Systems; the Precambrian, ed. K. Rankama, p. 263-415, Interscience Publishers, New York
- Wilson, R.L. (1962): An instrument for measuring vector magnetization at high temperatures; Geophys. J. Royal Astr. Soc., 7, p. 125-130
- Wilson, R.L., S.E. Haggerty and N.D. Watkins (1968): Variation of palaeomagnetic stability and other parameters in a vertical traverse of a single Icelandic lava; Geophys. J. Royal Astr. Soc., 16, p. 79-96
- Wilson, R.L. and N.D. Watkins (1967): Correlation of petrology and natural magnetic polarity in Columbia Plateau basalts; Geophys. J. Royal Astr. Soc., 12, p. 405-424
- Wright, J.B. (1968): Polarity reversals and oxidation state in rocks; Geophys. J. Royal Astr. Soc., 16, p. 161-167

TABLE A1

SPECIMEN MAGNETIZATION DIRECTIONS OF ANORTHOSITES (NRM)

SPECIMEN	AZIMUTH DEG	INCL DEG	INTENSITY EMU/CC
ANO11A	265.5	49.0	0.123E-02
ANO11B	278.0	44.0	0.116E-02
ANO12A	277.0	52.5	0.142E-02
ANO12B	253.0	64.0	0.140E-02
ANO13A	271.0	19.5	0.167E-02
ANO13B	270.0	25.5	0.186E-02
ANO14A	270.0	43.0	0.135E-02
ANO14B	251.0	20.0	0.243E-02
ANO15A	271.0	46.0	0.117E-02
ANO15B	280.5	40.0	0.137E-02
ANO16A	254.0	42.0	0.199E-02
ANO16B	260.0	34.0	0.200E-02
ANO21A	219.0	12.5	0.280E-02
ANO21B	243.0	6.0	0.345E-02
ANO23A	273.0	-3.0	0.252E-02
ANO23B	257.0	26.0	0.342E-02
ANO24A	220.0	-17.0	0.290E-03
ANO24B	247.0	61.0	0.641E-02
ANO25A	272.0	34.0	0.531E-02
ANO25B	253.0	26.0	0.227E-02
ANO26A	271.0	14.5	0.102E-01
ANO26B	281.5	12.5	0.759E-02
ANO31A	67.0	58.0	0.240E-03
ANO31B	40.0	51.0	0.330E-03
ANO32A	23.0	45.0	0.120E-03
ANO32B	190.0	33.5	0.170E-03
ANO33A	243.0	68.0	0.104E-01
ANO33B	135.0	65.0	0.127E-01
ANO34A	251.0	67.0	0.878E-02
ANO34B	250.0	60.5	0.646E-02
ANO35A	257.0	22.0	0.301E-02
ANO35B	267.0	26.0	0.391E-02
ANO41A	278.0	2.5	0.108E-01
ANO41B	287.0	16.0	0.117E-01
ANO42A	277.5	-13.5	0.371E-02
ANO42B	274.0	-10.0	0.296E-02
ANO43A	287.0	-4.0	0.333E-02
ANO43B	261.0	-12.0	0.306E-02
ANO44A	260.0	2.0	0.514E-02

TABLE A1 (CONTD)

SPECIMEN	AZIMUTH DEG	INCL DEG	INTENSITY EMU/CC
ANO44B	261.0	2.0	0.567E-02
ANO51A	311.0	25.0	0.135E-02
ANO51B	300.0	28.0	0.960E-03
ANO52A	248.0	-8.0	0.837E-02
ANO52B	273.5	-9.0	0.884E-02
ANO53A	278.0	-19.0	0.980E-02
ANO53B	278.0	-6.0	0.793E-02
ANO54A	258.5	9.0	0.114E-01
ANO54B	262.0	-3.0	0.106E-01
ANO55A	272.0	-9.5	0.848E-02
ANO55B	260.0	-17.0	0.930E-02
ANO61A	285.0	34.0	0.236E-02
ANO61B	273.0	34.0	0.224E-02
ANO62A	254.0	18.5	0.259E-02
ANO62B	244.0	16.0	0.277E-02
ANO63A	268.0	28.0	0.304E-02
ANO63B	268.0	28.0	0.234E-02
ANO64A	255.0	6.0	0.304E-02
ANO64B	264.0	22.5	0.159E-02

TABLE A2

SAMPLE MAGNETIZATION DIRECTIONS OF ANORTHOSITES (NRM)

SAMPLE	NN	AZIMUTH	INCL	THETA
ANO11	2	272.04	46.67	9.93
ANO12	2	266.98	58.80	16.89
ANO13	2	270.51	22.50	6.07
ANO14	2	259.30	31.85	27.99
ANO15	2	275.98	43.10	9.17
ANO16	2	257.16	38.04	9.29
ANO21	2	231.11	9.45	24.55
ANO23	2	265.42	11.61	32.88
ANO24	2	229.01	22.50	80.95
ANO25	2	262.11	30.34	18.25
ANO26	2	276.27	13.55	10.40
ANO31	2	52.32	55.25	17.02
ANO32	2	142.33	80.30	100.62
ANO33	2	184.26	75.62	37.68
ANO34	2	250.44	63.75	6.51
ANO35	2	261.92	24.08	9.97
ANO41	2	282.41	9.28	16.15
ANO42	2	275.74	-11.76	4.90
ANO43	2	274.13	-8.21	26.94
ANO44	2	260.50	2.00	1.00
ANO51	2	305.57	26.61	10.29
ANO52	2	260.73	-8.71	25.23
ANO53	2	278.00	-12.50	13.00
ANO54	2	260.26	3.00	12.50
ANO55	2	266.09	-13.32	13.87
ANO61	2	279.00	34.15	9.94
ANO62	2	248.97	17.31	9.87
ANO63	2	268.00	28.00	0.0
ANO64	2	259.33	14.29	18.65

NN = NUMBER OF SPECIMENS FROM EACH CORE

K = ESTIMATE OF FISHER PRECISION PARAMETER K

ALPHA = RADIUS OF 95% CONFIDENCE LIMIT

THETA = ANGLE BETWEEN THE TWO VECTORS OF
MAGNETIZATION FOR EACH CORE

TABLE A3

STEPWISE A.F. DEMAGNETIZATION OF SOME REPRESENTATIVE
ANORTHOSITE SPECIMENS

DEMAGNETIZATION HISTORY OF AN012A

STATE	AZIM	INCL	PSI	J	J/J0
0	275.3	52.5	0.0	0.245E-02	1.0000
50	277.8	28.5	24.0	0.221E-02	0.9022
100	275.0	24.2	5.0	0.196E-02	0.7989
150	273.0	24.3	1.8	0.174E-02	0.7117
200	274.3	25.5	1.7	0.161E-02	0.6587
300	270.1	25.6	3.8	0.143E-02	0.5843
400	272.1	25.9	1.8	0.126E-02	0.5128
500	270.8	25.7	1.2	0.106E-02	0.4330
600	264.7	24.3	5.7	0.828E-03	0.3382
700	268.1	27.0	4.1	0.697E-03	0.2846

DEMAGNETIZATION HISTORY OF AN023B

STATE	AZIM	INCL	PSI	J	J/J0
0	257.4	26.0	0.0	0.596E-02	1.0000
50	275.5	12.5	21.7	0.404E-02	0.6773
100	275.0	13.4	1.1	0.294E-02	0.4933
200	278.5	13.1	3.4	0.225E-02	0.3779
300	280.3	13.2	1.8	0.165E-02	0.2766
400	277.3	13.8	3.0	0.115E-02	0.1937
500	277.6	15.3	1.5	0.820E-03	0.1376
600	275.7	16.7	2.3	0.635E-03	0.1066
700	273.2	17.8	2.6	0.466E-03	0.0782

DEMAGNETIZATION HISTORY OF AN024A

STATE	AZIM	INCL	PSI	J	J/J0
0	220.7	-17.3	0.0	0.510E-03	1.0000
100	222.0	-14.8	2.8	0.380E-03	0.7441
200	221.8	-12.8	2.0	0.287E-03	0.5630
300	221.3	-8.8	4.0	0.227E-03	0.4438
400	220.3	-1.2	7.7	0.186E-03	0.3635

DEMAGNETIZATION HISTORY OF AN031A

STATE	AZIM	INCL	PSI	J	J/J0
0	67.1	57.5	0.0	0.425E-03	1.0000
50	48.0	31.0	29.7	0.102E-03	0.2396
100	273.1	0.6	126.8	0.163E-03	0.3839
150	261.8	0.5	11.4	0.159E-03	0.3736
200	271.6	2.4	10.0	0.173E-03	0.4068
250	267.2	0.7	4.8	0.151E-03	0.3558
300	267.7	-3.4	4.1	0.130E-03	0.3052
400	258.5	-4.4	9.2	0.120E-03	0.2821
500	265.8	-10.3	9.3	0.107E-03	0.2526
600	263.4	-9.1	2.6	0.915E-04	0.2153
700	271.3	-9.5	7.8	0.768E-04	0.1808

DEMAGNETIZATION HISTORY OF AN034A

STATE	AZIM	INCL	PSI	J	J/J0
0	250.3	66.4	0.0	0.154E-01	1.0000
50	249.4	30.7	35.8	0.306E-02	0.1982
100	244.0	58.6	28.2	0.133E-02	0.0862
150	240.2	63.9	5.6	0.999E-03	0.0648
200	236.9	63.9	1.5	0.826E-03	0.0536
300	230.0	67.0	4.2	0.610E-03	0.0396
400	224.9	69.9	3.4	0.434E-03	0.0281
500	226.2	79.2	9.3	0.404E-03	0.0262

DEMAGNETIZATION HISTORY OF AN034B

STATE	AZIM	INCL	PSI	J	J/J0
0	250.0	60.3	0.0	0.114E-01	1.0000
50	255.4	30.5	30.0	0.241E-02	0.2126
100	243.5	44.3	16.6	0.101E-02	0.0898
150	239.7	43.8	2.8	0.764E-03	0.0673
200	238.4	45.0	1.5	0.620E-03	0.0546
300	223.1	43.8	10.9	0.430E-03	0.0378
400	221.6	45.0	1.6	0.316E-03	0.0279
500	222.6	37.8	7.2	0.277E-03	0.0244
600	195.5	32.7	22.7	0.197E-03	0.0174
700	210.7	42.8	15.7	0.197E-03	0.0173

DEMAGNETIZATION HISTORY OF AN035B

STATE	AZIM	INCL	PSI	J	J/J0
0	267.2	25.8	0.0	0.676E-02	1.0000
50	264.6	20.8	5.6	0.247E-02	0.3657
100	267.6	19.8	3.0	0.127E-02	0.1883
200	268.0	15.1	4.7	0.829E-03	0.1225
300	270.0	10.9	4.6	0.587E-03	0.0868
400	275.8	2.4	10.3	0.334E-03	0.0493
500	292.3	-2.4	17.1	0.241E-03	0.0356
600	301.2	-10.7	12.2	0.156E-03	0.0230

DEMAGNETIZATION HISTORY OF AN041B

STATE	AZIM	INCL	PSI	J	J/J0
0	286.7	17.2	0.0	0.208E-01	1.0000
200	288.8	23.9	7.0	0.325E-02	0.1559
300	291.6	27.2	4.2	0.217E-02	0.1041
400	287.5	32.1	6.1	0.145E-02	0.0695
500	298.9	34.6	9.8	0.115E-02	0.0551
600	279.0	55.5	25.0	0.698E-03	0.0335
700	273.5	70.7	15.4	0.583E-03	0.0280

DEMAGNETIZATION HISTORY OF AN042A

STATE	AZIM	INCL	PSI	J	J/J0
0	278.3	-13.0	0.0	0.646E-02	1.0000
50	266.1	-9.6	12.5	0.582E-02	0.9003
100	182.5	-19.2	80.9	0.445E-02	0.6882
200	262.6	-8.6	77.9	0.225E-02	0.3475
300	261.8	-8.1	0.8	0.143E-02	0.2210
400	258.2	-7.5	3.6	0.107E-02	0.1661
500	262.9	-9.2	4.8	0.675E-03	0.1044
600	266.8	-8.5	3.9	0.444E-03	0.0688
700	262.3	-3.6	6.6	0.302E-03	0.0467

DEMAGNETIZATION HISTORY OF AN053A

STATE	AZIM	INCL	PSI	J	J/J0
0	278.5	-19.4	0.0	0.169E-01	1.0000
50	277.7	-19.4	0.8	0.162E-01	0.9595
100	276.9	-18.3	1.3	0.136E-01	0.8068
150	275.0	-17.2	2.1	0.108E-01	0.6400
200	273.2	-16.4	1.9	0.892E-02	0.5283
300	269.1	-15.0	4.2	0.607E-02	0.3592
400	266.6	-14.0	2.5	0.452E-02	0.2675
500	262.9	-12.6	3.9	0.322E-02	0.1907
600	267.5	-10.5	5.0	0.239E-02	0.1415
700	256.1	-8.9	11.3	0.151E-02	0.0893

DEMAGNETIZATION HISTORY OF AN061A

STATE	AZIM	INCL	PSI	J	J/J0
0	283.2	34.1	0.0	0.417E-02	1.0000
100	283.1	33.4	0.7	0.403E-02	0.9665
200	279.1	30.0	4.8	0.327E-02	0.7856
300	278.4	25.7	4.3	0.277E-02	0.6655
400	275.5	23.5	3.5	0.227E-02	0.5460
500	273.6	22.1	2.3	0.180E-02	0.4313
600	274.6	23.5	1.7	0.147E-02	0.3534
700	272.9	25.4	2.5	0.115E-02	0.2758

TABLE A4

SPECIMEN MAGNETIZATION DIRECTIONS OF ANORTHOSITES
AFTER OPTIMUM DEMAGNETIZATION

SPECIMEN	AZIMUTH DEG	INCL DEG	INTENSITY EMU/CC
ANO11A	258.5	18.0	0.650E-03
ANO11B	255.5	12.0	0.650E-03
ANO12A	273.0	24.0	0.820E-03
ANO12B	262.0	29.5	0.690E-03
ANO13B	257.5	10.5	0.115E-02
ANO14A	249.0	25.0	0.900E-03
ANO14B	254.0	9.0	0.165E-02
ANO15A	252.0	25.0	0.770E-03
ANO15B	256.0	23.0	0.770E-03
ANO16A	251.0	21.0	0.129E-02
ANO16B	248.5	16.0	0.123E-02
ANO21A	241.0	20.5	0.980E-03
ANO21B	274.0	13.5	0.129E-02
ANO23A	276.0	-21.0	0.130E-02
ANO23B	280.5	14.0	0.202E-02
ANO24A	221.0	-9.0	0.130E-03
ANO24B	257.0	-12.0	0.240E-03
ANO25A	275.0	20.0	0.930E-03
ANO25B	251.0	23.5	0.810E-03
ANO26A	270.5	11.5	0.150E-02
ANO26B	278.0	0.0	0.126E-02
ANO31A	267.0	2.0	0.600E-04
ANO31B	231.0	28.0	0.120E-03
ANO32A	269.5	-17.0	0.900E-04
ANO32B	278.0	-28.5	0.300E-04
ANO33A	275.0	37.0	0.340E-03
ANO33B	255.0	52.0	0.260E-03
ANO34A	232.0	68.0	0.350E-03
ANO34B	224.0	45.0	0.250E-03
ANO35A	264.5	14.0	0.260E-03
ANO35B	270.0	12.0	0.330E-03
ANO41A	283.5	-3.5	0.202E-02
ANO41B	286.5	24.0	0.192E-02
ANO42A	262.0	-10.0	0.126E-02
ANO42B	257.0	-7.5	0.116E-02
ANO43A	284.5	-1.5	0.111E-02
ANO43B	259.0	-13.0	0.930E-03
ANO44A	250.0	-6.0	0.900E-03

TABLE A4 (CONTD)

SPECIMEN	AZIMUTH DEG	INCL DEG	INTENSITY EMU/CC
ANO44B	258.5	-1.0	0.123E-02
ANO51A	261.0	-13.5	0.730E-03
ANO51B	266.0	-13.0	0.800E-03
ANO52A	247.5	-6.0	0.261E-02
ANO52B	273.0	-7.5	0.282E-02
ANO53A	270.0	-15.0	0.349E-02
ANO53B	276.0	-11.0	0.318E-02
ANO54A	251.5	4.0	0.337E-02
ANO54B	258.0	-6.0	0.366E-02
ANO55A	262.0	-7.0	0.239E-02
ANO55B	260.0	-13.0	0.268E-02
ANO61A	279.0	26.5	0.148E-02
ANO61B	271.5	26.0	0.148E-02
ANO62A	264.0	21.5	0.167E-02
ANO62B	262.0	18.0	0.173E-02
ANO63A	265.5	20.5	0.212E-02
ANO63B	265.5	20.5	0.162E-02
ANO64A	259.0	12.0	0.183E-02
ANO64B	254.0	20.5	0.990E-03

TABLE A5

SAMPLE MAGNETIZATION DIRECTIONS OF ANORTHOSITES
AFTER OPTIMUM DEMAGNETIZATION

SAMPLE	NN	AZIMUTH	INCL	THETA
ANO11	2	256.98	15.00	6.66
ANO12	2	273.00	24.00	0.02
ANO13	2	257.75	10.00	1.11
ANO14	2	251.61	17.02	16.69
ANO15	2	254.02	24.01	4.17
ANO16	2	249.73	18.50	5.53
ANO21	2	257.82	17.69	32.26
ANO23	2	278.29	-3.50	35.28
ANO24	2	238.91	-11.03	35.50
ANO25	2	263.15	22.19	22.54
ANO26	2	274.29	5.76	13.70
ANO31	2	250.15	15.73	43.09
ANO32	2	273.57	-22.81	13.91
ANO33	2	266.31	44.93	20.57
ANO34	2	226.77	56.56	23.38
ANO35	2	267.26	13.01	5.72
ANO41	2	284.93	10.25	27.65
ANO42	2	259.49	-8.76	5.54
ANO43	2	271.92	-7.43	27.74
ANO44	2	254.26	-3.51	9.85
ANO51	2	263.50	-13.26	4.89
ANO52	2	260.23	-6.92	25.36
ANO53	2	273.02	-13.02	7.08
ANO54	2	254.74	-1.00	11.92
ANO55	2	261.01	-10.00	6.31
ANO61	2	275.24	26.30	6.74
ANO62	2	262.99	19.75	3.97
ANO63	2	265.50	20.50	0.0
ANO64	2	256.55	16.26	9.76

NN = NUMBER OF SPECIMENS FROM EACH CORE

K = ESTIMATE OF FISHER PRECISION PARAMETER K

ALPHA = RADIUS OF 95% CONFIDENCE LIMIT

THETA = ANGLE BETWEEN THE TWO VECTORS OF
MAGNETIZATION FOR EACH CORE

TABLE B1

A.F. DEMAGNETIZATION OF REPRESENTATIVE ANORTHOSITE
SPECIMENS UP TO 1800 DE.

DEMAGNETIZATION HISTORY OF AN014B

STATE	AZIM	INCL	PSI	J	J/J0
0	250.9	20.2	0.0	0.430E-02	1.0000
50	256.7	12.6	9.4	0.176E-02	0.4095
100	254.2	7.2	6.0	0.362E-02	0.8416
150	250.5	6.2	3.8	0.333E-02	0.7743
200	249.3	6.2	1.2	0.319E-02	0.7408
300	248.6	6.7	0.8	0.291E-02	0.6778
400	246.2	6.2	2.5	0.262E-02	0.6087
500	249.9	5.9	3.7	0.229E-02	0.5318
600	242.9	6.4	6.9	0.184E-02	0.4269
700	243.9	5.1	1.6	0.150E-02	0.3486
800	245.6	8.4	3.7	0.117E-02	0.2720
900	191.9	8.7	53.1	0.854E-03	0.1986
1000	247.9	7.6	55.4	0.641E-03	0.1492
1200	237.3	7.7	10.6	0.406E-03	0.0943
1400	251.9	7.7	14.5	0.245E-03	0.0570
1600	260.3	18.8	13.8	0.133E-03	0.0309
1800	282.1	23.2	20.9	0.109E-03	0.0253

DEMAGNETIZATION HISTORY OF AN021A

STATE	AZIM	INCL	PSI	J	J/J0
0	216.8	12.3	0.0	0.483E-02	1.0000
50	240.8	18.5	24.0	0.412E-02	0.8521
100	239.1	21.2	3.2	0.330E-02	0.6835
200	237.2	21.9	1.9	0.240E-02	0.4964
250	239.8	20.6	2.7	0.206E-02	0.4256
300	240.0	20.3	0.4	0.174E-02	0.3597
400	238.1	20.3	1.8	0.126E-02	0.2606
500	235.7	19.8	2.4	0.830E-03	0.1718
600	235.5	20.1	0.4	0.601E-03	0.1243
700	235.4	18.1	1.9	0.435E-03	0.0900
800	231.0	18.4	4.2	0.349E-03	0.0722
900	238.4	17.3	7.1	0.259E-03	0.0537
1000	226.2	18.5	11.7	0.192E-03	0.0397

DEMAGNETIZATION HISTORY OF AN021A CONTD

STATE	AZIM	INCL	PSI	J	J/J0
1200	237.5	11.9	12.8	0.159E-03	0.0328
1400	227.4	13.7	10.0	0.111E-03	0.0229
1600	218.5	15.3	8.7	0.859E-04	0.0178
1800	189.8	9.3	28.7	0.548E-04	0.0113

DEMAGNETIZATION HISTORY OF AN051A

STATE	AZIM	INCL	PSI	J	J/J0
0	309.3	24.2	0.0	0.243E-02	1.0000
50	268.6	-0.2	46.3	0.189E-02	0.7802
100	266.0	-11.5	11.6	0.165E-02	0.6807
150	263.3	-11.8	2.7	0.151E-02	0.6223
200	263.4	-11.2	0.6	0.142E-02	0.5835
300	261.5	-13.4	2.9	0.129E-02	0.5315
400	262.8	-10.7	3.0	0.111E-02	0.4593
500	260.5	-10.0	2.3	0.927E-03	0.3818
600	259.9	-7.7	2.4	0.787E-03	0.3242
700	258.8	-15.4	7.8	0.689E-03	0.2838
800	269.1	-10.6	11.1	0.527E-03	0.2170
900	268.3	-10.6	0.8	0.379E-03	0.1563
1000	265.6	-2.5	8.5	0.228E-03	0.0941
1200	276.1	-9.0	12.4	0.336E-03	0.1383
1400	247.2	-23.5	31.2	0.987E-04	0.0407

DEMAGNETIZATION HISTORY OF AN064B

STATE	AZIM	INCL	PSI	J	J/J0
0	264.0	21.3	0.0	0.285E-02	1.0000
50	248.6	27.2	15.2	0.287E-02	1.0096
100	248.4	25.8	1.5	0.261E-02	0.9163
150	249.3	24.4	1.6	0.234E-02	0.8216
200	250.7	22.8	2.0	0.214E-02	0.7531
300	253.2	20.3	3.4	0.178E-02	0.6241
400	254.5	19.5	1.5	0.151E-02	0.5313
500	254.6	18.0	1.4	0.121E-02	0.4253
600	253.5	19.0	1.4	0.976E-03	0.3427
700	253.2	20.6	1.7	0.755E-03	0.2650
800	253.4	20.8	0.3	0.546E-03	0.1917

DEMAGNETIZATION HISTORY OF AN064B CONTD

STATE	AZIM	INCL	PSI	J	J/J0
900	251.1	21.2	2.2	0.364E-03	0.1279
1000	246.4	23.8	5.0	0.268E-03	0.0942
1200	244.8	20.9	3.3	0.184E-03	0.0647
1400	237.2	31.6	12.6	0.114E-03	0.0399
1600	224.6	23.7	13.6	0.695E-04	0.0244
1800	223.3	24.7	1.6	0.658E-04	0.0231

TABLE B2

SATURATION IRM OF SPECIMEN AN041A

Saturating Field (gauss)	IRM Moment (gauss-cm ³)
200	0.719
500	1.014
1000	1.108
1500	1.161
2000	1.168
3500	1.176
5000	1.175
7500	1.172
10000	1.178
12500	1.179
14500	1.178

TABLE B3

THE CRITICAL SINGLE-DOMAIN SIZE OF MAGNETITE
AS A FUNCTION OF AXIAL RATIO

Axial Ratio a/b	Length of Single-Domain Grain $2b$ (μ)
0.020	49.500
0.040	13.100
0.050	8.600
0.100	2.360
0.166	0.948
0.200	0.680
0.250	0.448
0.333	0.270
0.500	0.140
0.750	0.083

TABLE C1

SPECIMEN MAGNETIZATION DIRECTIONS OF GRENVILLE DIKES
NATURAL REMANENT MAGNETIZATION

SPECIMEN	AZIMUTH DEG	INCL DEG	INTENSITY EMU/CC
GRO11A	282.91	-24.71	0.379E-00
GRO11B	293.54	-25.96	0.493E-01
GRO12A	18.27	30.30	0.550E-03
GRO12B	349.79	43.63	0.341E-03
GRO14B	64.11	35.04	0.916E-03
GRO14D	301.41	24.90	0.327E-03
GRO15A	345.35	87.42	0.494E-03
GRO15B	199.00	32.22	0.658E-03
GRO16A	352.92	60.68	0.173E-03
GRO16B	51.63	54.64	0.487E-03
GRO21A	3.19	52.02	0.217E-02
GRO21B	25.16	19.49	0.198E-02
GRO22A	324.24	54.47	0.180E-02
GRO22B	346.92	38.65	0.168E-02
GRO23A	98.83	43.01	0.760E-03
GRO23B	141.38	41.28	0.117E-02
GRO24A	116.14	47.63	0.150E-02
GRO24B	162.95	28.16	0.131E-02
GRO25A	16.50	63.25	0.131E-02
GRO25B	107.72	58.81	0.102E-02
GRO31A	177.00	60.04	0.626E-03
GRO31B	219.32	41.13	0.640E-03
GRO32A	262.86	56.88	0.824E-03
GRO32B	308.32	34.59	0.846E-03
GRO33A	63.86	73.69	0.411E-03
GRO33B	51.04	63.70	0.447E-03
GRO34A	351.12	49.66	0.684E-03
GRO34B	84.88	70.51	0.652E-03
GRO35A	247.99	57.74	0.608E-03
GRO35B	357.27	62.55	0.482E-03
GRO41A	20.12	-7.87	0.377E-03
GRO41B	279.06	20.60	0.574E-03
GRO42A	354.11	17.98	0.645E-03
GRO42B	20.63	-28.34	0.645E-03
GRO43A	303.24	-51.38	0.221E-02
GRO43B	89.08	-32.42	0.407E-03
GRO44A	278.15	-51.90	0.298E-03

TABLE C1 (CONTD)

SPECIMEN	AZIMUTH DEG	INCL DEG	INTENSITY EMU/CC
GR044B	341.83	-43.08	0.510E-03
GR045A	333.78	-82.32	0.122E-01
GR045B	57.97	-86.21	0.128E-01
GR046A	166.25	47.05	0.668E-03
GR046B	184.85	19.71	0.246E-03
GR051A	34.02	74.69	0.152E-02
GR051B	29.81	56.72	0.951E-03
GR052A	117.16	-17.24	0.263E-02
GR052B	128.89	-22.88	0.153E-02
GR053A	358.70	62.47	0.285E-02
GR053B	16.37	54.18	0.250E-02
GR054A	343.04	71.37	0.254E-02
GR054B	82.33	77.64	0.168E-02
GR055A	354.27	62.94	0.233E-02
GR055B	6.24	70.60	0.163E-02
GR061A	335.39	64.98	0.723E-04
GR061B	105.49	55.65	0.534E-03
GR062A	171.41	29.58	0.944E-04
GR062B	17.61	-65.20	0.403E-02
GR063A	300.99	72.58	0.981E-04
GR063B	48.70	-69.90	0.758E-04
GR064A	351.07	56.59	0.165E-03
GR064B	331.09	76.30	0.178E-03
GR065A	54.33	64.18	0.130E-02
GR065B	321.74	68.07	0.288E-03
GR071A	21.57	68.12	0.163E-02
GR071B	352.35	62.64	0.154E-02
GR072A	325.51	64.56	0.172E-02
GR072B	336.59	49.72	0.127E-02
GR073A	312.79	52.06	0.117E-02
GR073B	257.76	49.88	0.614E-03
GR074A	341.29	66.91	0.125E-02
GR074B	43.04	69.58	0.916E-03
GR075A	4.97	69.13	0.173E-02
GR075B	5.67	69.45	0.172E-02
GR076A	341.97	52.09	0.130E-02
GR076B	338.11	31.48	0.153E-02
GR081A	332.35	70.06	0.261E-02
GR081B	341.43	77.15	0.244E-02
GR082A	35.01	64.34	0.173E-02

TABLE C1 (CONTD)

SPECIMEN	AZIMUTH DEG	INCL DEG	INTENSITY EMU/CC
GR082B	83.61	65.27	0.990E-03
GR083A	46.90	55.04	0.929E-03
GR083P	31.22	65.47	0.821E-03
GR084A	352.83	-79.28	0.368E 00
GR084B	338.08	-61.86	0.171E 00
GR085A	69.59	58.65	0.126E-02
GR085C	219.76	27.55	0.311E-03
GR181A	35.77	81.31	0.906E-03
GR181B	96.65	80.47	0.900E-03
GR182A	171.71	71.70	0.680E-03
GR182B	172.86	68.49	0.628E-03
GR183A	235.62	38.49	0.799E-03
GR183B	226.91	48.41	0.100E-02
GR184A	199.99	64.75	0.105E-02
GR184B	197.34	65.25	0.985E-03
GR185A	144.48	84.50	0.749E-03
GR185B	147.80	83.17	0.845E-03
GR186A	132.70	86.96	0.608E-03
GR186B	209.64	83.29	0.769E-03
GR201A	282.41	81.48	0.663E-03
GR201B	348.39	79.28	0.112E-02
GR202A	111.86	78.43	0.117E-02
GR202B	104.22	77.98	0.126E-02
GR203A	156.33	60.60	0.931E-03
GR203B	3.62	83.70	0.116E-02
GR204A	333.81	53.84	0.950E-03
GR204B	314.42	68.62	0.139E-02
GR205A	37.42	44.39	0.441E-03
GR205B	18.23	59.44	0.251E-03
GR211A	114.27	83.28	0.542E-03
GR211B	44.64	79.69	0.402E-03
GR212A	135.86	41.80	0.339E-03
GR212B	136.94	35.74	0.390E-03
GR213A	100.40	50.83	0.544E-03
GR213B	155.76	56.13	0.523E-03
GR221A	165.77	64.72	0.198E-03
GR221B	50.30	-18.75	0.303E-03
GR222A	155.69	89.03	0.921E-03
GR222B	182.66	82.61	0.103E-02
GR223A	104.57	71.95	0.740E-03

TABLE C1 (CONTD)

SPECIMEN	AZIMUTH DEG	INCL DEG	INTENSITO EMU/CC
GR223B	112.73	65.76	0.678E-03
GR224A	223.19	80.45	0.105E-02
GR224B	213.53	80.78	0.115E-02
GR225A	252.17	20.99	0.147E-03
GR225B	240.74	43.40	0.208E-03
GR226A	65.95	78.97	0.671E-03
GR226B	51.64	78.00	0.591E-03
GR231A	42.77	72.77	0.614E-03
GR231B	83.19	78.80	0.441E-03
GR232A	171.23	76.31	0.624E-03
GR232B	26.62	69.82	0.748E-03
GR233A	126.20	74.23	0.594E-03
GR233B	121.97	67.80	0.730E-03
GR234A	343.39	67.93	0.683E-03
GR234B	37.57	87.00	0.703E-03
GR235A	346.16	61.48	0.607E-03
GR235B	307.05	68.91	0.615E-03
GR241A	137.95	57.53	0.820E-04
GR241B	300.02	3.44	0.110E-01
GR242A	304.45	27.64	0.127E-02
GR242B	315.52	29.30	0.354E 00
GR243A	106.44	78.25	0.183E-03
GR243B	276.38	0.76	0.215E-02
GR251A	127.36	-5.56	0.172E-02
GR251B	126.39	-6.02	0.167E-02
GR252A	126.82	7.21	0.478E-03
GR252B	121.72	25.38	0.608E-03
GR253A	17.08	81.61	0.419E-03
GR253B	48.42	68.41	0.410E-03
GR254A	336.43	84.80	0.522E-03
GR254B	310.00	82.65	0.433E-03
GR261A	290.97	81.75	0.759E-03
GR261B	322.75	83.01	0.734E-03
GR262A	16.47	62.71	0.680E-03
GR263A	29.66	65.72	0.418E-03
GR263B	36.85	70.06	0.401E-03
GR264A	56.03	68.11	0.399E-03
GR264B	52.62	63.77	0.356E-03
GR271A	14.35	-3.26	0.702E-02

TABLE C1 (CONTD)

SPECIMEN	AZIMUTH DEG	INCL DEG	INTENSITY EMU/CC
GR271B	16.79	-6.29	0.654E-02
GR272A	310.47	74.49	0.795E-03
GR272B	315.18	74.96	0.110E-02
GR273A	74.40	-33.95	0.337E-01
GR273B	75.06	-38.24	0.612E-01
GR281A	118.31	9.02	0.314E-03
GR281B	117.20	22.74	0.345E-03
GR282A	243.57	30.48	0.228E-02
GR282B	250.33	33.73	0.384E-02
GR283	74.39	55.47	0.132E-02
GR284A	333.47	38.88	0.572E-03
GR284B	338.49	46.35	0.554E-03
GR312A	55.90	21.38	0.332E-02
GR312B	57.24	17.85	0.327E-02
GR313A	90.30	38.66	0.306E-02
GR313B	90.87	35.33	0.375E-02
GR314A	351.20	62.09	0.143E-02
GR314B	22.86	57.46	0.151E-02
GR315A	252.27	46.76	0.194E 00
GR315B	253.96	47.29	0.196E 00
GR316A	36.60	6.51	0.343E-02
GR316B	40.95	4.31	0.288E-02
GR321A	42.28	65.75	0.169E-02
GR321B	31.98	64.25	0.216E-02
GR322A	357.79	71.54	0.381E-02
GR322B	334.93	59.76	0.304E-02
GR323A	305.97	73.66	0.477E-02
GR323B	303.17	73.86	0.403E-02
GR324A	68.86	73.66	0.269E-02
GR324B	23.64	74.39	0.273E-02
GR325A	73.84	57.38	0.273E-02
GR325B	84.68	53.81	0.220E-02
GR331A	97.61	35.95	0.266E-04
GR331B	80.84	49.03	0.131E-04
GR332A	93.85	77.06	0.481E-04
GR332B	90.94	67.29	0.696E-04
GR333A	112.99	47.11	0.331E-04
GR333B	104.82	36.95	0.347E-04
GR334A	80.93	68.91	0.243E-03
GR334B	87.84	65.89	0.298E-03

TABLE C1 (CONTD)

SPECIMEN	AZIMUTH DEG	INCL DEG	INTENSITY EMU/CC
GR335A	55.29	59.62	0.120E-03
GR335B	53.45	47.65	0.114E-03
GR341A	318.44	35.55	0.366E-04
GR341B	317.24	31.90	0.354E-04
GR342A	325.77	40.91	0.205E-04
GR342B	330.34	35.97	0.201E-04
GR343A	325.89	30.08	0.180E-04
GR343B	322.58	30.41	0.142E-04
GR344A	80.34	-63.80	0.212E-02
GR344B	92.56	-65.73	0.270E-02
GR345A	54.73	32.23	0.140E-05
GR345B	260.62	-11.99	0.159E-05
GR351A	9.83	-68.24	0.230E-01
GR351B	15.78	-67.81	0.476E-01
GR352A	254.91	72.06	0.306E-01
GR352B	241.36	76.13	0.544E-01
GR353A	212.00	-55.83	0.311E-01
GR353B	219.36	-59.77	0.331E-01
GR354A	168.97	-45.02	0.510E-01
GR354B	169.83	-27.10	0.576E-01
GR355A	207.96	50.50	0.361E-01
GR355B	207.22	48.16	0.283E-01
GR356A	147.12	76.40	0.679E-02
GR356B	247.55	72.74	0.475E-02
GR361A	24.69	64.93	0.180E-02
GR361B	35.41	66.01	0.233E-02
GR362A	39.60	70.33	0.249E-02
GR363A	357.74	71.51	0.484E-02
GR363B	1.48	70.13	0.558E-02
GR364A	4.26	46.48	0.251E-02
GR364B	1.03	40.75	0.314E-02
GR365A	40.99	63.41	0.393E-02
GR365B	71.81	56.77	0.300E-02
GR371A	295.05	66.41	0.280E-02
GR371B	252.31	58.39	0.176E-02
GR372A	303.25	68.62	0.189E-02
GR372B	269.63	47.50	0.181E-02
GR373A	350.57	67.38	0.339E-02
GR373B	303.90	76.41	0.304E-02
GR374A	1.42	72.73	0.409E-02

TABLE C1 (CONTD)

SPECIMEN	AZIMUTH DEG	INCL DEG	INTENSITY EMU/CC
GR374B	4.36	61.88	0.354E-02
GR375A	8.50	71.60	0.366E-02
GR375B	345.59	71.74	0.281E-02
GR381A	2.01	54.92	0.161E-05
GR381B	342.84	55.56	0.137E-05
GR382A	28.96	84.56	0.150E-05
GR382B	173.44	73.90	0.217E-05
GR383A	337.35	60.58	0.351E-05
GR383B	357.70	57.24	0.188E-05
GR384A	67.18	75.42	0.193E-05
GR384B	57.13	70.60	0.110E-05
GR385A	330.44	64.00	0.219E-05
GR385B	160.96	56.92	0.130E-05
GR391A	310.47	43.66	0.563E-03
GR391B	278.97	57.57	0.112E-02
GR392A	323.11	27.84	0.879E-04
GR392B	333.23	23.98	0.918E-04
GR393A	309.91	49.51	0.118E-03
GR393B	310.29	53.62	0.105E-03
GR394A	192.08	74.42	0.562E-03
GR394B	182.91	71.53	0.648E-03
GR395A	318.65	43.47	0.767E-04
GR395B	346.16	56.57	0.797E-04
GR401A	49.96	64.79	0.150E-05
GR401B	47.71	76.74	0.148E-05
GR402A	47.95	62.92	0.234E-05
GR402B	59.31	63.00	0.241E-05
GR403A	359.68	72.49	0.754E-05
GR403B	348.10	62.42	0.141E-05
GR404A	281.27	75.28	0.783E-06
GR404B	117.96	71.89	0.574E-06
GR405A	60.56	70.01	0.445E-06
GR405B	311.50	34.71	0.348E-06
GR981A	185.07	61.79	0.386E-03
GR981B	36.14	80.89	0.576E-03
GR982A	19.01	75.18	0.780E-03
GR982B	275.87	78.94	0.114E-02
GR983A	359.02	66.58	0.740E-03
GR983B	57.23	59.90	0.432E-03
GR984A	247.88	57.23	0.782E-03

TABLE C1 (CONTD)

SPECIMEN	AZIMUTH DEG	INCL DEG	INTENSITY EMU/CC
GR984B	258.27	54.90	0.703E-03
GR985A	10.42	43.65	0.885E-03
GR985B	70.32	80.62	0.118E-02
GR986A	273.21	69.99	0.763E-03
GR986B	47.53	83.06	0.119E-02

TABLE C2

SAMPLE MAGNETIZATION DIRECTIONS OF
GRENVILLE DIKES (NRM)

SAMPLE	NN	AZIMUTH	INCL	THETA
GR011	2	288.20	-25.43	9.69
GR012	2	5.31	37.82	26.18
GR014	2	357.41	50.14	99.18
GR015	2	200.77	62.17	59.94
GR016	2	24.96	61.08	30.88
GR021	2	16.51	36.24	36.78
GR022	2	337.27	47.11	22.02
GR023	2	120.41	44.16	31.26
GR024	2	142.85	40.25	40.95
GR025	2	66.20	68.78	40.63
GR031	2	202.64	52.45	32.01
GR032	2	290.43	47.94	37.72
GR033	2	56.01	68.81	10.97
GR034	2	19.15	67.43	45.22
GR035	2	296.74	71.53	48.00
GR041	2	331.56	9.95	103.07
GR042	2	6.85	-5.32	52.95
GR043	2	42.15	-69.99	90.98
GR044	2	312.98	-52.05	42.50
GR045	2	358.89	-85.54	8.21
GR046	2	177.05	33.72	31.26
GR051	2	31.18	65.72	18.04
GR052	2	122.92	-20.16	12.37
GR053	2	8.58	58.63	12.37
GR054	2	19.60	79.56	23.85
GR055	2	359.32	66.88	8.96
GR061	2	57.54	75.88	53.53
GR062	2	150.83	-38.17	140.84
GR063	2	0.23	2.26	158.02
GR064	2	345.09	66.71	21.00
GR065	2	12.62	72.94	34.14

TABLE C2 (CONTD)

SAMPLE	NN	AZIMUTH	INCL	THETA
GR071	2	5.40	66.08	13.19
GR072	2	332.17	57.26	15.96
GR073	2	284.57	54.28	33.88
GR074	2	10.17	71.08	22.05
GR075	2	5.32	69.34	0.48
GR076	2	339.73	41.80	20.80
GR081	2	335.93	73.65	7.52
GR082	2	58.86	66.79	20.20
GR083	2	40.32	60.48	12.94
GR084	2	342.24	-70.69	17.97
GR085	2	189.03	68.96	90.30
GR181	2	67.75	82.13	9.23
GR182	2	172.33	70.10	3.23
GR183	2	231.62	43.53	11.75
GR184	2	198.68	65.01	1.23
GR185	2	146.32	83.84	1.38
GR186	2	187.79	86.01	6.71
GR201	2	319.61	81.89	10.60
GR202	2	107.97	78.23	1.62
GR203	2	149.04	78.00	35.11
GR204	2	326.43	61.56	17.31
GR205	2	29.46	52.29	19.00
GR211	2	71.17	82.92	10.14
GR212	2	136.42	38.77	6.12
GR213	2	126.20	56.73	32.46
GR221	2	77.10	34.28	117.68
GR222	2	179.60	85.87	6.54
GR223	2	109.22	68.90	6.84
GR224	2	218.44	80.65	1.61
GR225	2	247.17	32.32	24.35
GR226	2	58.50	78.57	3.01
GR231	2	58.60	76.59	11.26
GR232	2	68.66	83.88	32.29

TABLE C2 (CONTD)

SAMPLE	NN	AZIMUTH	INCL	THETA
GR233	2	123.74	71.03	6.57
GR234	2	349.35	78.02	20.45
GR235	2	329.46	66.44	17.62
GR241	2	281.29	60.34	117.34
GR242	2	309.94	28.58	9.87
GR243	2	273.83	51.12	100.81
GR251	2	126.88	-5.79	1.07
GR252	2	124.39	16.31	18.81
GR253	2	39.66	75.44	15.04
GR254	2	320.92	83.88	3.55
GR261	2	305.52	82.67	4.33
GR262	1	16.47	62.71	23.78
GR263	2	32.92	67.93	5.11
GR264	2	54.18	65.95	4.56
GR271	2	15.57	-4.78	3.88
GR272	2	312.79	74.74	1.33
GR273	2	74.72	-36.10	4.32
GR281	2	117.77	15.88	13.76
GR282	2	246.89	32.15	6.58
GR283	1	74.39	55.47	90.73
GR284	2	335.83	42.64	8.33
GR312	2	56.58	19.62	3.75
GR313	2	90.59	37.00	3.36
GR314	2	8.16	60.72	16.41
GR315	2	253.11	47.03	1.27
GR316	2	38.78	5.41	4.86
GR321	2	36.99	65.09	4.60
GR322	2	343.72	66.06	14.89
GR323	2	304.58	73.76	0.81
GR324	2	46.78	75.20	12.17
GR325	2	79.51	55.71	7.08

TABLE C2 (CONTD)

SAMPLE	NN	AZIMUTH	INCL	THETA
GR331	2	90.11	42.79	17.92
GR332	2	92.01	72.18	9.81
GR333	2	108.58	42.10	11.82
GR334	2	84.60	67.44	4.02
GR335	2	54.24	53.64	12.02
GR341	2	317.83	33.73	3.78
GR342	2	328.13	38.46	6.10
GR343	2	324.24	30.26	2.88
GR344	2	86.23	-64.89	5.54
GR345	2	320.17	37.23	148.78
GR351	2	12.83	-68.05	2.27
GR352	2	248.98	74.20	5.48
GR353	2	35.48	-57.85	5.55
GR354	2	169.45	-36.06	17.93
GR355	2	207.58	49.33	2.39
GR356	2	205.25	79.89	23.71
GR361	2	29.94	65.56	4.57
GR362	1	39.60	70.33	4.59
GR363	2	359.67	70.83	1.85
GR364	2	2.57	43.63	6.19
GR365	2	58.04	60.98	16.57
GR371	2	270.68	64.01	20.85
GR372	2	281.28	59.07	26.92
GR373	2	333.18	73.20	16.41
GR374	2	3.22	67.31	10.91
GR375	2	357.09	72.01	7.16
GR381	2	352.50	55.62	10.91
GR382	2	158.05	83.94	20.76
GR383	2	348.02	59.31	10.97
GR384	2	61.46	73.07	5.63
GR385	2	195.84	85.39	58.81
GR391	2	297.12	51.66	24.01
GR392	2	328.25	26.03	9.90

TABLE C2 (CONTD)

GR393	2	310.09	51.57	4.12
GR394	2	187.12	73.03	3.94
GR395	2	330.48	50.82	21.76
GR981	2	171.44	79.48	36.29
GR982	2	337.65	81.74	20.34
GR983	2	31.81	66.18	25.99
GR984	2	253.23	56.17	6.24
GR985	2	20.35	64.01	42.25
GR986	2	291.75	81.99	25.33

TABLE C3

SITE MEAN DIRECTIONS OF GRENVILLE DIKES (NRM)
WITH EACH SPECIMEN GIVEN UNIT WEIGHT

SITE	NN	AZIMUTH	INCL	R	K	ALPHA
GR02	10	66.38	67.57	7.4228	3.49	23.69
GR03	10	297.58	79.68	8.3587	5.48	18.91
GR04	12	342.34	-53.92	4.5260	1.47	33.31
GR05	10	51.03	66.22	7.1809	3.19	24.78
GR06	10	20.68	72.63	5.2040	1.88	32.32
GR07	12	338.81	63.25	11.2826	15.33	10.32
GR08	10	23.90	68.33	5.2794	1.91	32.06
GR18	12	200.34	75.96	11.3567	17.10	9.77
GR21	6	127.78	60.56	5.5497	11.10	17.15
GR22	12	171.83	84.62	9.4568	4.33	19.43
GR23	10	32.00	82.65	9.5500	20.00	9.90
GR24	6	295.78	44.13	4.0920	2.62	35.31
GR25	8	117.19	48.62	5.6766	3.01	28.52
GR26	7	30.31	73.31	6.8354	36.45	8.76
GR27	6	32.27	10.38	3.2488	1.82	42.40
GR28	7	127.88	88.46	3.7823	1.86	38.75
GR31	10	46.02	49.33	6.9247	2.93	25.88
GR32	10	29.25	73.77	9.4954	17.84	10.48
GR33	10	87.05	57.12	9.5508	20.04	9.89
GR34	10	331.30	20.74	5.2985	1.91	32.00
GR35	12	186.36	21.75	1.7729	1.08	38.97
GR36	9	22.74	63.39	8.6777	24.82	9.37
GR37	10	315.14	71.92	9.5382	19.49	10.03
GR38	10	5.35	77.00	9.1947	11.18	13.24
GR39	10	312.72	56.11	8.9251	8.37	15.30
GR98	12	329.29	83.08	10.9475	10.45	12.50

NN = NUMBER OF SPECIMENS FROM EACH SITE

R = RESULTANT OF NN UNIT VECTORS

K = ESTIMATE OF FISHER'S PRECISION PARAMETER

ALPHA = SEMIANGLE OF CONE OF 95% CONFIDENCE FOR MEAN DIRECTION

TABLE C5

SPECIMEN MAGNETIZATION DIRECTIONS OF GRENVILLE DIKES
AFTER OPTIMUM DEMAGNETIZATION

SPECIMEN	AZIMUTH DEG	INCL DEG	INTENSITY EMU/CC
GR011A	285.43	-25.11	0.269E-02
GR011B	282.92	-30.05	0.800E-04
GR012A	337.59	-53.19	0.111E-04
GR012B	1.54	-10.00	0.284E-04
GR014B	36.45	-17.64	0.180E-04
GR014D	315.89	39.29	0.768E-05
GR015A	30.60	51.17	0.519E-04
GR015B	311.10	-49.24	0.226E-04
GR016A	90.83	-68.39	0.384E-04
GR016B	32.08	19.38	0.106E-04
GR021A	83.05	59.86	0.122E-03
GR021B	88.46	55.33	0.110E-03
GR022A	89.67	84.21	0.955E-04
GR022B	11.74	77.93	0.980E-04
GR023A	96.95	59.60	0.645E-04
GR023B	139.50	60.81	0.559E-04
GR024A	122.98	49.77	0.524E-04
GR024B	121.28	41.62	0.578E-04
GR025A	79.48	54.90	0.562E-04
GR025B	110.99	48.17	0.803E-04
GR031A	152.42	77.82	0.228E-03
GR031B	187.69	64.50	0.179E-03
GR032A	277.55	80.12	0.320E-03
GR032B	313.50	71.31	0.222E-03
GR033A	79.29	77.98	0.291E-03
GR033B	87.74	74.53	0.302E-03
GR034A	353.14	55.69	0.223E-03
GR034B	32.44	68.45	0.178E-03
GR035A	274.04	68.56	0.254E-03
GR035B	42.25	75.30	0.276E-03
GR041A	301.98	-74.87	0.184E-03
GR041B	294.56	-53.80	0.102E-03
GR042A	324.00	-66.42	0.166E-03
GR042B	314.12	-63.75	0.139E-03
GR043A	295.23	-60.36	0.114E-02
GR043B	294.90	-52.62	0.269E-03
GR044A	293.12	-66.83	0.242E-03

TABLE C5 (CONTD)

SPECIMEN	AZIMUTH DEG	INCL DEG	INTENSITY EMU/CC
GR044B	306.52	-60.41	0.286E-03
GR045A	314.80	-76.16	0.265E-03
GR045B	344.44	-81.11	0.242E-03
GR046A	278.82	-11.64	0.472E-04
GR046B	272.14	-54.03	0.523E-04
GR051A	346.61	77.36	0.307E-03
GR051B	316.67	62.87	0.179E-03
GR052A	46.30	86.62	0.165E-03
GR052B	255.94	61.33	0.146E-03
GR053A	4.39	73.33	0.162E-03
GR053B	38.23	60.41	0.142E-03
GR054A	335.79	74.80	0.110E-02
GR054B	110.55	74.18	0.363E-03
GR055A	354.53	64.11	0.318E-03
GR055B	356.80	72.92	0.186E-03
GR061A	330.18	18.78	0.112E-04
GR061B	133.32	-59.08	0.828E-04
GR062A	122.51	-50.37	0.108E-03
GR062B	129.35	-58.55	0.159E-03
GR063A	12.57	0.47	0.127E-04
GR063B	65.11	-74.03	0.180E-03
GR064A	8.30	52.14	0.111E-04
GR064B	119.25	-4.13	0.268E-05
GR065A	88.22	53.18	0.570E-04
GR065B	337.20	67.21	0.833E-04
GR071A	42.78	85.45	0.132E-03
GR071B	339.12	79.08	0.132E-03
GR072A	332.31	79.73	0.327E-03
GR072B	325.61	82.03	0.194E-03
GR073A	321.56	39.89	0.165E-03
GR073B	297.86	48.93	0.108E-03
GR074A	348.88	81.19	0.273E-03
GR074B	130.89	70.28	0.153E-03
GR075A	350.64	82.44	0.285E-03
GR075B	227.86	85.84	0.219E-03
GR076A	342.10	62.49	0.202E-03
GR076B	329.93	67.00	0.115E-03
GR081A	130.18	-0.32	0.473E-04
GR081B	109.57	-43.88	0.490E-04
GR082A	84.75	-20.87	0.643E-04

TABLE C5 (CONTD)

SPECIMEN	AZIMUTH DEG	INCL DEG	INTENSITY EMU/CC
GR082B	74.65	-43.27	0.511E-04
GR083A	79.85	-45.71	0.825E-04
GR083B	108.21	-40.09	0.129E-03
GR084A	126.12	-59.32	0.233E-01
GR084B	122.66	-65.05	0.518E-02
GR085A	111.10	-43.26	0.716E-04
GR085C	142.21	-63.71	0.828E-04
GR181A	82.62	84.15	0.103E-03
GR182A	180.54	74.37	0.142E-03
GR183A	240.61	62.45	0.280E-03
GR184A	196.70	60.74	0.276E-03
GR185A	133.43	85.22	0.117E-03
GR186A	31.04	79.64	0.148E-03
GR201A	202.64	73.06	0.227E-03
GR201B	152.56	87.18	0.372E-03
GR202A	143.63	59.92	0.368E-03
GR202B	138.12	63.56	0.416E-03
GR203A	165.74	35.91	0.327E-03
GR203B	349.49	-73.19	0.308E-03
GR204A	286.46	74.93	0.269E-03
GR204B	274.83	75.68	0.500E-03
GR205A	145.21	63.68	0.164E-03
GR205B	199.19	69.93	0.910E-04
GR211A	143.39	34.69	0.123E-03
GR211B	136.02	28.56	0.966E-04
GR212A	142.16	0.99	0.134E-03
GR212B	141.59	-1.58	0.143E-03
GR213A	126.80	9.48	0.154E-03
GR213B	148.63	10.58	0.148E-03
GR221A	130.19	-60.19	0.319E-04
GR222A	72.62	-68.19	0.375E-04
GR223A	123.89	-66.27	0.438E-04
GR224A	216.54	-65.55	0.362E-04
GR225A	150.98	-5.13	0.103E-03
GR225B	157.26	-14.13	0.935E-04
GR226A	176.39	-56.65	0.957E-04
GR226B	151.16	3.55	0.598E-04
GR231A	86.84	82.37	0.186E-03
GR231B	150.80	68.20	0.152E-03

TABLE C5 (CONTD)

SPECIMEN	AZIMUTH DEG	INCL DEG	INTENSITY EMU/CC
GR232A	183.14	49.68	0.245E-03
GR232B	40.72	87.92	0.218E-03
GR233A	144.57	63.77	0.210E-03
GR233B	140.48	55.85	0.268E-03
GR234A	341.80	67.09	0.200E-03
GR235A	36.37	61.90	0.164E-03
GR235B	307.29	86.11	0.147E-03
GR251A	135.07	48.62	0.816E-04
GR252A	129.81	59.62	0.744E-04
GR252B	105.63	48.52	0.901E-04
GR253A	95.28	68.53	0.658E-04
GR253B	82.47	54.04	0.805E-04
GR254A	127.39	63.27	0.168E-03
GR261A	327.89	67.57	0.388E-04
GR261B	13.44	61.96	0.296E-04
GR262A	30.77	60.77	0.332E-04
GR263A	28.40	71.89	0.122E-04
GR263B	43.41	74.74	0.114E-03
GR264A	22.46	23.79	0.684E-05
GR271A	313.07	58.03	0.409E-04
GR271B	304.68	59.80	0.468E-04
GR272A	320.48	68.45	0.246E-03
GR273A	348.61	69.10	0.343E-04
GR273B	42.45	44.91	0.138E-04
GR281A	114.98	-49.47	0.341E-04
GR281B	123.03	-44.64	0.340E-04
GR282A	144.18	-57.79	0.113E-03
GR282B	144.47	-56.89	0.902E-04
GR283	322.72	14.50	0.199E-03
GR284A	24.35	-55.10	0.230E-04
GR284B	31.60	-60.04	0.262E-04
GR312A	112.09	34.02	0.382E-03
GR312B	111.70	33.51	0.380E-03
GR313A	109.46	31.38	0.304E-03
GR313B	115.23	-9.11	0.388E-01
GR314A	101.70	35.83	0.287E-03
GR314B	112.84	35.92	0.295E-03
GR315A	253.10	47.35	0.112E-01
GR315B	252.16	46.76	0.102E-01

TABLE C5 (CONTD)

SPECIMEN	AZIMUTH DEG	INCL DEG	INTENSITY EMU/CC
GR316A	97.90	28.33	0.210E-03
GR316B	102.74	17.59	0.174E-03
GR321A	121.33	15.94	0.252E-03
GR321B	117.03	15.00	0.255E-03
GR322A	111.17	45.82	0.235E-03
GR322B	109.50	33.39	0.171E-03
GR323A	116.01	39.39	0.189E-03
GR323B	120.77	29.34	0.181E-03
GR324A	119.22	33.34	0.397E-03
GR324B	118.26	26.52	0.252E-03
GR325A	121.53	18.55	0.358E-03
GR325B	118.91	15.50	0.384E-03
GR331A	101.03	23.76	0.228E-04
GR331B	81.25	34.99	0.847E-05
GR332A	110.96	46.58	0.118E-04
GR332B	108.04	47.50	0.273E-04
GR333A	114.35	22.96	0.249E-04
GR333B	110.15	21.93	0.288E-04
GR334A	57.44	72.78	0.451E-04
GR334B	57.12	75.42	0.531E-04
GR335A	79.58	79.56	0.181E-04
GR335B	76.68	59.86	0.101E-04
GR351A	27.90	-56.73	0.103E-03
GR351B	112.16	61.37	0.715E-04
GR352A	248.30	77.15	0.201E-03
GR352B	125.99	58.72	0.383E-04
GR353A	210.44	-60.67	0.671E-03
GR353B	358.08	60.36	0.623E-04
GR354A	164.48	-37.67	0.780E-04
GR354B	173.13	55.76	0.223E-04
GR355A	148.27	58.07	0.320E-04
GR355B	90.69	76.95	0.276E-04
GR356A	109.97	21.05	0.692E-04
GR356B	98.92	13.15	0.644E-04
GR361A	107.75	31.28	0.295E-03
GR361B	109.71	31.57	0.308E-03
GR362A	109.93	27.18	0.309E-03
GR363A	100.17	30.08	0.319E-03
GR363B	99.23	28.38	0.321E-03
GR364A	102.66	25.80	0.290E-03

TABLE C5 (CONTD)

SPECIMEN	AZIMUTH DEG	INCL DEG	INTENSITY EMU/CC
GR364B	102.86	28.31	0.311E-03
GR365A	111.56	30.73	0.329E-03
GR365B	109.92	30.45	0.310E-03
GR371A	109.54	38.91	0.277E-03
GR371B	110.72	28.83	0.255E-03
GR372A	128.62	33.99	0.251E-03
GR372B	127.31	35.57	0.252E-03
GR373A	116.55	36.14	0.385E-03
GR373B	114.22	33.04	0.362E-03
GR374A	117.76	35.44	0.284E-03
GR374B	115.42	32.12	0.283E-03
GR375A	120.90	46.24	0.249E-03
GR375B	129.55	36.65	0.205E-03
GR391A	309.15	44.91	0.457E-04
GR391B	353.79	57.37	0.461E-04
GR392A	321.75	30.13	0.345E-04
GR392B	337.03	31.23	0.362E-04
GR393A	323.92	49.47	0.381E-04
GR393B	326.68	61.72	0.338E-04
GR394A	144.95	40.50	0.134E-03
GR394B	149.28	40.01	0.151E-03
GR395A	323.16	55.52	0.112E-04
GR395B	211.94	67.15	0.245E-04
GR981A	225.08	55.73	0.544E-04
GR982A	334.62	67.16	0.877E-04
GR983A	332.99	69.57	0.125E-03
GR983B	62.13	73.65	0.692E-04
GR984A	250.98	43.36	0.233E-03
GR985A	350.16	51.81	0.280E-03
GR985B	277.53	81.95	0.305E-03
GR986A	260.61	54.64	0.190E-03

TABLE C6

SAMPLE MAGNETIZATION DIRECTIONS OF
GRENVILLE DIKES AFTER OPTIMUM
DEMAGNETIZATION

SAMPLE	NN	AZIMUTH	INCL	THETA
GR011	2	284.20	-27.59	5.42
GR012	2	352.52	-32.13	47.29
GR014	2	1.19	14.02	94.07
GR015	2	349.89	1.25	121.03
GR016	2	47.59	-26.92	97.37
GR021	2	85.92	57.62	5.37
GR022	2	34.94	82.76	12.23
GR023	2	117.81	61.92	20.81
GR024	2	122.44	45.70	8.18
GR025	2	96.43	52.59	20.52
GR031	2	176.26	71.89	16.98
GR032	2	301.13	76.32	12.11
GR033	2	84.04	76.29	3.98
GR034	2	8.48	63.40	21.80
GR035	2	317.75	81.36	32.55
GR041	2	296.83	-64.37	21.27
GR042	2	318.81	-65.17	4.94
GR043	2	295.05	-56.49	7.74
GR044	2	300.58	-63.77	8.72
GR045	2	326.36	-78.99	7.51
GR046	2	276.32	-32.88	42.72
GR051	2	326.27	70.66	17.28
GR052	2	259.83	77.10	31.65
GR053	2	25.92	67.71	18.07
GR054	2	45.85	83.90	28.58
GR055	2	355.44	68.52	8.85
GR061	2	348.32	-48.22	137.88
GR062	2	125.59	-54.51	9.08
GR063	2	23.17	-38.75	80.83
GR064	2	82.87	36.59	106.01
GR065	2	50.07	71.23	49.10
GR071	2	356.68	83.21	9.78
GR072	2	329.38	80.90	2.53
GR073	2	310.64	45.02	19.08
GR074	2	107.38	83.02	27.19

TABLE C6 (CONTD)

SAMPLE	NN	AZIMUTH	INCL	THETA
GR075	2	317.18	86.82	10.41
GR076	2	336.52	64.87	6.86
GR081	2	121.56	-22.42	47.27
GR082	2	80.33	-32.17	23.94
GR083	2	94.69	-43.78	21.40
GR084	2	124.55	-62.20	5.95
GR085	2	122.78	-54.44	27.05
GR181	1	82.62	84.15	
GR182	1	180.54	74.37	
GR183	1	240.61	62.45	
GR184	1	196.70	68.74	
GR185	1	133.43	85.22	
GR186	1	31.04	79.64	
GR201	2	195.98	80.56	15.28
GR202	2	141.04	61.77	4.47
GR203	2	168.95	56.34	40.40
GR204	2	280.79	75.38	3.04
GR205	2	168.49	69.06	21.35
GR211	2	139.58	31.68	8.77
GR212	2	141.87	-0.30	2.64
GR213	2	137.70	10.21	21.52
GR221	2	134.36	-56.54	9.58
GR222	2	76.41	-71.28	6.87
GR223	2	208.55	-54.44	78.98
GR224	1	218.00	-65.00	46.23
GR225	2	160.72	-0.27	139.11
GR226	2	170.57	-54.15	9.24
GR231	2	135.28	76.92	19.62
GR232	2	181.09	70.65	41.98
GR233	2	142.28	59.83	8.18
GR234	1	341.80	67.09	56.03
GR235	2	28.19	75.76	28.28
GR251	2	134.12	52.31	7.49
GR252	2	116.07	54.67	17.84

TABLE C6 (CONTD)

SAMPLE	NN	AZIMUTH	INCL	THETA
GR253	2	87.38	61.43	15.67
GR254	2	130.50	59.66	7.80
GR261	2	353.16	66.49	19.70
GR262	1	30.77	60.77	8.36
GR263	2	35.28	73.45	5.14
GR264	1	22.46	23.79	52.12
GR271	2	308.98	58.98	4.68
GR272	2	316.37	67.77	3.35
GR273	2	25.04	59.59	36.04
GR281	2	119.19	-47.13	7.30
GR282	2	144.33	-57.34	0.91
GR284	2	27.73	-57.62	6.28
GR312	2	111.89	33.77	0.60
GR313	2	107.99	32.20	2.98
GR314	2	107.27	36.00	9.02
GR315	2	252.63	47.06	0.87
GR316	2	100.42	22.98	11.62
GR321	2	119.18	15.48	4.25
GR322	2	110.26	39.61	12.50
GR323	2	118.53	34.39	10.79
GR324	2	118.72	29.93	6.87
GR325	2	120.21	17.03	3.95
GR331	2	91.69	29.74	20.51
GR332	2	109.51	47.05	2.19
GR333	2	112.24	22.46	4.02
GR334	2	57.29	74.10	2.64
GR335	2	77.45	69.71	19.72
GR351	2	66.53	3.12	135.04
GR352	2	151.14	76.41	39.51
GR353	2	105.20	-0.56	164.23
GR354	2	168.07	9.07	93.72
GR355	2	131.93	69.62	27.03
GR356	2	104.33	17.18	13.18

TABLE C6 (CONTD)

SAMPLE	NN	AZIMUTH	INCL	THETA
GR361	2	108.73	31.43	1.70
GR362	1	109.93	27.18	4.39
GR363	2	99.70	29.23	1.89
GR364	2	102.76	27.06	2.52
GP365	2	110.74	30.59	1.44
GR371	2	110.16	33.92	10.03
GR372	2	127.97	34.78	1.91
GR373	2	115.36	34.60	3.65
GR374	2	116.57	33.79	3.85
GR375	2	125.55	41.53	11.56
GR391	2	328.29	53.26	29.97
GR392	2	329.35	30.90	13.18
GR393	2	325.08	55.60	12.35
GR394	2	147.14	40.27	3.32
GR395	2	282.77	72.25	47.15
GR981	1	225.08	55.73	
GP982	1	334.62	67.16	
GR983	1	332.99	69.57	
GR984	1	250.98	43.36	
GR985	1	350.16	51.81	
GR986	1	260.61	54.64	

TABLE C7

SITE MEAN DIRECTIONS OF GRENVILLE DIKES
WITH EACH SPECIMEN GIVEN UNIT WEIGHT

GR02	10	103.22	61.71	9.5237	18.90	10.18
GR03	10	3.33	85.36	9.4394	16.05	11.05
GR04	12	296.59	-61.63	11.3749	17.60	9.63
GR05	10	349.61	77.65	9.5731	21.08	9.64
GR06	10	63.05	-12.43	3.1239	1.31	38.70
GR07	12	327.20	76.68	11.3800	17.74	9.59
GR08	10	106.72	-44.85	9.1435	10.51	13.66
GR21	6	139.75	13.83	5.7955	24.45	11.56
GR22	11	162.18	-63.05	8.2281	3.61	22.22
GR23	9	132.64	80.42	8.3231	11.82	13.57
GR24	5	307.33	63.16	2.7342	1.77	47.12
GR25	8	118.50	58.27	7.8224	39.42	7.88
GR26	6	18.39	62.11	5.6551	14.50	15.01
GR27	6	336.13	66.52	5.6733	15.30	14.61
GR28	6	104.37	-63.71	5.3904	8.20	19.96
GR31	10	114.43	44.42	7.9864	4.47	20.94
GR32	10	117.63	27.32	9.8216	50.46	6.23
GR33	10	97.43	49.87	9.1220	10.25	13.83
GR35	12	122.26	44.99	6.3556	1.95	28.95
GR36	9	105.94	29.38	8.9744	312.95	2.64
GR37	10	118.98	35.90	9.9228	116.57	4.10
GR39	10	320.31	68.35	7.7974	4.09	21.90

NN = NUMBER OF SPECIMENS FROM EACH SITE

R = RESULTANT OF NN UNIT VECTORS

K = ESTIMATE OF FISHER'S PRECISION PARAMETER

ALPHA = SEMIANGLE OF CONE OF 95% CONFIDENCE FOR MEAN DIRECTION

TABLE C8

THERMAL DEMAGNETIZATION OF GRENVILLE DIKES

DEMAGNETIZATION HISTORY OF GRO21C

STATE	AZIM	INCL	PSI	J	J/J0
0	54.5	37.8	0.0	0.21E-02	1.0000
121	63.1	49.3	13.0	0.15E-02	0.7157
248	67.3	51.6	3.6	0.91E-03	0.4236
276	63.6	49.9	2.9	0.82E-03	0.3806
331	89.9	43.2	19.2	0.73E-03	0.3395
394	80.5	43.4	6.9	0.44E-03	0.2058
456	78.3	44.0	1.7	0.37E-03	0.1743
502	85.8	46.6	5.8	0.23E-03	0.1067
544	79.9	35.4	12.1	0.46E-04	0.0216
565	14.0	-60.3	109.7	0.88E-05	0.0041
603	71.8	-9.3	66.4	0.19E-04	0.0089

DEMAGNETIZATION HISTORY OF GRO23C

STATE	AZIM	INCL	PSI	J	J/J0
0	281.5	80.5	0.0	0.95E-03	1.0000
179	193.8	85.0	10.5	0.53E-03	0.5558
279	153.9	70.6	15.9	0.40E-03	0.4240
311	158.5	83.7	13.1	0.36E-03	0.3733
361	171.7	72.5	11.4	0.33E-03	0.3510
423	172.9	73.7	1.2	0.28E-03	0.2903
479	115.9	69.0	18.1	0.23E-03	0.2424
536	103.7	-14.7	84.2	0.49E-04	0.0509
556	327.9	-1.4	133.4	0.45E-04	0.0470
610	49.2	-1.3	81.2	0.12E-04	0.0124

DEMAGNETIZATION HISTORY OF GRO24C

STATE	AZIM	INCL	PSI	J	J/J0
0	251.8	78.5	0.0	0.10E-02	1.0000
147	144.1	79.5	17.8	0.53E-03	0.5189
235	140.0	71.1	8.5	0.41E-03	0.3999
301	127.2	67.1	6.1	0.34E-03	0.3262
382	123.1	59.1	8.2	0.33E-03	0.3224
455	102.3	63.2	10.8	0.24E-03	0.2311
524	212.0	87.9	27.6	0.54E-04	0.0527
595	216.5	76.5	11.4	0.10E-04	0.0098

DEMAGNETIZATION HISTORY OF GR025C

STATE	AZIM	INCL	PSI	J	J/J0
0	104.2	76.3	0.0	0.12E-02	1.0000
197	91.3	75.1	3.4	0.86E-03	0.7151
295	97.4	73.4	2.4	0.68E-03	0.5639
387	23.7	69.5	22.2	0.14E-03	0.1199
498	25.4	71.4	2.1	0.40E-04	0.0331
561	32.0	48.0	23.7	0.14E-04	0.0116

DEMAGNETIZATION HISTORY OF GR031C

STATE	AZIM	INCL	PSI	J	J/J0
0	277.9	53.6	0.0	0.53E-03	1.0000
153	260.5	69.3	17.6	0.40E-03	0.7614
240	233.6	70.8	9.2	0.27E-03	0.5065
309	207.0	73.4	8.5	0.19E-03	0.3655
371	220.4	65.3	9.3	0.16E-03	0.3013
440	202.4	64.5	7.7	0.12E-03	0.2223
508	203.6	66.2	1.8	0.75E-04	0.1421
568	172.3	-25.3	94.6	0.19E-04	0.0359

DEMAGNETIZATION HISTORY OF GR032C

STATE	AZIM	INCL	PSI	J	J/J0
0	17.1	61.2	0.0	0.77E-03	1.0000
179	3.7	70.8	11.0	0.33E-03	0.4248
279	1.3	68.8	2.1	0.16E-03	0.2065
311	5.0	67.6	1.8	0.13E-03	0.1697
361	16.8	70.4	5.0	0.90E-04	0.1172
423	48.7	66.9	12.0	0.80E-04	0.1047
479	78.9	51.9	21.0	0.49E-04	0.0644
536	175.2	77.7	41.0	0.50E-04	0.0653
556	350.9	77.6	24.6	0.15E-04	0.0195
610	163.9	-14.0	116.3	0.22E-04	0.0284

DEMAGNETIZATION HISTORY OF GR033C

STATE	AZIM	INCL	PSI	J	J/J0
0	89.3	68.9	0.0	0.50E-03	1.0000
197	103.2	66.6	5.7	0.52E-03	1.0458
295	107.9	65.6	2.2	0.36E-03	0.7327
387	101.7	65.0	2.6	0.22E-03	0.4438
498	90.4	60.1	7.2	0.35E-04	0.0712
561	263.6	62.9	56.9	0.11E-04	0.0222

DEMAGNETIZATION HISTORY OF GR035C

STATE	AZIM	INCL	PSI	J	J/J0
0	101.4	75.8	0.0	0.24E-03	1.0000
131	104.6	82.4	6.7	0.28E-03	1.1619
233	23.0	80.8	11.0	0.23E-03	0.9789
270	39.3	82.7	2.9	0.19E-03	0.7945
326	7.5	67.1	17.1	0.17E-03	0.7183
379	349.4	68.8	7.0	0.14E-03	0.5903
455	338.1	73.6	6.0	0.94E-04	0.3957
501	4.0	78.7	7.9	0.89E-04	0.3747
549	324.0	79.8	7.4	0.65E-04	0.2724
559	325.1	1.9	77.9	0.18E-04	0.0758
609	336.8	22.9	23.9	0.78E-05	0.0327

DEMAGNETIZATION HISTORY OF GR041C

STATE	AZIM	INCL	PSI	J	J/J0
0	267.3	19.9	0.0	0.46E-03	1.0000
131	273.1	-25.1	45.3	0.33E-03	0.7219
233	269.6	-42.6	17.8	0.34E-03	0.7437
270	265.9	-51.0	8.8	0.35E-03	0.7554
326	264.0	-57.2	6.3	0.40E-03	0.8662
378	259.5	-59.0	3.0	0.37E-03	0.8037
455	262.5	-60.6	2.2	0.42E-03	0.9034
501	257.5	-60.2	2.5	0.40E-03	0.8776
549	267.2	-44.2	17.1	0.64E-04	0.1394
565	250.0	-67.6	25.2	0.34E-04	0.0732
609	258.6	-21.6	46.4	0.14E-04	0.0311

DEMAGNETIZATION HISTORY OF GR043C

STATE	AZIM	INCL	PSI	J	J/J0
0	359.5	12.3	0.0	0.28E-03	1.0000
205	47.5	7.0	47.6	0.78E-04	0.2769
267	52.9	-57.8	65.0	0.13E-03	0.4427
364	55.5	-59.0	1.8	0.77E-04	0.2715
472	59.3	-59.1	1.9	0.34E-04	0.1194
565	146.8	-69.0	36.0	0.12E-04	0.0414

DEMAGNETIZATION HISTORY OF GR045C

STATE	AZIM	INCL	PSI	J	J/J0
0	75.2	-80.2	0.0	0.15E-01	1.0000
214	75.7	-80.1	0.2	0.13E-01	0.8764
284	81.0	-79.8	1.0	0.10E-01	0.6922

DEMAGNETIZATION HISTORY OF GR045D CONTD

STATE	AZIM	INCL	PSI	J	J/J0
343	78.3	-79.4	0.6	0.83E-02	0.5660
408	71.5	-79.6	1.2	0.71E-02	0.4800
471	76.2	-79.1	1.0	0.58E-02	0.3938
528	72.7	-79.6	0.8	0.44E-02	0.2969
562	81.5	-79.9	1.6	0.18E-02	0.1198
607	37.6	-37.7	45.4	0.12E-04	0.0008

DEMAGNETIZATION HISTORY OF GR054C

STATE	AZIM	INCL	PSI	J	J/J0
0	281.5	77.9	0.0	0.90E-03	1.0000
197	250.7	75.7	7.3	0.65E-03	0.7252
295	228.6	73.7	6.1	0.46E-03	0.5105
387	338.3	63.1	35.6	0.19E-03	0.2142
498	330.3	74.8	12.1	0.66E-04	0.0735
561	315.4	60.4	15.4	0.32E-04	0.0351

DEMAGNETIZATION HISTORY OF GR055C

STATE	AZIM	INCL	PSI	J	J/J0
0	19.0	84.9	0.0	0.13E-02	1.0000
121	36.5	81.3	4.1	0.13E-02	0.9482
229	55.2	81.8	2.8	0.92E-03	0.6870
242	50.5	81.0	1.1	0.88E-03	0.6542
300	61.9	83.6	3.0	0.73E-03	0.5480
373	43.7	81.8	2.9	0.53E-03	0.3994
430	53.8	78.9	3.4	0.41E-03	0.3046
480	32.7	80.6	4.1	0.33E-03	0.2433
522	359.4	74.6	9.1	0.18E-03	0.1342
587	38.4	21.4	57.0	0.17E-04	0.0129

DEMAGNETIZATION HISTORY OF GR061C

STATE	AZIM	INCL	PSI	J	J/J0
0	12.5	69.5	0.0	0.82E-04	1.0000
131	71.6	75.7	17.8	0.17E-03	2.0635
207	88.7	50.0	26.6	0.77E-04	0.9323
276	113.1	-18.9	72.2	0.60E-04	0.7285
337	130.0	-34.6	21.8	0.10E-03	1.2233
398	136.4	-42.7	9.5	0.12E-03	1.5107
451	143.8	-59.0	16.9	0.14E-03	1.7330
511	150.0	-62.1	4.4	0.15E-03	1.8034
534	100.6	-47.5	31.0	0.47E-04	0.5777
592	152.3	57.8	113.6	0.17E-04	0.2093

DEMAGNETIZATION HISTORY OF GR064C

STATE	AZIM	INCL	PSI	J	J/J0
0	279.9	28.2	0.0	0.50E-03	1.0000
202	238.0	69.6	47.8	0.31E-03	0.6185
311	212.7	73.1	8.7	0.23E-03	0.4597
407	184.4	71.3	8.8	0.11E-03	0.2225
511	178.7	70.4	2.1	0.45E-04	0.0906
571	180.2	72.1	1.8	0.14E-04	0.0290

DEMAGNETIZATION HISTORY OF GR065C

STATE	AZIM	INCL	PSI	J	J/J0
0	40.7	30.2	0.0	0.12E-02	1.0000
147	50.7	41.8	14.1	0.52E-03	0.4447
235	57.7	41.4	5.2	0.41E-03	0.3526
301	64.0	32.4	10.3	0.31E-03	0.2637
382	73.0	38.3	9.3	0.27E-03	0.2299
455	79.3	41.5	5.8	0.22E-03	0.1875
524	119.5	-65.8	111.7	0.64E-04	0.0549
568	342.8	68.7	163.4	0.18E-04	0.0158

DEMAGNETIZATION HISTORY OF GR072C

STATE	AZIM	INCL	PSI	J	J/J0
0	338.5	59.4	0.0	0.13E-02	1.0000
140	323.8	63.6	8.2	0.10E-02	0.7960
248	314.3	67.8	5.7	0.69E-03	0.5334
276	314.2	65.1	2.7	0.67E-03	0.5152
331	301.2	69.8	6.9	0.56E-03	0.4315
394	301.0	70.5	0.6	0.47E-03	0.3626
456	283.5	74.5	6.6	0.35E-03	0.2680
502	274.4	75.4	2.5	0.30E-03	0.2356
544	313.2	68.4	13.6	0.69E-04	0.0534
565	51.7	-49.7	138.1	0.21E-04	0.0159
603	222.3	55.8	171.7	0.13E-04	0.0102

DEMAGNETIZATION HISTORY OF GR073C

STATE	AZIM	INCL	PSI	J	J/J0
0	267.1	35.3	0.0	0.70E-03	1.0000
205	285.8	43.4	16.5	0.61E-03	0.8717
267	282.3	45.3	3.1	0.50E-03	0.7131
364	285.2	41.2	4.6	0.32E-03	0.4608
472	283.3	44.4	3.5	0.14E-03	0.2047
565	259.7	78.2	35.1	0.15E-04	0.0214

DEMAGNETIZATION HISTORY OF GR074C

STATE	AZIM	INCL	PSI	J	J/J0
0	329.1	81.1	0.0	0.83E-03	1.0000
147	312.2	82.6	2.8	0.68E-03	0.8228
231	285.7	80.0	4.7	0.55E-03	0.6643
290	280.0	82.2	2.4	0.48E-03	0.5716
348	262.6	78.2	4.9	0.44E-03	0.5293
411	257.5	79.4	1.6	0.36E-03	0.4296
477	15.7	74.8	22.3	0.36E-03	0.4298
534	331.4	59.5	22.1	0.27E-03	0.3239

DEMAGNETIZATION HISTORY OF GR076C

STATE	AZIM	INCL	PSI	J	J/J0
0	352.1	30.0	0.0	0.14E-02	1.0000
201	350.2	32.8	3.2	0.12E-02	0.8189
280	345.1	32.7	4.3	0.93E-03	0.6449
341	348.2	33.8	2.8	0.77E-03	0.5286
403	349.7	34.0	1.3	0.61E-03	0.4226
471	348.1	36.5	2.8	0.45E-03	0.3077
526	330.1	54.2	21.6	0.86E-04	0.0598
544	320.0	51.0	6.9	0.37E-05	0.0025

DEMAGNETIZATION HISTORY OF GR083C

STATE	AZIM	INCL	PSI	J	J/J0
0	3.8	48.3	0.0	0.47E-03	1.0000
140	12.8	51.6	6.7	0.31E-03	0.6635
248	25.4	61.8	12.2	0.43E-04	0.0909
276	70.1	-20.5	89.7	0.72E-04	0.1539
331	69.8	-72.7	52.2	0.94E-04	0.2007
394	48.2	-76.2	6.7	0.10E-03	0.2131
456	161.5	-80.0	20.0	0.11E-03	0.2434
502	118.4	-78.1	8.2	0.11E-03	0.2457
544	164.7	-74.8	11.0	0.14E-03	0.2891
565	61.0	-41.2	53.9	0.40E-04	0.0845
603	318.6	-20.9	85.2	0.12E-04	0.0246

DEMAGNETIZATION HISTORY OF GR084C

STATE	AZIM	INCL	PSI	J	J/J0
0	337.4	-51.5	0.0	0.76E-01	1.0000
147	335.3	-53.2	2.1	0.81E-01	1.0655
231	337.3	-55.9	3.0	0.74E-01	0.9791
290	338.9	-56.1	1.0	0.70E-01	0.9212

DEMAGNETIZATION HISTORY OF GR084C CONTD

STATE	AZIM	INCL	PSI	J	J/J0
348	342.1	-57.8	2.4	0.66E-01	0.8680
411	335.7	-57.8	3.4	0.59E-02	0.0774
477	344.0	-61.1	5.3	0.49E-01	0.6440
534	343.1	-63.6	2.6	0.30E-01	0.4031
568	339.5	-57.7	6.1	0.14E-02	0.0185
611	321.0	-39.5	21.7	0.15E-04	0.0002

DEMAGNETIZATION HISTORY OF GR085D

STATE	AZIM	INCL	PSI	J	J/J0
0	312.2	21.1	0.0	0.32E-03	1.0000
202	310.5	-1.0	22.2	0.87E-04	0.2725
311	283.9	-67.4	68.9	0.93E-04	0.2933
407	281.7	-67.7	0.9	0.62E-04	0.1945
511	281.7	-67.0	0.7	0.34E-04	0.1056
571	332.2	21.8	96.4	0.87E-05	0.0274

DEMAGNETIZATION HISTORY OF GR181B

STATE	AZIM	INCL	PSI	J	J/J0
0	103.0	81.8	0.0	0.88E-03	1.0000
149	113.6	78.3	3.9	0.76E-03	0.8590
233	120.3	77.5	1.6	0.60E-03	0.6795
261	123.4	75.6	2.1	0.56E-03	0.6364
319	130.5	75.4	1.8	0.46E-03	0.5279
375	120.2	74.8	2.7	0.38E-03	0.4278
449	119.0	74.4	0.5	0.29E-03	0.3335
497	115.2	77.6	3.3	0.24E-03	0.2777
543	134.6	83.4	6.6	0.83E-04	0.0946
559	343.3	-3.4	99.2	0.11E-04	0.0125
605	164.2	24.2	159.2	0.42E-05	0.0048

DEMAGNETIZATION HISTORY OF GR183B

STATE	AZIM	INCL	PSI	J	J/J0
0	226.4	49.5	0.0	0.85E-03	1.0000
257	227.5	53.1	3.7	0.77E-03	0.9061
350	224.2	55.7	3.3	0.67E-03	0.7927
471	214.2	62.1	8.2	0.13E-03	0.1529
563	173.0	71.8	18.3	0.29E-04	0.0341

DEMAGNETIZATION HISTORY OF GR184B

STATE	AZIM	INCL	PSI	J	J/J0
0	196.1	64.4	0.0	0.10E-02	1.0000
147	191.0	61.7	3.5	0.93E-03	0.9170
231	186.9	60.1	2.5	0.81E-03	0.7964
290	186.3	58.6	1.5	0.73E-03	0.7229
348	197.3	61.8	6.3	0.70E-03	0.6947
411	198.6	68.1	6.3	0.60E-03	0.5908
477	238.1	74.0	13.8	0.12E-02	1.1390
534	234.6	30.3	43.7	0.22E-03	0.2194
568	336.3	24.9	87.0	0.15E-04	0.0145
611	28.8	-6.7	60.0	0.17E-04	0.0173

DEMAGNETIZATION HISTORY OF GR185B

STATE	AZIM	INCL	PSI	J	J/J0
0	159.8	82.6	0.0	0.88E-03	1.0000
201	152.0	80.3	2.6	0.70E-03	0.8016
280	158.1	80.6	1.0	0.61E-03	0.6943
341	159.8	79.5	1.1	0.54E-03	0.6129
403	161.1	79.0	0.6	0.45E-03	0.5152
471	162.1	81.9	2.9	0.44E-03	0.5063
526	219.7	80.6	8.5	0.10E-03	0.1190
544	330.8	84.2	12.7	0.79E-05	0.0090

DEMAGNETIZATION HISTORY OF GR224B

STATE	AZIM	INCL	PSI	J	J/J0
0	220.8	80.5	0.0	0.12E-02	1.0000
131	210.1	78.0	3.2	0.10E-02	0.8750
207	219.2	77.5	2.0	0.80E-03	0.6912
276	230.2	74.9	3.7	0.63E-03	0.5430
337	231.4	73.3	1.7	0.52E-03	0.4512
398	239.9	66.9	7.0	0.39E-03	0.3402
451	244.7	66.1	2.0	0.26E-03	0.2255
511	257.9	31.3	35.8	0.11E-03	0.0932
534	296.2	5.1	44.4	0.49E-04	0.0427
592	80.3	9.7	141.3	0.11E-04	0.0098

DEMAGNETIZATION HISTORY OF GR234B

STATE	AZIM	INCL	PSI	J	J/J0
0	42.5	85.7	0.0	0.42E-03	1.0000
170	74.5	85.8	2.3	0.42E-03	1.0227
247	87.2	85.9	0.9	0.38E-03	0.9137

DEMAGNETIZATION HISTORY OF GR234B CONTD

STATE	AZIM	INCL	PSI	J	J/J0
306	80.9	85.4	0.7	0.34E-03	0.8260
391	84.5	84.8	0.7	0.30E-03	0.7130
462	76.2	84.9	0.7	0.24E-03	0.5709
529	319.9	63.1	29.5	0.47E-04	0.1140
562	279.4	49.7	25.4	0.10E-04	0.0246

DEMAGNETIZATION HISTORY OF GR264B

STATE	AZIM	INCL	PSI	J	J/J0
0	50.4	60.0	0.0	0.37E-03	1.0000
201	56.4	52.2	8.5	0.22E-03	0.5791
280	57.2	52.1	0.5	0.17E-03	0.4650
341	57.6	51.9	0.3	0.15E-03	0.3935
403	57.3	51.6	0.3	0.11E-03	0.2933
471	53.5	45.5	6.6	0.61E-04	0.1643
526	356.7	-6.6	72.6	0.59E-05	0.0158
544	229.0	35.3	124.2	0.27E-05	0.0071

DEMAGNETIZATION HISTORY OF GR282A

STATE	AZIM	INCL	PSI	J	J/J0
0	152.5	-43.5	0.0	0.54E-04	1.0000
170	139.5	-56.0	15.0	0.84E-04	1.5495
247	138.4	-55.8	0.6	0.11E-03	1.9852
306	144.5	-55.0	3.5	0.79E-04	1.4625
391	142.5	-57.7	2.9	0.86E-04	1.5929
462	142.6	-56.7	1.1	0.84E-04	1.5523
529	140.9	-62.0	5.4	0.24E-04	0.4429
562	177.4	-35.3	35.0	0.41E-05	0.0754

DEMAGNETIZATION HISTORY OF GR984B

STATE	AZIM	INCL	PSI	J	J/J0
0	252.4	55.0	0.0	0.75E-03	1.0000
131	250.5	54.2	1.4	0.63E-03	0.8497
233	255.1	54.0	2.7	0.54E-03	0.7176
261	258.8	53.4	2.3	0.52E-03	0.6947
319	262.5	51.0	3.3	0.47E-03	0.6263
375	255.5	50.7	4.4	0.41E-03	0.5493
449	260.7	48.5	4.0	0.34E-03	0.4538
497	261.5	47.5	1.1	0.27E-03	0.3593
543	81.0	47.7	84.8	0.85E-04	0.1145
605	40.9	-19.7	76.4	0.11E-04	0.0149

DEMAGNETIZATION HISTORY OF GR986B

STATE	AZIM	INCL	PSI	J	J/J0
0	53.6	84.1	0.0	0.12E-02	1.0000
147	46.0	82.9	1.4	0.87E-03	0.7336
235	45.8	83.3	0.4	0.72E-03	0.6044
301	23.9	88.7	5.5	0.63E-03	0.5283
382	352.1	82.9	6.0	0.47E-03	0.3992
455	326.6	81.9	3.5	0.36E-03	0.3049
524	292.3	31.1	52.3	0.54E-04	0.0456
568	250.4	-66.7	102.8	0.45E-05	0.0038

DEMAGNETIZATION HISTORY OF GR312C

STATE	AZIM	INCL	PSI	J	J/J0
0	57.6	16.7	0.0	0.42E-02	1.0000
137	60.5	13.7	4.1	0.40E-02	0.9573
214	65.4	13.1	4.8	0.35E-02	0.8272
284	69.7	13.7	4.2	0.30E-02	0.7260
343	73.7	14.4	4.0	0.26E-02	0.6313
408	74.7	14.8	1.0	0.21E-02	0.4976
471	83.7	16.4	8.8	0.16E-02	0.3797
528	81.8	19.5	3.5	0.11E-02	0.2725
562	78.7	8.6	11.3	0.92E-04	0.0219
607	154.2	-17.5	78.9	0.18E-04	0.0042

DEMAGNETIZATION HISTORY OF GR322C

STATE	AZIM	INCL	PSI	J	J/J0
0	127.2	79.7	0.0	0.20E-02	1.0000
149	87.6	79.7	6.9	0.16E-02	0.7997
229	96.8	74.8	5.3	0.13E-02	0.6220
242	100.6	70.6	4.4	0.12E-02	0.5754
300	101.4	66.2	4.4	0.85E-03	0.4175
373	113.6	53.2	14.3	0.70E-03	0.3400
430	110.1	47.1	6.5	0.56E-03	0.2759
480	112.7	38.2	9.2	0.53E-03	0.2570
522	111.1	37.4	1.4	0.44E-03	0.2160
538	114.0	37.8	2.3	0.33E-03	0.1600
587	165.0	-20.0	75.1	0.33E-04	0.0161

DEMAGNETIZATION HISTORY OF GR324C

STATE	AZIM	INCL	PSI	J	J/J0
0	108.2	46.2	0.0	0.27E-02	1.0000
187	115.4	44.0	5.5	0.10E-02	0.3742
291	118.9	40.9	4.0	0.76E-03	0.2859

DEMAGNETIZATION HISTORY OF GR324C CONTO

STATE	AZIM	INCL	PSI	J	J/J0
396	124.9	32.2	9.9	0.77E-03	0.2880
477	131.1	27.2	7.4	0.69E-03	0.2573
568	139.5	22.2	9.2	0.18E-03	0.0668
613	82.8	59.3	54.3	0.28E-04	0.0104

DEMAGNETIZATION HISTORY OF GR325C

STATE	AZIM	INCL	PSI	J	J/J0
0	99.7	47.1	0.0	0.20E-02	1.0000
137	103.3	50.1	3.8	0.22E-02	1.0640
214	108.6	45.1	6.1	0.20E-02	0.9721
284	111.0	38.7	6.6	0.18E-02	0.9057
343	114.9	34.4	5.3	0.17E-02	0.8341
408	119.9	32.6	4.5	0.16E-02	0.7656
471	120.0	27.2	5.4	0.14E-02	0.7079
528	121.8	21.5	5.9	0.13E-02	0.6264
562	128.7	19.5	6.8	0.71E-03	0.3484
607	164.1	-74.3	96.5	0.19E-04	0.0092

DEMAGNETIZATION HISTORY OF GR331C

STATE	AZIM	INCL	PSI	J	J/J0
0	99.5	30.1	0.0	0.44E-04	1.0000
140	100.7	28.5	1.9	0.48E-04	1.0863
233	100.1	26.5	2.1	0.45E-04	1.0316
261	99.9	26.0	0.5	0.44E-04	1.0110
319	98.6	22.7	3.5	0.42E-04	0.9512
375	99.6	21.7	1.3	0.40E-04	0.9086
449	100.8	20.5	1.7	0.38E-04	0.8783
497	99.9	18.7	2.0	0.37E-04	0.8557
543	100.2	18.5	0.3	0.35E-04	0.8098
605	98.3	16.4	2.7	0.21E-05	0.0491

DEMAGNETIZATION HISTORY OF GR333C

STATE	AZIM	INCL	PSI	J	J/J0
0	99.5	36.6	0.0	0.26E-04	1.0000
257	107.2	29.1	9.8	0.24E-04	0.9072
350	110.9	23.5	6.6	0.23E-04	0.8646
471	111.2	7.5	16.0	0.14E-04	0.5321
563	110.1	11.6	4.3	0.95E-05	0.3585

DEMAGNETIZATION HISTORY OF GR334C

STATE	AZIM	INCL	PSI	J	J/J0
0	9.5	70.0	0.0	0.21E-03	1.0000
170	79.3	71.0	22.1	0.17E-03	0.8334
247	83.9	69.4	2.2	0.11E-03	0.5303
306	81.8	72.0	2.7	0.73E-04	0.3496
391	66.9	71.4	4.7	0.52E-04	0.2497
462	79.5	57.0	15.3	0.32E-04	0.1525
529	321.4	76.4	41.0	0.13E-04	0.0636
562	148.4	17.1	86.4	0.19E-02	*****

DEMAGNETIZATION HISTORY OF GR341

STATE	AZIM	INCL	PSI	J	J/J0
0	312.5	34.3	0.0	0.36E-04	1.0000
149	315.3	32.8	2.7	0.32E-04	0.8975
233	305.8	34.4	8.0	0.18E-04	0.4911
270	293.4	39.1	11.0	0.11E-04	0.3022
326	268.5	31.0	21.8	0.30E-05	0.0824
379	169.9	-34.6	113.5	0.17E-05	0.0469
455	261.2	30.8	107.8	0.11E-04	0.3036
501	325.6	23.3	57.1	0.74E-06	0.0205

DEMAGNETIZATION HISTORY OF GR343C

STATE	AZIM	INCL	PSI	J	J/J0
0	323.4	12.9	0.0	0.12E-04	1.0000
257	331.7	12.0	8.2	0.40E-05	0.3296
350	67.1	-24.3	99.8	0.10E-05	0.0824

DEMAGNETIZATION HISTORY OF GR351C

STATE	AZIM	INCL	PSI	J	J/J0
0	11.2	-64.7	0.0	0.76E-01	1.0000
205	15.7	-64.3	2.0	0.65E-01	0.8570
267	15.9	-63.2	1.1	0.54E-01	0.7060
364	6.4	-65.9	4.9	0.46E-01	0.5996
472	13.2	-66.1	2.7	0.86E-02	0.1123
565	346.8	-59.6	13.5	0.21E-02	0.0280

DEMAGNETIZATION HISTORY OF GR353C

STATE	AZIM	INCL	PSI	J	J/J0
0	206.2	-53.0	0.0	0.61E-01	1.0000
131	207.5	-54.0	1.3	0.65E-01	1.0498

DEMAGNETIZATION HISTORY OF GR353C CONTO

STATE	AZIM	INCL	PSI	J	J/J0
207	207.4	-54.3	0.3	0.58E-01	0.9427
276	207.8	-53.6	0.7	0.52E-01	0.8537
337	207.3	-53.4	0.4	0.46E-01	0.7468
398	207.1	-53.0	0.4	0.35E-01	0.5754
451	206.9	-52.9	0.1	0.29E-01	0.4776
511	207.8	-52.7	0.6	0.18E-01	0.2919
534	266.4	-63.3	31.5	0.14E-01	0.2268
592	206.1	-75.9	22.9	0.13E-03	0.0022

DEMAGNETIZATION HISTORY OF GR355C

STATE	AZIM	INCL	PSI	J	J/J0
0	219.7	65.6	0.0	0.21E-01	1.0000
153	227.8	65.5	3.3	0.20E-01	0.9826
240	225.0	66.1	1.3	0.16E-01	0.7919
309	225.9	65.1	1.0	0.13E-01	0.6541
371	224.0	66.3	1.4	0.11E-01	0.5255
440	220.4	66.7	1.5	0.82E-02	0.3958
508	225.1	65.6	2.2	0.52E-02	0.2523
566	269.7	70.3	16.9	0.62E-03	0.0302

DEMAGNETIZATION HISTORY OF GR361C

STATE	AZIM	INCL	PSI	J	J/J0
0	73.6	77.8	0.0	0.24E-02	1.0000
121	56.5	75.0	4.9	0.25E-02	1.0267
229	67.5	73.0	3.6	0.19E-02	0.7660
242	67.0	72.4	0.6	0.17E-02	0.7160
300	79.3	70.1	4.6	0.14E-02	0.5864
373	83.0	67.0	3.3	0.11E-02	0.4336
430	84.5	65.1	2.0	0.94E-03	0.3897
480	95.6	39.2	26.6	0.84E-03	0.3475
522	96.2	57.3	18.0	0.60E-03	0.2477
538	89.2	61.2	5.4	0.41E-03	0.1699
587	50.9	-25.3	91.9	0.24E-04	0.0098

DEMAGNETIZATION HISTORY OF GR363C

STATE	AZIM	INCL	PSI	J	J/J0
0	350.4	68.2	0.0	0.58E-02	1.0000
207	12.2	68.5	8.0	0.40E-02	0.7012
311	22.5	69.1	3.8	0.29E-02	0.4971
407	11.5	67.8	4.3	0.45E-03	0.0784
511	39.0	59.6	14.5	0.12E-03	0.0214
571	45.6	49.4	10.9	0.29E-04	0.0050

DEMAGNETIZATION HISTORY OF GR365C

STATE	AZIM	INCL	PSI	J	J/J0
0	352.3	60.2	0.0	0.55E-02	1.0000
187	30.3	64.5	17.9	0.48E-02	0.8753
291	27.7	65.0	1.3	0.28E-02	0.5095
396	19.6	64.5	3.5	0.48E-03	0.0866
477	42.7	52.7	16.7	0.16E-03	0.0290
568	42.4	51.9	0.9	0.31E-04	0.0056
613	146.0	51.1	58.6	0.14E-04	0.0026

DEMAGNETIZATION HISTORY OF GR371C

STATE	AZIM	INCL	PSI	J	J/J0
0	285.0	48.5	0.0	0.69E-03	1.0000
187	282.4	56.5	8.2	0.84E-03	1.2122
291	100.5	28.9	94.5	0.43E-03	0.6263
396	198.6	84.5	62.0	0.10E-03	0.1498
477	125.9	59.4	29.4	0.40E-04	0.0580
568	166.9	-22.5	88.6	0.10E-04	0.0150

DEMAGNETIZATION HISTORY OF GR372C

STATE	AZIM	INCL	PSI	J	J/J0
0	296.2	35.8	0.0	0.20E-02	1.0000
153	296.8	48.0	12.2	0.10E-02	0.5006
240	287.1	62.2	15.3	0.75E-03	0.3666
309	260.5	68.2	12.5	0.62E-03	0.3042
371	251.5	80.0	12.0	0.55E-03	0.2689
440	180.7	73.5	16.2	0.45E-03	0.2216
508	145.8	55.3	22.9	0.39E-03	0.1893
566	190.5	5.2	61.5	0.69E-04	0.0341

DEMAGNETIZATION HISTORY OF GR373C

STATE	AZIM	INCL	PSI	J	J/J0
0	311.2	62.7	0.0	0.21E-02	1.0000
179	348.8	72.4	16.9	0.15E-02	0.7408
279	11.7	76.9	7.5	0.12E-02	0.5907
311	33.7	77.9	4.9	0.11E-02	0.5222
361	67.6	73.0	9.6	0.82E-03	0.3959
423	87.2	70.0	6.8	0.66E-03	0.3193
479	107.3	57.2	15.5	0.60E-03	0.2887
536	120.5	52.1	9.2	0.40E-03	0.1898
556	57.8	14.2	62.2	0.10E-03	0.0492
610	63.8	-7.3	22.2	0.35E-04	0.0167

APPENDIX D

SUPPLEMENTARY NOTES TO THE PRECAMBRIAN PALEOMAGNETIC DATA OF NORTH AMERICA

- P1 BERGH(1968): NINE SITES, AFTER CORRECTION FOR TILT, ARE CONSIDERED TO REFLECT THE DIRECTION OF THE PRIMARY STILLWATER TRM. RB-SR ISOCHRON METHOD YIELDS A RELIABLE AGE OF 3100 200M.Y.
- P2 FAHRIG ET AL (1965), STRANGWAY(1964): FAHRIG AND WANLESS(1963) REPORT A SINGLE K-AR WHOLE ROCK AGE WHICH IS LISTED. CAMPBELL (1962) REPORTED AN AGE OF 1740 200 M.Y. FOR A NORTHEPLY STRIKING DIKE AND THIS AGE IS TAKEN AS THE RESULT OF POST-INTRUSION ARGON LOSS. STRANGWAY(1964) LISTS GEOLOGICAL EVIDENCE WHICH INDICATES THAT THE DIKES ARE OLDER THAN 1.5 B.Y..
- P3,P7 SYMONS (1967): BOTH NIPISSING DIABASE SILL AND COBALT GROUP SEDIMENTS ARE SHOWN TO CARRY PRIMARY REMANENCES BY MEANS OF STABILITY INDEX VALUES OF TARLING AND SYMONS (1967)
- P4,P5,P6 SYMONS (1967): SYMONS SUGGESTS A TIME INTERVAL OF THE ORDER OF 'TENS OF MILLIONS OF YEARS' BETWEEN THE GENESIS OF THE GOETHITE ORE AND DEPOSITION OF THE HANGING WALL ASHROCK A TIME DIFFERENCE OF 'HUNDREDS OF MILLIONS OF YEARS' IS SUGGESTED BETWEEN THE ASHROCK AND THE BASIC EXTRUSIVES.
- P8,P22 FAHRIG ET AL (1965): THE AGE DETERMINATIONS AND PALED MAGNETIC RESULTS ARE ONLY APPROXIMATE, THE RESULTS BEING BASED ON FEW SAMPLES. THE AGE OF 1445 M.Y. FOR MOLSON DIKES IS BEING EFFECTED BY THE LOW POTASSIUM CONTENT IN THE ROCK.
- P9,P10,P11 LAROCHELLE (1966),FAHRIG ET AL (1965),STRANGWAY(1964): GSC AGE DETERMINATIONS (63-118,63-149) SUGGEST A 585 M.Y. DIFFERENCE BETWEEN THE WHOLE ROCK AGES. STRANGWAY(1964)'S ENF DIKES PARALLEL TO GRENVILLE FRONT.
- P12 HODD(1961),SOPHER(1963): IRVING'S POLE 1.49. RADIOMETRIC AGE BETWEEN 1200 AND 1800 M.Y. IS ASSIGNED.
- P13,P14 NAIRN ET AL (1959)
- P15 EGGLE AND LARSON (1968): AGE DETERMINATIONS BY THE RB-SR ISOCHRON METHOD. POLE 9.144 OF MCELHINNY (1968)
- P16,P17 HAYS AND SCARDON (1966), HSU ET AL (1966): THESE TWO POLES ARE FOR ROCK UNITS OF SIMILAR AGE. FOR POLE P16, THE MAGNETIZATION IS INFERRED TO BE CHEMICAL REMANENT, AND WAS SHOWN TO BE STABLE IN FIELDS OF 500-800 OE. THE MEAN IS CALCULATED GIVING UNIT WEIGHT TO EACH SITE.

P18 BLACK (1963): POLE 1.73 OF IRVING

P19,P24 COLLINSON AND RUNCORN (1960),RUNCORN (1964): IRVING'S POLE NUMBERS 1.21-1.27. OBRADOVICH AND PETERMAN(1968) POINTED OUT THAT THREE DISTINT PERIODS OF SEDIMENTATION EXIST FOR THE BELT SERIES, AT 1300,1100,AND 900 M.Y.. THE BELT SERIES ARE CHARACTERIZED BY DISCONTINUOUS SEDIMENTATION. THERE IS EVIDENCE THE MCNAMARA FORMATION IS YOUNGER THAN 1085 M.Y.. GILETTI (1966,1968) POINTED OUT THAT BELT SERIES POST DATE 1600M.Y.. THUS COMPUTATION OF A SINGLE MEAN POLE MAY BE MISLEADING. COLLINSON AND RUNCORN AND RUNCORN DID NOT REPORT ANY LABORATORY STABILITY TESTS MADE ON THESE ROCK UNITS.

P20 SPALL(1968): AGE DETERMINATIONS INDICATE AN AGE OF 1360 M.Y.. ONLY SPECIMENS WITH Q' VALUES NEAR UNITY WERE CONSIDERED IN THE ESTIMATION OF POLE POSITIONS.

P21 PALMER (1969): THE FORMATION IS RELIABLY DATED AT 1475 50 M.Y.. A.C.DEMAGNETIZATION IN 75 DE IMPROVED THE GROUPING. SAMPLE DIPECTION IS GIVEN UNIT WEIGHT IN THE ANALYSIS.

P25 ROBERTSON (1964): THE DIRECTION QUOTED IS THE MEAN AFTER TREATMENT IN 75 DE.. GEOCHRONOLOGIC DATA INDICATE AN AGE SIMILAR TO THE SUDBURY DIKE SWARM.

P26 LAROCHELLE(1967),SOPHER(1963),STRANGWAY(1964): THE NORTHWEST TRENDING DIKES AROUND SUDBURY WHICH ARE DATED AT 1285 M.Y.., YIELD THREE SIMILAR POLE POSITIONS

P27 RESULTS OF FAHRIG AND JONES (1969) AND FAHRIG ET AL (1965) YIELD SIMILAR POLE POSITIONS

P28-P31,P33 DUBOIS(1962): DUBOIS SUGGESTED A RAPID POLAR WANDER FROM HIS RESULTS.

P34 VINCENZ(1968) AND DUBOIS(1962) OBTAINED SIMILAR RESULTS ON THESE LAVAS WHOSE AGE IS KNOWN RELIABLY AS 1000M.Y.. VINCENZ OBSERVED PARTIAL SELF REVERSAL OF MAGNETIZATION AT CERTAIN SITES. IT IS DEMONSTRATED THAT PARTIAL SELF REVERSAL HAS NO EFFECT ON THE VALIDITY OF PALEOMAGNETIC DATA.

P35,P36 DATED AS UPPER MIDDLE KEWEENAWAN. DEMAGNETIZATION IN 75 DE IMPROVED THE GROUPING. 27 SITES OF FERROGABBRO NOT INCLUDED IN THE FINAL RESULT BECAUSE OF MAGNETIC ANISOTROPY. THE AUTHOPS CONCLUDE THAT POLE POSITIONS OF KEWEENAWAN AGE FALL INTO TWO GROUPS; AN OLDER GROUP OF POSITIVE POLARITY AND SCATTERED POLES AND A YOUNGER GROUP OF NEGATIVE POLARITY AND TIGHTLY GROUPED POLES.

P37-P41 HOOD (1958)

P42 HARGRAVES AND BURT (1967): K-AR AGE DETERMINATIONS BY THE GSC AVERAGE AROUND 1000M.Y. WHICH REFLECTS GRENVILLE METAMORPHISM. ALLARD LAKE ANORTHOSITES ARE PRESUMED TO HAVE ACQUIRED THEIR MAGNETISM DURING GRENVILLE OROGENY.

P44 THESE EAST WEST TRENDING DIKES ARE YOUNGER THAN JACOBSTOWN SANDSTONE. STRANGWAY(1964) COMPARES THEM TO SIMILAR TRENDING DIKES NORTH OF OTTAWA(GRENVILLE DIKES DESCRIBED IN CHAPTER 5) WHICH YIELD DATES YOUNGER THAN GRENVILLE OROGENY.

B29933